DECIPHERING THE ROLE OF GTPASES AND THE CYTOSKELETON IN AQUAPORIN-4 VESICULAR TRAFFICKING

Andrea Markou

Doctor of Philosophy

Aston University

September 2022

Aston University

Deciphering the role of GTPases and the cytoskeleton in aquaporin-4 vesicular trafficking

Andrea Markou, Doctor of Philosophy, 2022

The AQP4 water channel is abundantly expressed in brain glial cells and contributes to swelling following brain trauma. Cell surface localization of AQP4 in mammalian cells fluctuates rapidly in response to changes in oxygen and tonicity, suggesting a role for vesicular trafficking in its translocation, but the molecular mechanism of this is not fully understood. The aim of this thesis was to decipher the role of key elements of vesicular trafficking in the movement of AQP4 to the plasma membrane.

Early and recycling endosomes were selected as likely candidates of rapid AQP4 translocation. HEK293 cells were transiently transfected with AQP4-EGFP and either mCherry-Rab5 or mCherry-Rab11. It was found that AQP-EGFP colocalized with mCherry-Rab5 positive early endosomes and mCherry-Rab11 positive recycling endosomes. Under hypotonic conditions, AQP4-EGFP translocated from intracellular vesicles to the plasma membrane within 90 seconds. Co-expression of dominant negative forms of the mCherry-tagged Rab5 and Rab11 with AQP4-EGFP resulted in no changes in the relative membrane expression of AQP4 following changes in tonicity. Inhibition of dynamin impaired internalisation of AQP4. Cytoskeleton modifying compounds also affected AQP4 translocation to and from the plasma membrane. Findings in HEK293 cells were confirmed and validated in human primary astrocytes using cell surface biotinylation.

Through the work completed in this thesis, dynamin has been shown to be necessary for the internalisation of AQP4. Whether the mechanism is either clathrin-dependent or clathrin-independent would need to be determined with further studies. The role of actin and microtubules is less clear; the results showed an involvement of actin and microtubules, but future work will determine whether F-actin or G-actin is involved, as well as whether microtubules are required for AQP4 vesicular targeting, or whether they are required for untargeted movement within the cell.

Key words: Water channel, Aquaporin, AQP4, Vesicular Trafficking, GTPase, Cytoskeleton

for my grandfather, Dr Andreas Markou

Acknowledgements

This project would not have been possible without the support of my supervisor, Dr Zita Balklava. I am extremely grateful for her patience, advice, and continuous question-answering throughout my PhD studies. An enormous thank you to my associate supervisor, Professor Roslyn Bill, for imparting her wisdom, and for her encouragement in steering me towards the completion of this work.

My thanks to Dr Phil Kitchen for his time, work and guidance throughout my research. I am indebted to Dr Mariaelena Repici for sharing her imaging expertise, and for all the time given to talk about my project among other things. I would like to thank everyone in Team AQP, It was more than a pleasure to work with people of such deep and wide knowledge.

Special thanks to Dr Ivana Milic, for her support both in and out of the lab, her endless patience, and her invaluable friendship. A big thanks to Parbata Chauhan, for the sit-down time and the inside jokes. A special mention to Nestor for keeping me entertained throughout this journey.

Finally, I would be remiss in not expressing my endless gratitude to my family: my grandmother Christina, for helping to keep my spirits high and for enduring this journey with me, and my mother, Dr Eleni Markou, for the continuous support, motivation, for being the inspiration behind my academic journey and for often being the wind beneath my wings.

List of Contents

List of Abbreviations

AM	Astrocyte medium
AP2	Adaptor protein 2
APS	Ammonium persulfate
AQP	Aquaporin
BBB	Blood-brain barrier
BSA	Bovine serum albumin
C.elegans	*Caenorhabditis elegans*
CaM	Calmodulin
CAV	Caveolin
CIE	Clathrin-independent endocytosis
CKII	Casein kinase II
CME	Clathrin-mediated endocytosis
CNS	Central nervous system
CVR	Cell volume regulation
DMEM	Dulbecco's modified Eagle's medium
DMSO	Dimethyl sulfoxide
EEA1	Early endosome antigen 1
ER	Endoplasmic reticulum
FCHSD1	FCH and double SH3 domains protein 1
FIPs	Rab11-family interacting proteins
FBS	Foetal bovine serum
GAP	GTPase activating protein
GDI	GDP dissociation inhibitor
GDP	Guanosine diphosphate
GEF	Guanine nucleotide exchange factor
GFP	Green fluorescent protein
GTP	Guanosine triphosphate

HEK293	Human embryonic kidney 293 cells
HRP	Horseradish peroxidase
ICP	Intracranial pressure
NGM	Nematode Growth Medium
OAP	Orthogonal arrays of particles
PBS	Phosphate-buffered saline
PCC	Pearson's correlation coefficient
PCR	Polymerase chain reaction
PEI	Polyethylenimine
RAB	Ras-associated binding protein
REP	Rab escort protein
RME	Relative membrane expression
RNAi	RNA interference
RVD	Regulatory volume decrease
RVI	Regulatory volume increase
SDS-PAGE	Sodium dodecyl sulphate polyacrylamide gel electrophoresis
SNARE	Soluble NSF-attachment protein receptor
TEMED	Tetramethylenediamine
TRPV4	Transient receptor potential vanilloid 4
WASP	Wiskott-Aldrich syndrome protein

List of Tables

List of Figures

1 Introduction

1.1 AQP family

Aquaporin (AQP) water channels are transmembrane proteins responsible for the bidirectional transport of water across the cell membrane. There have been 13 AQPs identified in humans (Table 1) and APQs are present in all organisms. AQPs can be subcategorised into classical AQPs (selective for transporting water), aquaglyceroporins (capable of transporting small neutral solutes such as glycerol and urea, as well as water) and superaquaporins – these have sequences with differences such as the unique NPA box compared to that of AQPs previously described and their roles are yet to be fully elucidated (Ishibashi, Tanaka & Morishita, 2021). More recently, some of these AQPs have been shown to share similar properties with regards to the similarity of the solutes they transport. These can be subdivided into ammoniaporins (transport of ammonia), and peroxiporins (H_2O_2), with some AQPs showing permeability to both (Prata, Hrelia & Fiorentini, 2019; da Silva et al., 2022).

Table 1: Thirteen human AQPs which are found throughout the human body.

AQP name	Subcategory information adapted from (Kozono et al., 2002)	Permeability information adapted from (Kitchen et al., 2015)	Location in the human body information adapted from (Day et al., 2014)
AQP0	Classical AQP	Water	Lens fibre
AQP1	Classical AQP	Water	Inner ear, brain, spinal cord, kidney, pancreas, blood vessels, liver, skin
AQP2	Classical AQP	Water	Kidney
AQP3	Aquaglyceroporin	Water, glycerol, urea, ammonia	Kidney, spinal cord, gastrointestinal tract, sperm, lungs, skin
AQP4	Classical AQP	Water	Brain, retina, nasal cavity, inner ear, spinal cord, heart, kidney, gastrointestinal tract, lungs
AQP5	Classical AQP	Water	Salivary glands, gastrointestinal tract, lungs, skin
AQP6	Classical AQP	Water (very low), glycerol, urea, ammonia	Kidney

AQP7	Aquaglyceroporin	Water, glycerol, urea, ammonia	Kidney, sperm, ovaries, adipocytes
AQP8	Classical AQP	Water, urea, ammonia	Spinal cord, pancreas, ovaries, liver
AQP9	Aquaglyceroporin	Water, glycerol, urea, ammonia	Osteoclasts, gastrointestinal tract, ovaries, liver
AQP10	Aquaglyceroporin	Water, glycerol, urea	Skin, small intestine
AQP11	Superaquaporin	Water, glycerol, H_2O_2	Male reproductive system
AQP12	Superaquaporin	Water, glycerol, H_2O_2	Pancreas

1.1.1 AQP structure

Recent reports of high-resolution X-ray structures of AQPs have been published, showing that the family has been conserved in structure (Kreida & Törnroth-Horsefield, 2015), something which had already been reported for quite a few years before this (Hedfalk et al., 2006), with each AQP monomer consisting of two helices that do not cross the membrane and six transmembrane helices encompassing a central pore (figure 1-1)(Kreida & Törnroth-Horsefield, 2015). This pore contains two highly conserved asparagine-proline-alanine water-conducting motifs, and Kosinska Eriksson *et al.* (2014) suggest that the asparagine residues and carbonyl groups form hydrogen bonds with water molecules, the water permeability of the AQP depends on the number of these bonds. The selectivity filters present in AQP pores, differentially effect the permeability to substances (Kitchen et al., 2019). The aromatic arginine motif which is present in the extracellular region of the pore, is comprised of four residues: arginine, and three others depending on the AQP subgroup. The arginine contributes to the selectivity, as well as proton exclusion, through its positive charge.

The AQP monomers form tetramers, with each pore staying intact (Jung et al., 1994b; Mathai & Agre, 1999). It should be noted that in the group of superaquaporins, the asparagine-proline alanine motifs are not as highly conserved (Ishibashi, 2006).

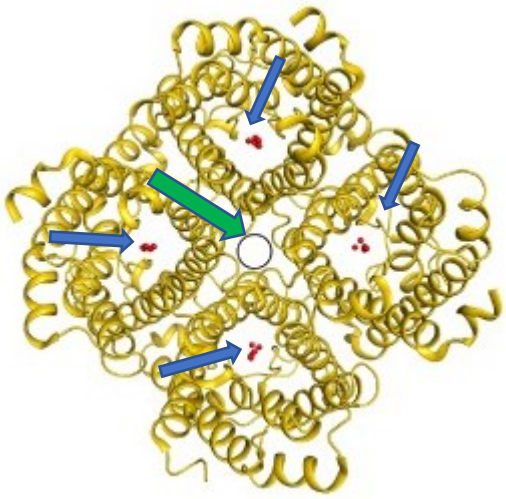

Figure 1-1: The structure of an AQP tetramer. Each monomer contains its own pore (blue arrow) and the four monomers surround a central pore (green arrow) (adapted from Kreida & Törnroth-Horsefield, 2015).

1.1.2 AQP4 structure and function

There are multiple roles AQP4 has in the brain: neuroexcitation, astrocyte migration and, of course, water transport (Fukuda & Badaut, 2012; Saadoun et al., 2005; Jung et al., 1994a). The expression of AQP4 in the brain is predominantly in the areas close to fluid-filled compartments, indicating that AQP4 plays a role in its movement. It should be noted that AQP1 and AQP9 are also expressed in the brain to a much lesser extent (Badaut et al., 2002). In astrocytes, AQP4 is attached to the membrane with a dystrophin complex (Iacovetta *et al.*, 2013). The expression of AQP4 is abundant in the subpial processes and the endfeet, the former forming part of the interface between the central nervous system and cerebrospinal fluid and the latter forming part of the interface between the blood and the central nervous system (Papadopoulos and Verkman, 2013). The osmotic gradient across the cell membrane determines the flow of water through AQP4, with the rate of this changing, depending on the actual number of AQP4 present.

Like other AQPs, AQP4 consists of tetramers surrounding a central pore (figure 1-2). These tetramers then form structures called orthogonal arrays of particles (OAPs) (Nagelhus and Ottersen, 2013). The transport of water through AQP4, again, like other AQPs, is due to the pore narrowing to approximately 2.8 Å, allowing only water to pass through and excluding any larger molecules and positively charged dipoles block the passage of protons (Nagelhus and Ottersen, 2013).

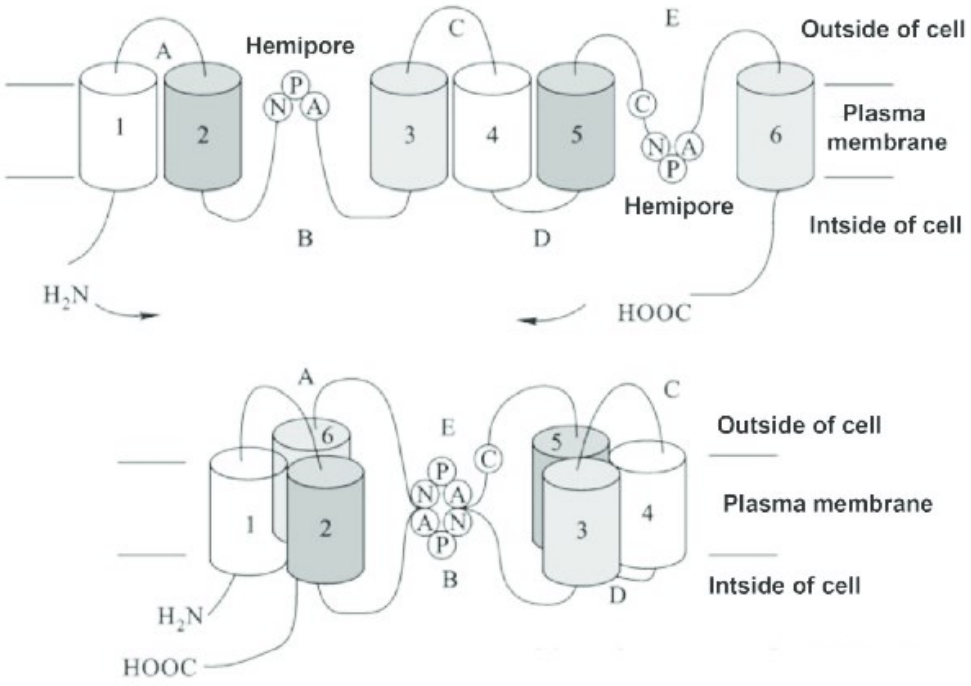

Figure 1-2: The transmembrane structure of an AQP4 monomer (Chu et al., 2016).

AQP4 has several isoforms that have been described: M1 and M23 (Iacovetta *et al.*, 2013) and, more recently, AQP4b, AQP4d, AQP4e and AQP4f (Potokar *et al.*, 2013). The presence of the M1 and M23 isoforms in astrocytes, although not having been described decisively, has been established and a model proposed by Jin *et al.* (2011) of the M1:M23 ratio provided insight into the formation of OAPs from these isoforms. In 2004, Rash *et al.* showed using combined confocal microscopy and freeze-fracture immunogold labelling, that the size of the OAPs formed by AQP4 was dependent on the presence of M1 and M23, the latter of the two stabilizing the OAP and, when expression increased, enlarging it. The presence of the AQP4e isoform in the astrocytic endfeet was also recently described (Sorbo *et al.*, 2008). The directionality and mobility of vesicles carrying AQP4e were shown to have a correlation with their localisation in the plasma membrane in response to a hypotonic environment (Sorbo *et al.*, 2008).

The passive movement of water facilitated by AQPs is varied across tissues, however, it triggers cellular mechanisms that determine cell volume. Cell volume regulation (CVR) is a constituent of water transport by AQPs and is a response to either hypotonic or hypertonic changes in the cell through RVD and regulatory volume increase (RVI), respectively (Day *et al.*, 2014). Hoffmann *et al.* (2009) showed that the mechanism of each of these seems to depend on the cell type, however, the results of all of these tend to be the same; in hypotonicity-induced swelling, RVD is dependent upon water efflux to alter the cell volume

and in comparison, hypertonicity-induced shrinkage depends on water influx to alter the cell volume.

The involvement of AQPs in CVR has been demonstrated by studies carried out in knockout experiments. Both in AQP5 knockout cells and AQP3 deficient mice, when exposed to hypotonic conditions, were unable to undergo RVD (Chen et al., 2010; Liu et al., 2006). Additionally, Galizia *et al*. (2012) demonstrated that in AQP2 non-expressing cells, there was no occurrence of RVD, however, when the same cells expressed AQP2, RVD was present; suggesting AQPs act as a signal in RVD. Such examples have not been published for RVI but given the similarity in both RVI and RVD, the AQPs may very well play a role in this.

AQP4 has been shown to also contribute to regulatory volume decrease (RVD) in astrocytes, a protective mechanism that acts as a response to hypotonic stress. In RVD, a complex of transient receptor potential vanilloid 4 (TRPV4) and AQP4 respond to a change in extracellular tonicity triggering the downstream effects. Benfenati *et al.* (2011) compared the astrocytes of AQP4 knockout mice to wild type mice that were exposed to hypotonic conditions. When undergoing hypotonic stress, the astrocytes of the wild type mice responded firstly with an increase in volume followed by a decrease. On the other hand, the astrocytes of the AQP4 knockout mice responded at a much slower rate of volume increase and were unable to undergo RVD. This experiment was a good indicator that AQP4 is an essential component of RVD in astrocytes.

1.2 Cytotoxic oedema

1.2.1 Pathology

Following a trauma to the brain, swelling of the tissue occurs with potentially devastating outcomes for a patient that range from disability to even death. This swelling arises as a consequence of the water flow between the astrocytic syncytium and the interstitial space having changed; the altered transport leads to the increase in both ions and water intracellularly, with a reduction in these in the extracellular area, this is called cytotoxic oedema. All of this occurs with the blood-brain barrier (BBB) remaining undamaged. Apart from cytotoxic oedema, there are two other categories of brain swelling: vasogenic oedema, which usually occurs as a continuum from cytotoxic oedema (figure 1-3), and hydrocephalic oedema (Liang *et al.*, 2007).

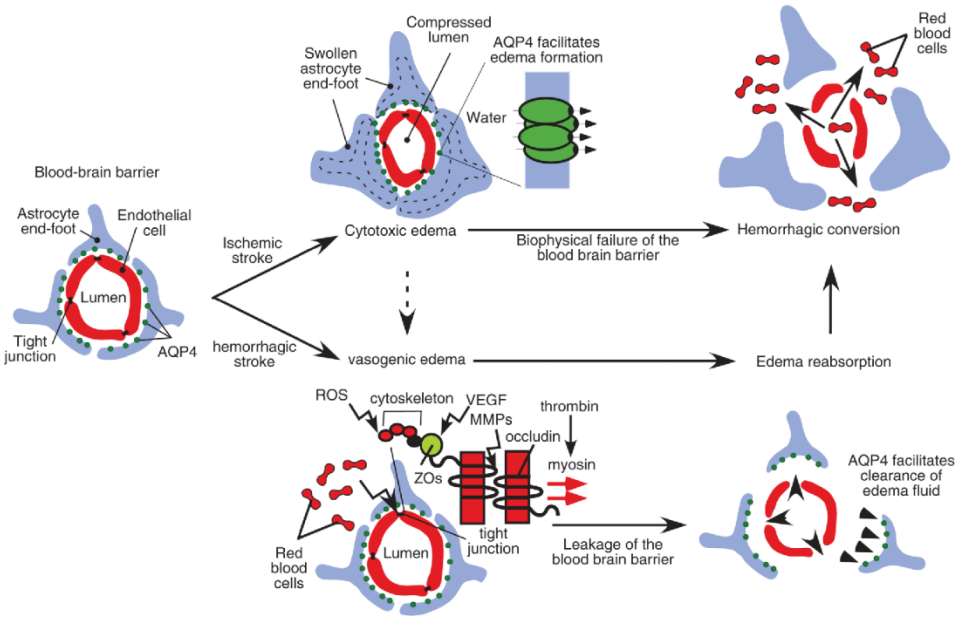

Figure 1-3: The brain swelling process (Zador et al., 2009). Following injury, in this case, stroke, cytotoxic and/or vasogenic oedema forms with swelling of astrocytes after an influx of water, or a breakdown of the blood-brain barrier, ultimately ending in AQP4 involvement in the clearance of the accumulated fluid.

In 2005, Kimelberg reviewed data on astrocytic swelling following injury and concluded that there was a direct detrimental effect on the function of the astrocytes themselves as well as the surrounding neurons. Different proposals of a complete mechanism of the formation of cytotoxic oedema have been put forward, with the three main ones being proposed by Kimelberg (2004), Davalos *et al* (2004) and Walz and Mukerji (1988). All three propose that trauma leads to a change in the osmotic gradient, allowing the passive transport of water into the astrocytes, clearly implicating AQP4 in this process as an important component.

1.2.2 AQP4 in cytotoxic oedema

It is important to note, that as the most abundantly expressed water channel in the central nervous system (CNS), AQP4 does not only play a role in cerebral oedema (Vandebroek & Yasui, 2020). Recently, AQP4 has been shown to contribute to clearance of proteins related to Alzheimer's disease, and has even been associated with a poor cognitive performance in patients with Parkinson's Disease (Silva et al., 2021; Fang et al., 2022). However, the focus of this thesis will be understanding the role of AQP4 movement in relation to cytotoxic oedema. Following a trauma to the brain, ischaemia, inflammation or a tumour, an influx of water occurs - facilitated by AQP4 - and ions through separate channels, which leads to an increase in volume of the brain tissue. Once the brain tissue begins to swell, it presses against the skull, bringing about an increase in intracranial pressure (ICP) and a decrease in blood circulation

(Zador et al., 2009). This increase in volume can have devastating effects, both in terms of morbidity and mortality, and is a problem that disproportionately affects young people (NICE, 2019). Therefore, understanding the molecular mechanism that leads to brain swelling is vital in order to develop effective, targeted treatments.

As mentioned previously, oedema is usually either cytotoxic or vasogenic and it has been suggested that cytotoxic oedema is prevalent in trauma and ischaemia, whereas vasogenic oedema occurs more often in inflammation and tumours. This is not always the case, with the two occurring consecutively in most circumstances (Stokum, Gerzanich & Simard, 2016).

The role of AQP4 in the nervous system and cytotoxic oedema has been described in several articles, most notably by Vella (2015) and Papadopoulos and Verkman (2013). Whilst Papadopoulos and Verkman (2013) make note of the gaps in available information with regards to the cell-specific mechanisms of AQPs, Vella (2015) discusses the use of animal models and concludes that the understanding of the modulators of AQPs would provide a useful therapeutic target.

Animal studies have shown varying outcomes with AQP4 being both upregulated and downregulated. In rats, Sun *et al.* (2003) measured AQP4 mRNA expression following a traumatic brain injury and observed a significant upregulation of AQP4 mRNA in the area where the injury occurred, with no change in the areas of the brain that were not injured. In mice, Manley *et al.* (2000) compared wild-type mice to those with an AQP4 deletion and Yang *et al.* (2008) compared mice overexpressing AQP4 to those with an AQP4 deletion; in both publications, the authors observed a decrease in oedema formation in the AQP4-deficient mice and the mice overexpressing AQP4 had a much faster oedema formation as well as a more negative outcome. A similar experiment on APQ4 involvement in cytotoxic oedema formation was published by Verkman *et al.* (2006). Mice with an AQP4 deficiency were protected from cytotoxic oedema and overall had a much more positive outcome in terms of survival and the endfeet of the astrocytes were swollen to a much less significant degree.

In addition to using the model lacking AQP4 expression, mouse models deficient in polarized AQP4 localized to the membrane added another dimension to the understanding of AQP4 function (Amiry-Moghaddam, 2004). The distribution of AQP4 in the foot processes of the astrocytes is in a polarized manner. The dystrophin-α-syntrophin complex it relies on for this is localized to the astrocytic endfeet. In knockout mice lacking α-syntrophin, polarized AQP4 was not expressed and a phenotype similar to that of the aforementioned AQP4 knockout models was observed: a decreased occurrence of cytotoxic oedema (Amiry-Moghaddam, 2004).

Each publication has highlighted the importance of the presence of AQP4 as a water channel in terms of cytotoxic oedema and the outcomes associated with its correct and incorrect function.

More recently, AQP4 subcellular localisation was used as a potential target for oedema treatment. This was done through the administration of trifluoperazine to rats subjected to spinal crush injury, leading to a reduction in oedema and enhanced recovery (Kitchen et al., 2020). This data shows the subcellular localisation mechanism of AQP4 to be an attractive target.

1.3 Membrane trafficking

1.3.1 Endocytic pathways

The internal organization of a cell must sustain a balanced exchange between elements entering and exiting the cell. These must be transported rapidly in order to respond to the needs of compartmentalisation through the budding, fusion and fission of the compartments of the endosome (Alberts *et al.,* 2008). Intracellular trafficking compartments are comprised of the endoplasmic reticulum (ER), the Golgi apparatus, vesicles, cell membrane, the endosomes and lysosome (Alberts *et al.,* 2008).

The process of selectively transporting cargo into a cell through the phospholipid bilayer can occur through two different pathways, the clathrin-mediated and clathrin-independent. Clathrin-mediated endocytosis (CME) involves the formation of specific vesicles to transport molecules between the compartments of the endosome and the plasma membrane. These vesicles are formed and then released through a highly ordered process (figure 1-4). The initial step is the gathering of coat and adaptor proteins around the membrane, forming a coat around the pit (McMahon & Boucrot, 2011). One such coat protein is clathrin, responsible for moving vesicles from the plasma membrane to the endosome. The structure of clathrin is that of three heavy chains and three light chains, which form a curved basket that contributes to vesicle budding (Hurley *et al.*, 2010). This clathrin lattice formation at the plasma membrane is initiated by the Adaptor protein 2 (AP2) (Kovtun et al., 2020).

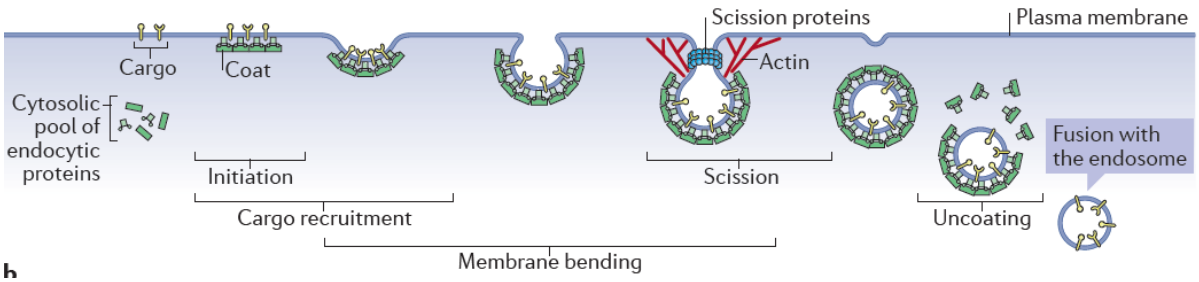

b

Figure 1-4: Formation of a vesicle through CME. The cargo is enveloped in a clathrin coat, and a vesicle slowly forms through membrane bending. Then, with the aid of the cytoskeleton and scission proteins, the vesicle comes away from the membrane and into the cell.

Once this initial coat has been created, a reorganisation of the cytoskeleton through actin polymerization contributes to the elongation of the neck of the pit (Ferguson et al., 2009). Actin polymerization begins with nucleation, where actin monomers accumulate to form polymers (Cooper, 2000). Actin filament nucleators, such as Actin-related protein 2 (Arp2) aid in the creation of additional branches of actin filaments. Arp2 along with Arp3 form a complex which binds to the actin filament; the Arp2/3 complex mimics actin subunit organisation and creates new sites for nucleation (Rodnick-Smith et al., 2016). The Arp2/3 function is modulated by Wiskott-Aldrich syndrome protein (WASP) proteins which recruit the complex to actin filaments; this process is activated by FCH and double SH3 domains protein 1 (FCHSD1) (Almeida-Souza et al., 2018). Following this, dynamin is recruited to the clathrin-coated pits.

Dynamin, a GTPase, assembles around the elongated neck, constricts and then cuts it. This scission of the vesicle is achieved through a “super twist” of the dynamin, which has recently been suggested as the main force required for the vesicle to separate from the membrane (Cheng et al., 2021).

The other main pathway of internalisation, clathrin-independent endocytosis (CIE), is not as well-described as CME. The most well-known mechanism is that involving the formation of caveolae (Mayor & Pagano, 2007). Caveolae are created through infolding of the plasma membrane and are mostly made up of caveolin-1 (cav-1), with caveolin-2 (cav-2) and caveolin-3 (cav-3) also part of the family of proteins involved in CIE. Interestingly, not all are required for invagination (only cav-1 and cav-3 for muscle cells) or for vesicular transport (here cav-1 and cav-2 serve that purpose) (Thomas & Smart, 2008). It has been suggested that CIE contributes to only approximately 5% of endocytic traffic, but this requires further elucidation (Bitsikas, Corrêa & Nichols, 2014).

However, it should be noted that whilst CME and CIE occur independently of each other, and not to the same extent, there are still proteins that are implicated in both. One such protein is dynamin - as mentioned above, CME is a dynamin-dependent process, whilst CIE can occur in a dynamin-dependent or dynamin-independent manner. The action of dynamin in CIE is similar to that in CME. Studies have shown that impaired dynamin function not only prevents internilsation of caveolae but also the initial budding from the membrane (Oh, McIntosh & Schnitzer, 1998).

1.3.2 The early endosome

Once the vesicle has entered the cytosol it is targeted to the early endosome, the function of which is to sort the vesicle cargo for various regions within the cell, whether it be recycling or degradation (Jovic et al., 2010).

The regulation of this transport is controlled by Ras-associated binding (Rab) proteins. Rabs, like other small G-proteins, switch between active GTP-bound and inactive GDP-bound states (figure 1-5). The GDP is removed and the inactive Rab undergoes a conformational change by a guanine nucleotide exchange factor (GEF), allowing the GTP to bind and activate the protein; conversely, the active Rabs become inactive through the hydrolysis of GTP through the GTPase activating protein (GAP) (Müller & Goody, 2017). In order for the cytosolic pool of inactive Rabs to remain available, the GDP dissociation inhibitor (GDI) regulates their removal from the membrane, whereas the Rab escort protein (REP) will aid in the Rab delivery to the membrane.

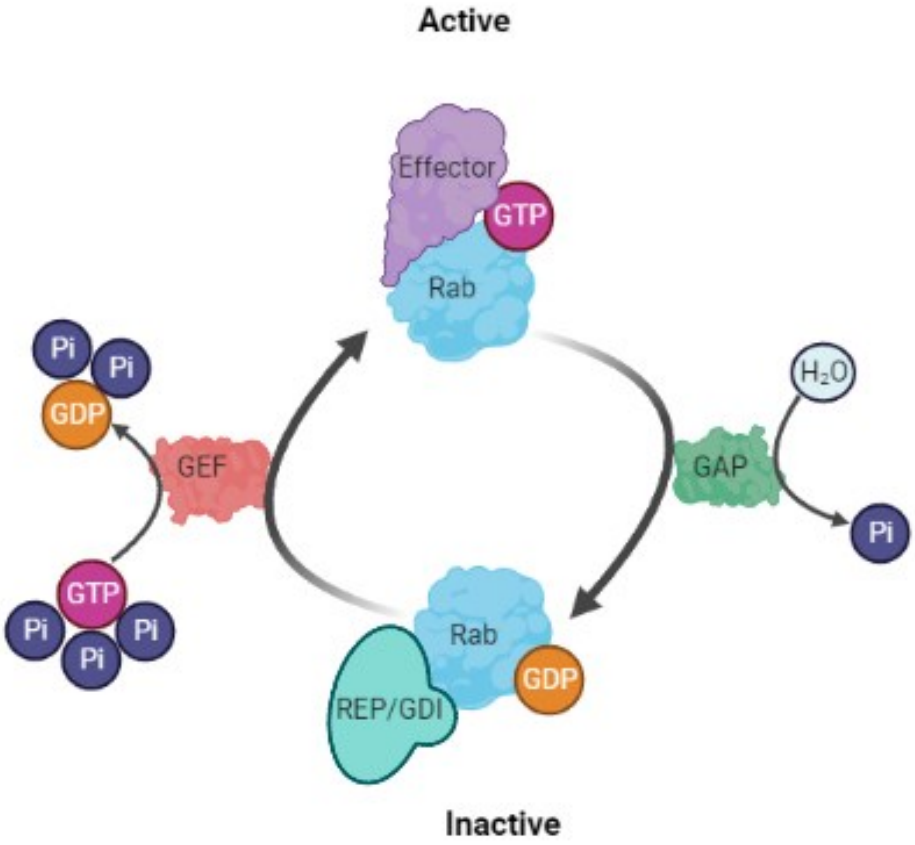

Figure 1-5 The Rab GTPase activation and inactivation cycle (Created with BioRender.com)

In relation to the plasma membrane and the early endosome, in particular, Rab5 has been identified as having a key role. Transport of clathrin-coated vesicles entering the cytosol is

regulated through Rab5 and its effector early endosome antigen 1 (EEA1). Following membrane fission, and uncoating of the vesicle, Rab5 plays a role in the uncoating of the vesicle, most likely to prepare for membrane fusion (Semerdjieva et al., 2008; Galperin & Sorkin, 2003).

For fusion to occur, soluble *N*-ethylmaleimide-sensitive factor protein receptors (SNAREs) aid vesicle attachment. SNAREs can be subdivided into vesicular (v-SNARES) and target (t-SNARES) depending on whether they originate on the transport vesicle or target membrane, respectively (Söllner et al., 1993). These SNAREs bridge with each other by forming a complex and "zippering" from the N-terminus to the C-terminus, bringing the vesicle closer to its target (Fiebig et al., 1999; Brandhorst et al., 2006). The cargo released following this fusion is sorted, either to the lysosome via the late endosome, the endocytic recycling compartment or released for fast recycling (Jovic et al., 2010; Grant & Donaldson, 2009).

1.3.3 The recycling endosome

Movement from the early endosome to the endocytic recycling compartment is regulated by several proteins, however, the targeting in itself is not specific (Maxfield & McGraw, 2004). In terms of Rab proteins, it has been shown that this involves a loss of Rab5 and a gain of Rab11 (Sönnichsen et al., 2000). Rab11-dependent recycling is regulated by Rab11-family interacting proteins (FIPs). Return to the plasma membrane requires the recruitment of motor proteins in addition to FIPs; these motor proteins include kinesin and dynein which are involved in the movement of microtubules. Studies have also shown that the recycling of CIE cargo to the plasma membrane is dependent on CDE cargo, however, it is still unclear to what extent (Lau & Chou, 2008).

In the absence of Rab11, knockout studies have shown that Rab11 is required for the homeostasis of the endosome-lysosomal pathway (Zulkefli et al., 2019). HeLa cell lines with Rab11 knockout showed a change in the morphology of the recycling endosome which was no longer functional, whilst the lysosome showed an increase in size and activity (Zulkefli et al., 2019).

The use of dominant negative Rabs is a useful tool to examine specific Rab functions, by binding GDP and out-competing the endogenous Rabs and blocking the GTP-bound ones (Caviglia et al., 2019). For vesicle docking to occur, the Rab interacts with tethering proteins, however, in order for fusion to occur, more specialised proteins called soluble NSF-attachment protein receptors are needed. Most Rabs are ubiquitously expressed, with a few being tissue specific. Additionally, certain Rabs associate with certain compartments (figure 1-6), for example, Rab5 and Rab22 associate with the early endosome and Rab7 and Rab9 with the late endosome.

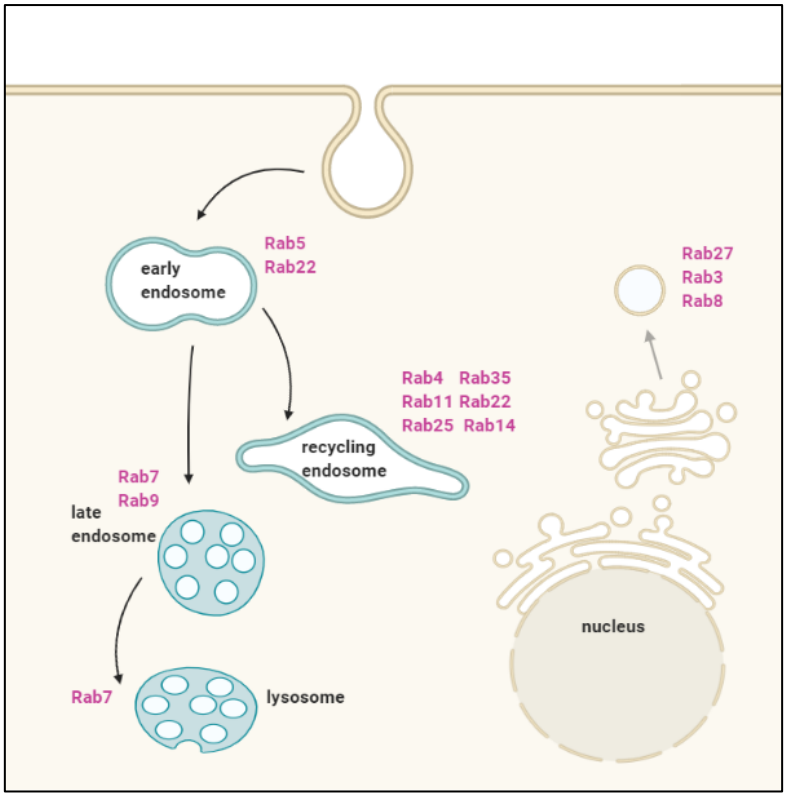

Figure 1-6: The localisation of several mammalian Rab proteins (Created with BioRender.com).

1.4 AQP trafficking

The translocation mechanisms of the 13 human AQPs have been described to varying degrees. The most well-understood is that of AQP2, which is found in the kidney and is triggered by vasopressin, however, several other triggers of AQPs are known (Table 2).

Table 2: A summary of triggers and molecules implicated in the mechanisms of AQP regulation (Markou *et al.*, 2022).

AQP	Regulation	Trigger(s)	Molecules implicated in the mechanism(s)
AQP0	Gating	pH	PKA, PKC, calmodulin, Ca^{2+}
AQP1	Trafficking, gating	secretin, hypotonicity, hypertonicity	PKA, PKC, cGMP, cAMP, Ca^{2+}, calmodulin, actin, microtubules, TRP channels
AQP2	Trafficking	vasopressin, hypertonicity	PKA, AKAPs, actin, TM5b, Arp2/3

AQP	Regulation	Trigger(s)	Molecules implicated in the mechanism(s)
AQP3	Trafficking	adrenaline, hypotonicity, hypertonicity	PKA, PKC, RalA, PI3K/Akt/mTOR
AQP4	Trafficking	vasopressin, histamine, glutamate, hypotonicity, hypoxia	PKA, PKC, PKG, ERK, p38-MAPK, actin, TRP channels, Ca^{2+}, calmodulin
AQP5	Trafficking	adrenaline, acetylcholine, hypotonicity	PKA, PKG, cAMP, Ca^{2+}, actin, microtubules, TRP channels
AQP6	Gating	pH	–
AQP7	Trafficking	lipolytic stimuli	PKA, PLIN1
AQP8	Trafficking	glucagon	cAMP, PKA, PI3K, microtubules
AQP9	Trafficking	unknown	PKA, PKC
AQP10	Trafficking	lipogenic stimuli, lipolytic stimuli	unknown
AQP11	Trafficking	unknown	unknown
AQP12	Trafficking	unknown	unknown

The translocation mechanisms broadly seem to share a number of similar characteristics. The trafficking of most AQPs in vesicles from the cytoplasm to the plasma membrane is a common one, following the synthesis of the protein. The protein can then remain inserted in the membrane, or will be present in vesicles that can be triggered, with different mechanisms as seen in Table 2, to reach the plasma membrane. The opposite movement, internalisation of the AQPs, has been shown to be either clathrin-dependent or clathrin-independent, which is something to be examined in the context of AQP4 in this thesis. The mechanisms of AQP0-5 are the most well-described (Markou et al., 2022). The cell-specific expression of the AQP family does not fundamentally alter the relocalisation to the plasma membrane or the endocytosis of the proteins. These mechanisms have broadly been described as involving the activation of a protein kinase, and the remodelling of the cytoskeleton to aid the targeting of the AQP either to the plasma membrane or from the plasma membrane. The added element of polarized AQP expression that is seen in a number of the water channels is also something to consider when examining the trafficking. The studies that contributed to the formation of

Table 2 may not have all been in cultures that accurately represent what is seen *in vivo*. Finally, AQP0, 1, 4 and 5 all show to have calmodulin (CaM) and calcium implicated in the trafficking mechanism. It has also been shown that AQP4 directly binds to CaM, and this is true of several other AQPs, the molecular mechanism is not fully understood (Kitchen et al., 2020).

1.4.1 AQP4 trafficking

AQP4 plays an important role in water transport in the brain and is an integral part of the formation of cytotoxic oedema following TBI or stroke. The animal studies published have shown that a reduction of the protein has a significant impact on oedema formation and a reduction in AQP4 number at the surface membrane leads to a much better outcome.

The trafficking mechanism of AQP4 has been shown to be CaM-dependent (figure 1-7). Triggered by changes to the extracellular environment, Ca^{2+} ions enter the cell via the TRPV4 channels and bind to CaM. Once activated, CaM binds directly to AQP4, as well as activating PKA through cyclic AMP which leads to phosphorylation of AQP4 and its subsequent translocation to the plasma membrane (Kitchen et al., 2020). The trafficking of AQP4 has been shown to depend on the polarization of the cell. A study showed that in epithelial cells the C-terminus of the AQP4 protein was the key determinant of the movement in endocytosis (Madrid et al., 2001). Additionally, a more recent study indicated that in astrocytes, *in vitro* so the results would need further validation, the M1 and M23 subtypes were present in diffferent compartments and in different states of activation for the astrocytes (Ciappelloni et al., 2019). This would indicate a need to use polarized models when carrying out work to address the trafficking of AQP4, but for the purpose of this thesis, this was not considered when creating the models.

1.4.2 AQP4 trafficking to the plasma membrane

It has been shown that AQP4 can relocalise to the plasma membrane in response to hypotonicity *in vitro*, both rapidly and reversibly (Kitchen et al., 2015) and AQP4 translocation has been demonstrated to involve PKA, calcium inflow and CaM activation. The calcium influx that occurs during cell swelling is due to the TRPV4 channel being activated by this – the only TRPV channel activated by hypotonic changes in the environment – and allows calcium to bind to CaM. This binding of calcium to CaM occurs through binding to EF-hand domains. CaM has 4 EF-hand domains, which consist of a 12-residue loop, and the calcium binds to residues 1,3,5,7,9 and 12. Following this, CaM undergoes a conformational change, meaning the calcium-CaM complex can bind to targets. Whilst it has been shown that CaM directly binds to AQP4, the target in the case of the AQP4 subcellular localisation pathway is adenylyl cyclase, which facilitates the catalytic conversion of ATP into cAMP through the cleavage of pyrophosphate. Then, PKA is activated by cAMP, which binds to one of the regulatory subunits

of PKA. Once this binding has happened, a conformational change occurs and the catalytic subunits of PKA are activated. This conformational change allows PKA to phosphorylate proteins through the removal of a phosphate from ATP, and the addition of that phosphate to a serine residue present on the protein it is targeting. This then allows the phosphorylated target protein to elicit a cellular response. In the case of AQP4, PKA facilitates the phosphorylation of AQP4 (Kitchen et al., 2015). This is achieved through the phosphorylation of the water channel at Ser276 by PKA, which in turn leads to an increase in AQP4 at the plasma membrane. The phosphorylation that occurs following PKA activation is most likely taking place in the late endosome. In addition to PKA, PKC has been shown to be a potential regulator of AQP4 translocation to the plasma membrane. A study conducted in *Xenopus* oocytes showed a downstream effect on AQP4 following treatment with PKC activators. Again, AQP4 was phosphorylated, although the phosphorylation site was not identified, it was most likely to be Ser180 as shown by subsequent work (Moeller et al., 2009; Zelenina et al., 2002).

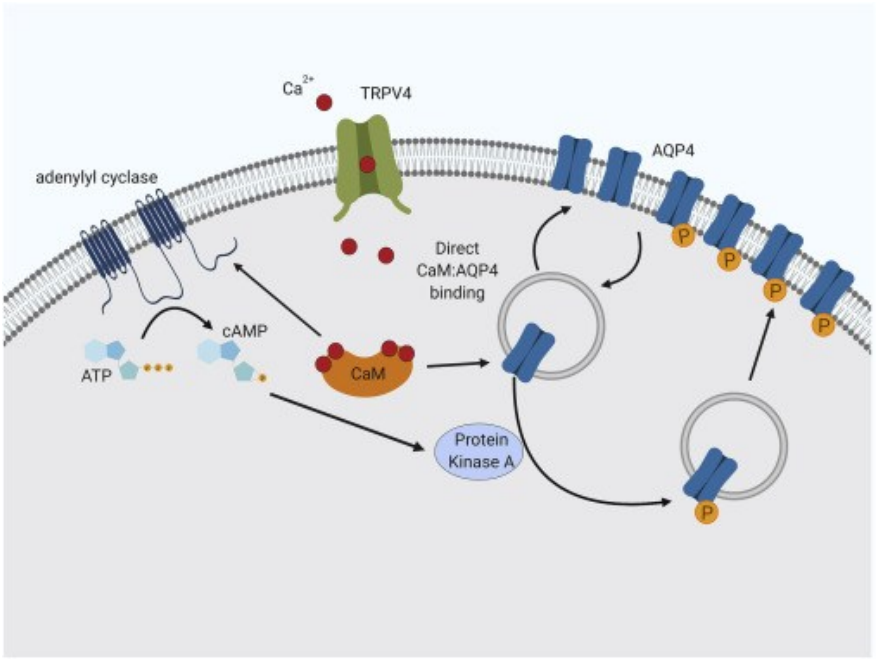

Figure 1-7: The trafficking mechanism of AQP4 (Kitchen et al., 2020).

Within the cytoplasm, AQP4 has been shown to be present in vesicles, and analysis of their movement indicated that the distance of the vesicle from the plasma membrane did not affect the rate or behaviour (Mazzaferri, Costantino & Lefrancois, 2013). Additionally, the rate at which the movement to the plasma membrane occurs is very similar to that of the movement from the plasma membrane.

In addition to this, the response of AQP4-carrying vesicles to changes in tonicity has been discussed in only one study, which concluded that AQP4 is transported along microtubules

(Mazzaferri *et al.* 2013). Interestingly, CKII has been described as being localized to microtubules (Lim *et al.*, 2003), but this does not fully show how AQP4 trafficking to the plasma membrane occurs, meaning a detailed understanding of the pathway has yet to be achieved.

The response of AQP4-carrying vesicles to changes in tonicity has been discussed in studies which concluded that AQP4 is transported along microtubules (Mazzaferri, Costantino & Lefrancois, 2013). More recent studies have concluded that a change in the tonicity of the local extracellular environment of cells causing them to swell (as mentioned before a key part of the mechanism of cytotoxic oedema), in combination with a protein kinase A inhibitor, prevented the translocation of AQP4 to the membrane (Kitchen et al., 2015). Other studies have shown that the knock-out of dystrophin affects the trafficking of AQP4 due to the contribution of the proteins to the polarization of the water channel (Belmaati Cherkaoui et al., 2021).

1.4.3 AQP4 trafficking from the plasma membrane

Studies in HGT1 cells have suggested that following AQP4 endocytosis and early endosome maturation, the protein is not directed for degradation, but instead is phosphorylated and subsequently recycled back to the plasma membrane (Carmosino et al., 2012). More recently, a study suggested a role of the CIE protein cav-1 in the surface expression of AQP4, with knockout studies in mice showing a decrease in cell surface expression and overall worse outcomes following stroke (Filchenko et al., 2020).

In epithelial cells, it has been shown that when degradation is the target, phosphorylation of AQP4 through CKII and clathrin-adaptors regulates the expression at the surface through endocytosis and movement to the lysosome (Madrid, 2001).

The importance of understanding the regulation of the AQP4 trafficking mechanism is vital as using it as a therapeutic target would be provide an alternative approach to current strategies. Blocking the pore completely has been shown to be possible using mercury ions (Savage & Stroud, 2007), however, this is not applicable as a therapy due to the cytotoxicity of the mercury ions. The recent description of trifluoperazine as an inhibitor of AQP4 translocation is an important step in developing a therapeutic strategy for cerebral oedema (Kitchen et al., 2020). Trifluoperazine binds CaM, leading to a conformational change in the protein's structure – from a dumbbell shape to a spherical shape – thus inhibiting enzyme binding to CaM (Vandonselaar et al., 1994). Consequently, a more detailed understanding of AQP4 trafficking is needed to evaluate its contribution to cytotoxic oedema.

To gain an understanding of how AQP4 is relocalised to the plasma membrane, a valuable starting point is the evaluation of translocation mechanisms of the other 12 human AQPs. Of

the AQP family, one of the most thoroughly characterized is AQP2. Despite similarities with other AQPs and AQP4, the selection of AQP2 was important due to this. The selection of both targets (dynamin, Rab11, Rab5, cytoskeletal elements), as well as the compounds, was made with the understanding that the AQP2 trafficking mechanism may not be as close to the AQP1 mechanism is to AQP4, but the literature available was more substantial for initial research. Additionally, AQP2 follows a polarized expression apically and subapically, and AQP4 has a polarized expression in astrocyte endfeet (Liu et al., 2023; Rice et al., 2015).

Found in the cells of the kidney's collecting duct, AQP2 translocation occurs in response to vasopressin, whereby the water channel moves to the basolateral membrane from the perinuclear region, undergoing endocytosis in Rab5-positive early endosomes; these endosomes allow AQP2 to reach the perinuclear region through transcytosis, allowing Rab11-positive recycling endosomes to transport AQP2 to the apical membrane (Takata et al., 2008; Kwon, Frøkiær & Nielsen, 2013:p.2). Consequently, these two Rab GTPases can provide a starting point for determining how membrane trafficking of AQP4 occurs. Furthermore, the translocation mechanism of several other AQPs has been described. However, the most common mechanism is that of vesicular transport, and mostly microtubule dependent.

So far, animal models have been used to attempt to understand the AQP4 relocalisation mechanism, but the conflicting results do not provide a clear picture of how the water channel is translocated. The animal studies published have shown that a reduction of AQP4 has a significant impact on oedema formation and a reduction in AQP4 number at the surface membrane leads to a much better outcome (Verkman et al., 2006).

However, the role of actin and microtubules in AQP4 trafficking has also not been fully described, and there is still little understanding of how vesicular trafficking of AQP4 occurs and the composition of those vesicles remains to be elucidated. Consequently, a more detailed description of AQP4 trafficking is needed to complete the understanding of its contribution to cytotoxic oedema. There are a number of compounds that can be used to examine the roles of the key proteins involved in membrane trafficking (Table 3).

Table 3: A summary of compounds that can be used to target membrane trafficking regulators.

Compound	Target	Action
Dynasore	Dynamin	Inhibitor
Jasplakinolide	Actin	Polymerisation enhancer
Paclitaxel	Microtubules	Stabiliser
Nocodazole	Microtubules	Polymerisation Inhibitor

Filipin	CIE	Disrupts caveolae
Cytochalasin D	Actin	Polymerisation Inhibitor

Dynasore is an inhibitor of the GTPase dynamin, needed for vesicle formation after membrane fission. The inhibitor blocks the development of these vesicles due to the dynamin being unable to function in the assembly which leads to abnormal and improperly-formed vesicles (Macia et al., 2006). Filipin disrupts the formation of caveolar structures (Schnitzer et al., 1994). Cytochalasin D inhibits the elongation phase of actin polymerisation, disrupting the formation of an organised network and instead leading to the development of filamentous aggregates (Casella, Flanagan & Lin, 1981). Nocodazole inhibits microtubule elongation, through its interaction with tubulin, and has also been shown to reduce the total number of microtubules in cells treated with the compound (Cassimeris, Wadsworth & Salmon, 1986). Jasplakinolide ensures the continuous polymerisation of F-actin in the target system (Holzinger, 2009), whereas paclitaxel stabilises microtubules through the inhibition of depolymerisation (Horwitz, 1994).

The aim of this thesis was to examine the membrane trafficking of aquaporin-4 (AQP4) and determine the key molecular players in this process. This was due to the importance of AQP4 in the CNS, both under homeostatic conditions and disease states. The already well-described trafficking of aquaporin-2 (AQP2) was used as a starting point for this, and cell lines were utilised to investigate the main trafficking pathways that were thought to be contributing to the movement of the water channel from within the cytosol to the plasma membrane. Additionally, the development of an *in vivo* model was investigated in the screening of potential membrane trafficking regulators, allowing for the faster determination of important components of the AQP4 vesicular trafficking mechanism.

Therefore, the main objectives of this thesis were to:

1. Further dissect the trafficking mechanism of AQP4 through the use of a cell-based system of HEK293 cells to determine the key players in the vesicular movement of AQP4 from inside the cell to the plasma membrane, as well as *vice versa.*
2. To demonstrate the importance of the key membrane trafficking regulators in a physiologically relevant cell-based system, human primary cortical astrocytes.
3. To determine whether or not *C. elegans* can be used as an appropriate *in vivo* model for screening potential trafficking partners of AQP4.

2 Materials and methods

2.1 Materials

2.1.1 Reagents

MELFORD, UK

- Bacto Peptone
- Sodium chloride
- Agar
- $CaCl_2$
- $MgSO_4$
- KH_2PO_4
- K_2HPO_4
- Cholesterol
- Nystatin
- Albumin Bovine Fraction V
- Glycine
- Triton X-100

SIGMA-ALDRICH, UK

- Geneticin G418
- Trypsin-EDTA
- Polyethylenimine (PEI)
- Phosphate buffered saline (PBS)
- Dulbecco's modified Eagle's medium (DMEM)
- Luminol
- p-Coumaric acid
- Ammonium persulfate (APS)
- GenElute™ Plasmid Midiprep Kit
- OPD – SigmaFast tablet set
- Anti-Actin Antibody, clone JLA20 mouse antibody
- MOWIOL mounting medium

THERMO-FISHER, UK

- Dimethyl sulfoxide (DMSO)
- EZ-Link Sulfo-NHS-SS-Biotin
- Neutravidin-coated high binding capacity 96-well plate

ABCAM, UK

- Dynasore
- Jasplakinolide
- Cytochalasin D
- Nocodazole
- Paclitaxel
- Filipin
- Anti-Aquaporin 4 rabbit antibody

CELL SIGNALING TECHNOLOGY

- Anti-rabbit IgG, HRP-linked antibody
- Anti-GFP rabbit antibody

SCIENCELL

- Astrocyte medium (AM)
- Astrocyte growth serum

2.1.2 Cell lines

- HEK293T (ATCC, USA)
- Human astrocytes (Sciencell, USA)
- *E. coli* OP50 (CGC, USA)

2.1.3 Worm strains

- RT2059 unc-119(ed3);pwIs716[pPD95.75-aqp-4], referred to as GFP-AQP-4 (CGC, USA)
- RT130 unc-119 (ed3);pwIs23 [vit-2::rfp], referred to as YP170 (CGC, USA)

2.1.4 Plasmids

- mCherry-Rab5a-7 (Addgene, USA)
- mCherry-Rab11a-7 (Addgene, USA)
- DsRed-rab11 DN was a gift from Richard Pagano (Addgene plasmid # 12680 ; http://n2t.net/addgene:12680 ; RRID:Addgene_12680)

- mCherry-Rab5DN(S34N) was a gift from Sergio Grinstein (Addgene plasmid # 35139; http://n2t.net/addgene:35139 ; RRID:Addgene_35139)

- CellLight LifeAct-RFP (Thermo Fisher Scientific, UK)
- Human AQP4 cloned into mammalian expression vector pDEST47 (Invitrogen)

2.1.5 Equipment

- Haemocytometer (Camlab Ltd, UK)
- Inverted fluorescence microscope (Zeiss Axiovert 200M, UK)
- Confocal microscope (SP8 TCS by Leica Microsystems, Germany)
- Mr. Frosty™ Freezing Container (Thermo Fisher Scientific, UK)
- EI800 BioTek plate reader (BioTek Instruments, UK)
- Multiskan Go plate reader (Thermo Fisher Scientific, UK)
- Nano drop spectrophotometer (Thermo Fisher Scientific, UK)
- Centrifuge 5418 (Eppendorf, Germany)
- Neutravidin Coated High Binding Capacity (HBC) Clear 96-Well Plates with SuperBlock Blocking Buffer (Thermo Fisher Scientific, UK).

2.1.6 Software

- ImageJ 1.53q (NIH, USA)
- GraphPad Prism 6.01 (GraphPad Software Inc., USA)

2.2 Methods

2.2.1 Freezing & thawing cells

Cells were centrifuged at 300xg and resuspended in a freezing medium made up of 5% (v/v) DMSO in foetal bovine serum (FBS) in cryovials. Cells were frozen using a Mr. Frosty™ Freezing Container and stored at -80°C for up to 5 days and then transferred to liquid nitrogen storage. When cells were needed, the cryovial was placed in a 37°C bead bath and thawed suspension was then transferred dropwise to a 15ml falcon tube containing prewarmed 7ml DMEM. Cells were pelleted at 300xg, the supernatant removed, and the pellet resuspended in prewarmed DMEM. Cells were transferred to a T25 flask and then grown in a 37°C incubator with 5% CO_2.

2.2.2 HEK293

Human embryonic kidney 293 (HEK293) cells were purchased from ATCC. Cells were cultured in DMEM supplemented with 10% FBS, penicillin (100 units/ml) and streptomycin (100 µg/ml) and L-glutamine (6 mM). Before use, DMEM was warmed to 37°C. Subculturing of cells was carried out by washing once with phosphate buffered saline (PBS) and trypsinizing (0.25%) at 37°C to detach cells from the flask surface. Cells were grown in a 37°C incubator with 5% CO_2.

2.2.3 Human primary astrocytes

Human cortical astrocytes at p1 following purchase from Sciencell were a gift from Dr Phil Kitchen. The cells were frozen in liquid nitrogen, and these were used as stocks for experimental work from p1 to p5. Cells were cultured in Astrocyte Medium (AM) (Sciencell, CA, USA), supplemented with 2% FBS, 1% Astrocyte Growth Supplement and 1% Penicillin/streptomycin solution. Before use, AM was warmed to 37°C. Subculturing of cells was carried out by washing once with phosphate buffered saline (PBS) and accutase at room temperature was used to detach cells from the flask surface. Cells were grown in a 37°C incubator with 5% CO_2.

2.3 Transient transfection

2.3.1 Transient transfection with PEI

A mixture containing 50µl serum-free DMEM, 1mg DNA and 12µl of 1mg/mL PEI in dH_2O was vortexed for 15 seconds and incubated at room temperature for 10 minutes. This was added to 300µl of DMEM with serum. Cell culture medium was removed from the plates and the transfection mixture was pipetted dropwise onto the cells grown in 35mm dishes. The cells were incubated for 3 hours, then 2mL DMEM with serum was added and the plates were returned to the incubator at 37°C for 24-hours.

2.3.2 Setting up cells for confocal microscopy

Cells were either grown on coverslips in 6-well plates or in 35mm fluorodishes and transfected with the plasmids when they had reached 60% confluency. After 24-hours the coverslips were mounted on slides using Mowiol solution and were then imaged on a Leica SPS with a 63x 1.4 oil immersion lens. The following laser lines were used for excitation of the fluorophores: 488nm and 594nm. The images of each channel were taken sequentially, to reduce overlap.

2.3.3 Live imaging of GFP-AQP4

The live cells were placed on a temperature-controlled stage and imaged after 90 seconds on a Zeiss Axiovert. Following this, a 3:1 mixture of water:DMEM replaced the DMEM and images were taken after 5 minutes. Finally, the hypotonic solution was replaced with DMEM and cells were imaged again after 5 minutes.

2.3.4 AQP4 translocation in the presence of selected compounds

In experiments where compounds were present, following the addition of each compound, the live cells were imaged as described above, with the concentrations and incubation times being

used as shown in Table 1. These were determined based on literature searches to establish optimal timepoints and concentrations.

Table 1: Compounds used to target membrane trafficking regulators, concentration used, and incubation time needed.

Compound	Conc (μM)	Incubation time (min)
Dynasore	80	30
Jasplakinolide	0.15	30
Paclitaxel	0.05	20
Nocodazole	30	45
Filipin	15	45
Cytochalasin D	5	45

2.3.5 Cell viability

Cell viability was assessed both by routine observation of morphology and by MTT assay. Cells were grown in 96-well plates in either DMEM or AM and incubated at different times with each compound according to table 1. A total of 20μl MTT (25mg/ml) was added to each well containing cells at a final concentration of 0.5mg/ml. Following an incubation of 2 hours at 37°C, the MTT was solubilized by adding 100μl acidified isopropyl alcohol (0.04N HCl). Following a 15-minute extraction at room temperature, plates were read on a spectrophotometer at 570nm.

2.3.6 Colocalisation Analysis

In order to examine the colocalisation, two methods of analysis were used: Pearson's correlation coefficient (PCC) and Mander's colocalisation coefficients, M1 and M2. The JaCoP plugin in ImageJ was used to analyze these images and calculate the two coefficients. The following formulae were applied in order to calculate PCC and M1 and M2, respectively:

$$r_p = \frac{\sum_i (A_i - a) \times (B_i - b)}{\sqrt{\sum_i (A_i - a)^2 \times \sum_i (B_i - b)^2}}$$

$$M_1 = \frac{\sum_i A_{i,coloc}}{\sum A_i} \quad with \quad A_{i,coloc} = A_i, if B_i > 0$$

$$M_2 = \frac{\sum_i B_{i,coloc}}{\sum B_i} \quad with \quad B_{i,coloc} = B_i, if A_i > 0$$

The use of these two coefficients gave rise to two different sets of information. The PCC gives an indication of whether the two proteins are associated within the same area and the strength of this association. A value of -1 shows no correlation and that the two proteins are present in the completely opposite space; a value of 0 shows no correlation and the two proteins are present in random spaces and a value of +1 shows perfect correlation, with the two proteins present in the same space. The M1 and M2 coefficients give an indication of co-occurrence, or, in other words, colocalisation. This is calculated by adding the fluorescence intensity of the pixels of the two channels and then dividing that by the integrated density of the pixels. A value of 0 shows that there is no colocalisation and a value of 1 shows there is complete colocalisation. This method measures only the pixels that are covered by both signals.

2.3.7 Relative Membrane Expression

Live cell images were analysed in ImageJ through the measurement of intensity profiles across each cell. Relative membrane expression (RME) was calculated as previously described (Conner *et al.*, 2010). Briefly, each line was drawn across the cell, from the extracellular space on one side to another, avoiding the nucleus. The average membrane intensity was calculated as the mean of the membrane peaks, and intracellular intensity as the average between the two peaks. The background was calculated as the mean of the extracellular pixels on either side of the membrane peaks and was subtracted from peak and intracellular intensity values. The RME was then calculated by dividing the membrane intensity by the total intensity at both peaks and internally. Each experimental repeat consisted of 3 profiles of at least 10 cells in each repeat.

An example calculation:

Background	*Mean 1st peak (minus background)*	*Mean 2nd peak (minus background)*	*Mean intracellular (minus background)*
11.168	*12.485*	*14.723*	*35.266*

Sum of both peaks	*Total intensity (1st + 2nd + intracellular)*	*RME (sum of both peaks divided by total intensity)*
27.208	*62.474*	*0.435509*

2.3.8 Cell surface biotinylation

Human astrocytes were plated in 48-well plates 24-hours before the experiment. The cells were placed in DMEM or DMEM diluted with dH_2O (in a ratio of 1:3)– both of these conditions also included each inhibitor and activator at the concentrations described in Table 1. Following

incubation, as described in Table 1, the plates were placed on ice and each well was washed 5 times by removing 375µl of the media and replacing with 375µl ice-cold PBS or PBS diluted to the same tonicity as the DMEM. The cells were then incubated on ice for 30 minutes with 600µl of EZ-Link Sulfo-NHS-SS-Biotin in PBS at the same tonicity as in previous steps. Following this, the quenching solution (25mM glycine in PBS) was added 3 times for 5 minutes. The cells were then lysed on ice for 45 minutes in Tris-Triton lysis buffer (1% v/v triton X-100, 100 mM NaCl, 2 mM $MgCl_2$, 25 mM Tris pH 7.4). Cell lysates were transferred to 1.5mL Eppendorf tubes and centrifuged at 4°C for 10 minutes at 20,000xg and then 100µl of supernatant were added to neutravidin-coated high binding capacity 96-well plates and were incubated at 4°C for 2 hours. The plates were then washed with 100µl 0.05% PBS-Tween and blocked for 1 hour in 100µl 3% w/v BSA in PBS at room temperature on an orbital shaker. Following this, plates were incubated with 100µl AQP4 antibody (Abcam, ab128906) diluted 1:2000 in 0.05% v/v PBS-Tween overnight at 4°C. The plates were then washed with 100µl 0.05% v/v PBS-Tween and incubated with 100µl HRP-conjugated secondary antibody for 1 hour at room temperature. Finally, plates were washed with 100µl 0.05% v/v PBS-Tween 3 times for 5 minutes and incubated with 100µl OPD HRP substrate for 45 minutes at room temperature, wrapped in foil to avoid exposure to light. Absorbance was read at 450nm.

2.4 *C. elegans* maintenance

C. elegans strains were maintained on plates with nematode growth medium (NGM), 500ml of which was made using 1.25g of Bacto Peptone, 1.5g of NaCl and 8.5g of agar dissolved in 487.5ml distilled water and autoclaved. Following autoclaving, 500µl of 1M $CaCl_2$, 500µl of 1M $MgSO_4$, 12.5ml of 1M KPO_4, 500µl of 5mg/ml cholesterol in ethanol and 500µl of nystatin (10mg/ml in DMSO) were added. Plates were seeded with an overnight culture of *E. coli* OP50, which was dried at room temperature to form a lawn and incubated at 20°C.

2.5 Incubation of *C. elegans* on NGM plates with different tonicities

Worms at L4 stage were transferred from NGM plates with 53mM NaCl to NGM plates containing 100mM and 400mM NaCl and agar plates. Worms were left on the different plates and collected and imaged after 24 and 48-hours.

2.6 Sodium Dodecyl Sulphate Polyacrylamide Gel Electrophoresis (SDS-PAGE)

SDS-PAGE gels were created with the two components, the stacking phase (6%) and the separating phase (10%) (Table 2) responsible for concentrating the proteins and separating the proteins depending on both molecular weight and charge, respectively.

The gels were polymerised using tetramethylenediamine (TEMED) and added to the sealed plates; a comb was placed for well formation and the gels were left to set.

Table 2: Composition of the stacking phase and separating phase of the gel.

Gel	H_2O	Tris	Sucrose	Acrylamide	SDS	APS
Stacking (6%)	1.6ml	0.8ml (0.5M, pH 6.8)	-----	0.5ml (40%)	33µl (10%)	20µl (10%)
Separating (10%)	4.4ml	1.7ml (1.5M, pH 8.8)	1.1ml (60%)	2.7µl (40%)	67µl (10%)	50µl (10%)

The samples were prepared in the following manner: 20 worms were added to a lysis buffer (100mM Tris @ pH 6.8, 8% SDS and 1% β-mercaptoethanol), incubated at 37°C for an hour and mixed with 2X Laemmli buffer (20% glycerol, 0.004% bromophenol blue, 4% SDS, 0.125 M Tris HCl and 10% 2-mercaptoethanol) and loaded onto the polyacrylamide gel. A prestained protein standard (New England Biolabs, Hitchin, UK) was also added to one of the wells and the gel was run at 100V for 15 minutes then 150V for 45 minutes in SDS running buffer, until the resolution of the bands was adequate.

2.7 Western Blotting

Following SDS-PAGE, the gel containing the proteins was added to a cassette and a transfer sandwich was created with sponge, Whatman filter paper and a nitrocellulose membrane. The cassette was added to a tank filled with buffer (25mM Tris, 200mM glycine and 20% (v/v) Methanol) and transfer was carried out at 200mA for 2 hours as described previously (Yang, Liu and Mahmood, 2014). The membrane was then incubated in 3% (w/v) bovine serum albumin (BSA) in 1x phosphate-buffered saline (PBS) blocking solution at room temperature for 1 hour and then incubated overnight in a 1:1000 dilution of anti-GFP primary antibody in blocking solution in PBS containing 3% (w/v) BSA and 0.05% (v/v) Tween-20 at 4°C. The membrane was then washed in PBS Tween for 2 minutes, 4 minutes and then 15 minutes at room temperature and the PBS Tween was then replaced with a solution containing 1:2000 dilution of anti-rabbit HRP-linked secondary antibody in a solution containing 3% (w/v) BSA and 0.05% (v/v) Tween-20 for 2 hours. The membrane was then washed again in PBS-T for 2 minutes, 4 minutes and then 15 minutes at room temperature and then washed for one final time in PBS for 20 minutes. Finally, the membrane was incubated with an enzyme substrate (1M Tris pH 8.5, 50 mM coumaric acid, 250 mM luminol and 30% $H_2O_{2)}$ and were either

exposed on an X-ray film in a dark room and bands were visualised using developer and fixer, or visualised using G:box (Syngene, Cambridge, UK).

2.8 RNAi

RNAi knockdown to investigate a loss-of-function phenotype in *C. elegans* can be carried out by feeding (Balklava and Sztul, 2013). The bacteria that are fed to the worms express dsRNA for the genes of interest. The gene of interest is amplified by PCR and cloned in an L4440 vector between two inverted T7 promoters. The *E. coli* are RNAse III deficient and have an IPTG inducible T7 polymerase. When the RNAi is performed, the worms feed on the bacteria the dsRNA is cleaved and forms siRNA, which then recognises and cleaves complementary mRNA leading to no protein expression.

Each clone was used to inoculate 3ml LB containing 100µg/ml ampicillin and seeded onto NGM Lite agar plates, 500mL of which was made using 1.0g NaCl, 2.0g Bactotryptone, 1.5g KH_2PO_4, 0.25g K_2HPO_4, in 500ml distilled water and autoclaved. Following autoclaving, 500µl of 1M $CaCl_2$, 500µl of 1M $MgSO_4$, 1M IPTG, 500µl of cholesterol and 500µl of nystatin were added. The plates were left overnight for induction and then L4 stage worms were added to the plates and incubated at 20^{o}C for 24-hours.

2.9 Dissection

C.elegans were maintained on NGM agar. Synchronised L4 stage worms were dissected using needles under a dissecting scope in dissection buffer containing 5%(w/v) sucrose and different concentrations of NaCl (0mM, 53mM, 100mM, 400mM) with 0.1M levamisole, diluted down in water to 0.5M for 10 minutes, fixed in dissection buffer containing 1.5% paraformaldehyde (PFA) for 10 minutes and washed with PTC (0.1% BSA, 1XPBS, 0.1%Tween-20,1mM EDTA) for 30 minutes, 4 times.

2.10 Microscopy and Image Analysis

A wide-field fluorescence microscope was used to image the samples (10 worms imaged per condition) using a 63x objective. Images were analysed using ImageJ software. The apical membrane area of GFP expression was measured using the mean grey value of the pixels.

2.11 Statistical Analysis

All results were added to Microsoft Excel and analysed in GraphPad using a one-way analysis of variance (ANOVA) multiple comparison and a *p*-value of <0.05 was used as a threshold for results that were considered to be statistically significant. The post-hoc test chosen for each

dataset was Tukey's. An ANOVA was selected as the most appropriate statistical test, due to the requirement that the datasets contained three or more means. Any *p*-value of <0.05 was an indication that the means of the groups were not all equal, however a post hoc test was need to examine the differences between these means. Tukey's was selected in order to minimise the experiment-wise error rate. Tukey's allows for the comparison of the means of each group, showed which results were truly statistically significant, and which results were false positives (Stoll, 2017). The *p*-values presented in the following results chapters were all obtained using an ANOVA, then Tukey's post hoc test, and are the adjusted *p*-values.

3. Results - Investigating AQP4 trafficking mechanisms in HEK293 cells

The main objective of this chapter was to investigate the role of Rab5, Rab11, dynamin and the cytoskeleton in the vesicular trafficking of AQP4 (Figure 3-0).

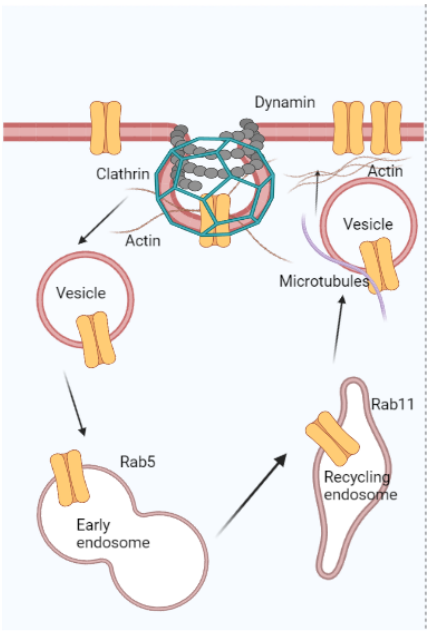

Figure 3-0: The location of Rab5, Rab11, dynamin, actin and microtubules in vesicular trafficking (Created with Biorender.com).

These were selected as the most likely candidates to be involved in the internalisation and recycling of AQP4, based on the reported membrane trafficking partners of AQP2 (Barile et al., 2005). The selected cell system, HEK293, was used due to previous studies demonstrating that AQP4 translocation occurs in these cells when transfected (Kitchen et al., 2015). HEK293 are also more cost-effective to maintain and transfect and can grow at a faster rate than primary cells. The experimental strategy used in this chapter was the co-transfection of mCherry-Rab5 and mCherry-Rab11 with AQP4-eGFP in HEK293 cells first under isotonic conditions in order to determine whether AQP4 is localised on Rab5-positive early endosomes and Rab11-positive recycling endosomes, as shown previously with AQP2 (Barile et al., 2005). Hypotonicity was used as a trigger for the translocation of AQP4 to the plasma membrane in the same cells. In these experiments, the role of the early endosome and recycling endosome in AQP4 translocation was determined by the inhibition of trafficking at the early endosome and recycling endosome. Co-transfection with dominant negative Rab5 and Rab11 was used to mimic a knockdown effect and to examine the role of Rab5 and Rab11 in the relocalisation of AQP4. Finally, a range of drugs to target different steps of membrane trafficking were used to treat HEK293 cells in order to elucidate which of these could play a role in the internalisation and recycling of AQP4.

3.1 Optimisation of transient transfection

Transient transfection is used to deliver plasmid DNA – containing the gene of interest – in an effective manner. A number of delivery systems have been described, however, polyethylenimine (PEI) was used for the experiments described in this chapter because it is a cost-effective and simple way to carry out this process.

To deliver plasmid DNA into mammalian cells, the polycationic PEI is mixed with anionic DNA to form a complex which can be introduced into cells. The PEI acts as a “proton sponge”, eventually leading to the avoidance of lysosomal degradation and endosomal rupture (Akinc et al., 2005; Boussif et al., 1995). In this case, branched PEI was used instead of linear. Whilst linear PEI usually is less cytotoxic, the branched PEI is more efficient for binding with nucleic acids (Zakeri et al., 2018).

As suggested in previous literature, the PEI to DNA ratio was evaluated before the final concentration to be used in the experimental setup was decided (Longo et al., 2013). A selection of ratios of PEI to DNA was made (Table 1). Images of the transiently transfected HEK293 cells were taken on an epifluorescence microscope, using the green and red fluorescence channels. The data indicated that there were areas of apparent overexpression in the PEI:DNA ratios 1:1, 3:1 and 4:1 (Figure 3-1). In others, mainly 5:1 and 6:1, there was a range of expression, but with minimal overexpression, potentially due to the size of the complexes formed between PEI and DNA and both were identified as the optimal example of transfection reagents and ratio to use. It was crucial to determine the optimal ratio for further fluorescence quantification analysis.

Table 1: Ratios of PEI:DNA used and the corresponding transfection efficiencies for each of these.

PEI 1mg/ml (µl)	DNA (µg)	PEI:DNA	Efficiency
6	1	6:1	74%
5	1	5:1	72%
4	1	4:1	62%
3	1	3:1	65%
2	1	2:1	68%
1	1	1:1	61%

Additionally, transfection efficiencies were calculated for each ratio (Table 1), indicating that for the ratio 6:1, the transfection efficiency was also at an appropriate level, so this was the one used for all subsequent experiments.

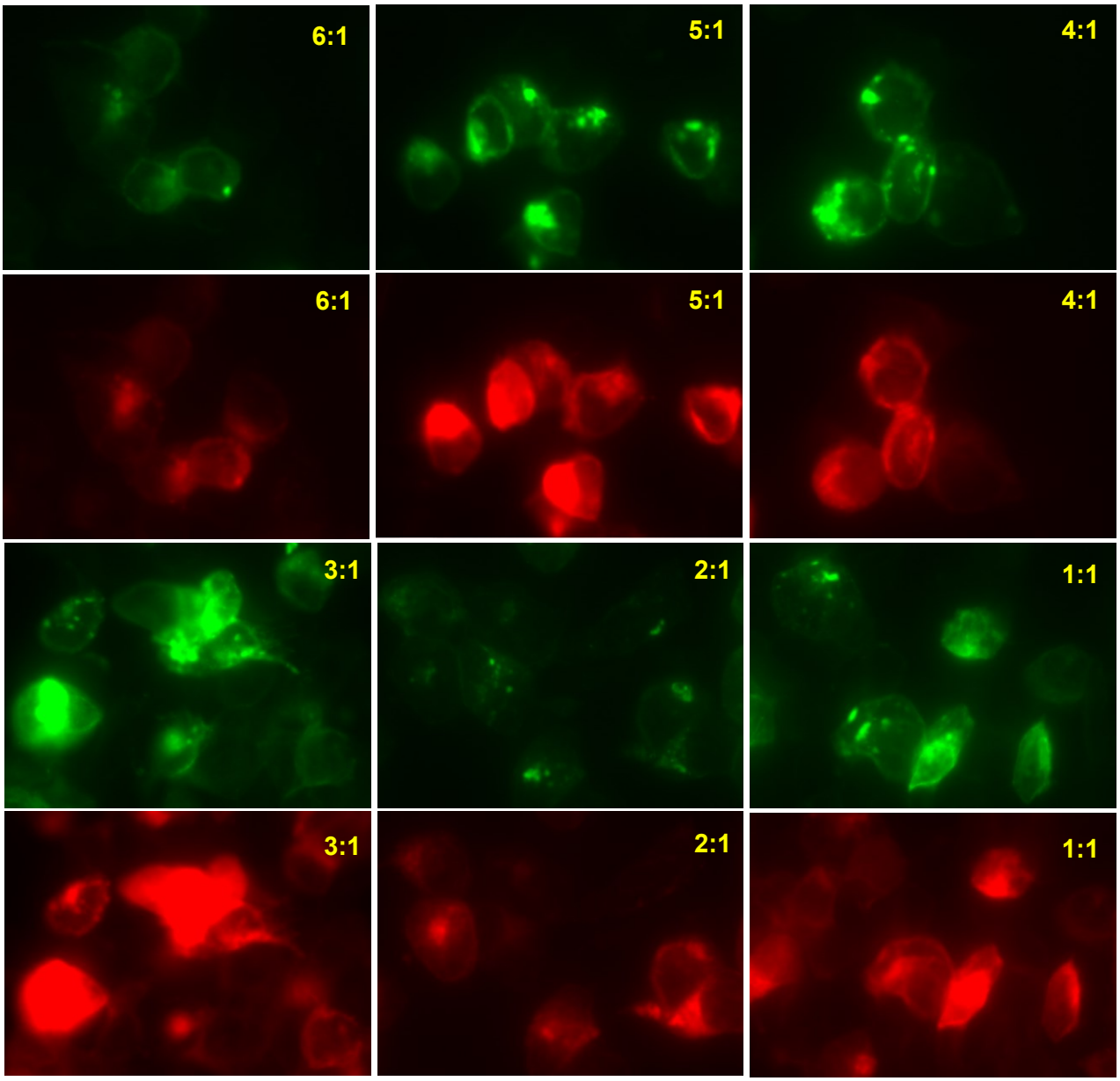

Figure 3-1: Optimisation of transfection efficiency in HEK293 cells. Representative images of the ratios of PEI:DNA used. Green (AQP4-eGFP) and red (mCherry-Rab5) channel pairs starting clockwise from top left: 6:1, 5:1, 4:1, 3:1, 2:1, 1:1.

3.1.1 AQP4-eGFP colocalizes with mCherry-Rab5 and mCherry-Rab11 in HEK293 cells

It has been shown previously that AQP2 can be found in Rab5-positive and Rab11-positive vesicles (Barile et al., 2005). Here, the hypothesis that these proteins play a role in AQP4 relocalisation was tested. To examine this relationship, the first step was to determine whether AQP4 colocalises with each Rab (Figure 3-2). Images were taken as described in Chapter 2, section 2.2.3.

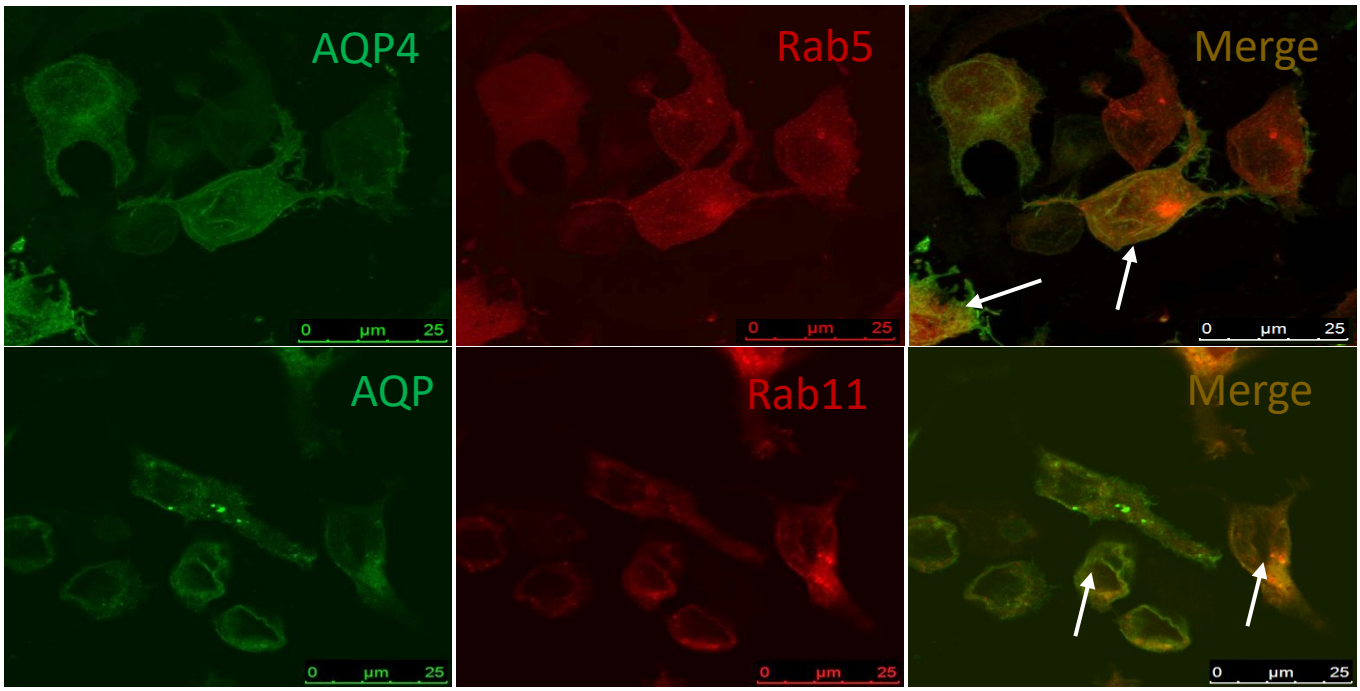

Figure 3-2: Colocalisation of AQP4 with Rab5 and Rab11 in HEK293 cells. Representative confocal images of HEK293 cells transiently transfected with AQP4-eGFP (green), mCherry-Rab5 or mCherry-Rab11 (red) and the merged images (yellow). Images of each channel were taken sequentially at 63x magnification. The localisation of AQP4-eGFP and mCherry-Rab5 overlaps in many areas (white arrows), as does the localisation of AQP4-eGFP and mCherry-Rab11 (white arrows). The scale bar is 25 µm.

The colocalisation and correlation of AQP4 with Rab5 and Rab11 were measured using the method mentioned in Chapter 2, section 2.3.6. The PCC of AQP4-eGFP and mCherry-Rab5 was found to be approximately 0.8 (Figure 3-3 A, B), which showed that the correlation between the two proteins was high. This indicates that the AQP4-eGFP and mCherry-Rab5 proteins strongly associate in the same space. However, the correlation of both proteins did not mean that colocalisation was 100%. Similar to this, AQP4-eGFP and mCherry-Rab11 had a PCC of approximately 0.77 (Figure 3-3A, B), which indicated a strong association between the two proteins. To ensure the accuracy of results, analysis was carried out in two ways - on selected cells (Figure 3-3B), and on whole images (Figure 3-3A). These results showed similar values, indicating that both methods were appropriate for quantification.

Following this, the colocalisation was examined with the calculation of M1 and M2, as described in Chapter 2, section 2.3.6 (Figure 3-3C). The M1 value for AQP4-eGFP and mCherry-Rab5 was 0.63 and the M2 was 0.55, showing that where AQP4-eGFP was present, mCherry-Rab5 overlapped in 63% of the pixels and where mCherry-Rab5 was present, AQP4-eGFP overlapped in 55% of the pixels. The M1 value for AQP4-eGFP and mCherry-Rab11 was 0.65 and the M2 was 0.50, showing that where AQP4-eGFP was present, mCherry-

Rab11 overlapped in 65% of the pixels and where mCherry-Rab11 was present, AQP4-eGFP overlapped in 50% of the pixels.

These results demonstrate that approximately 60% of Rab5-positive and Rab11-positive vesicles contain AQP4 and approximetaly 50% of AQP4 localizes with Rab5-positive and Rab11-positive vesicles.

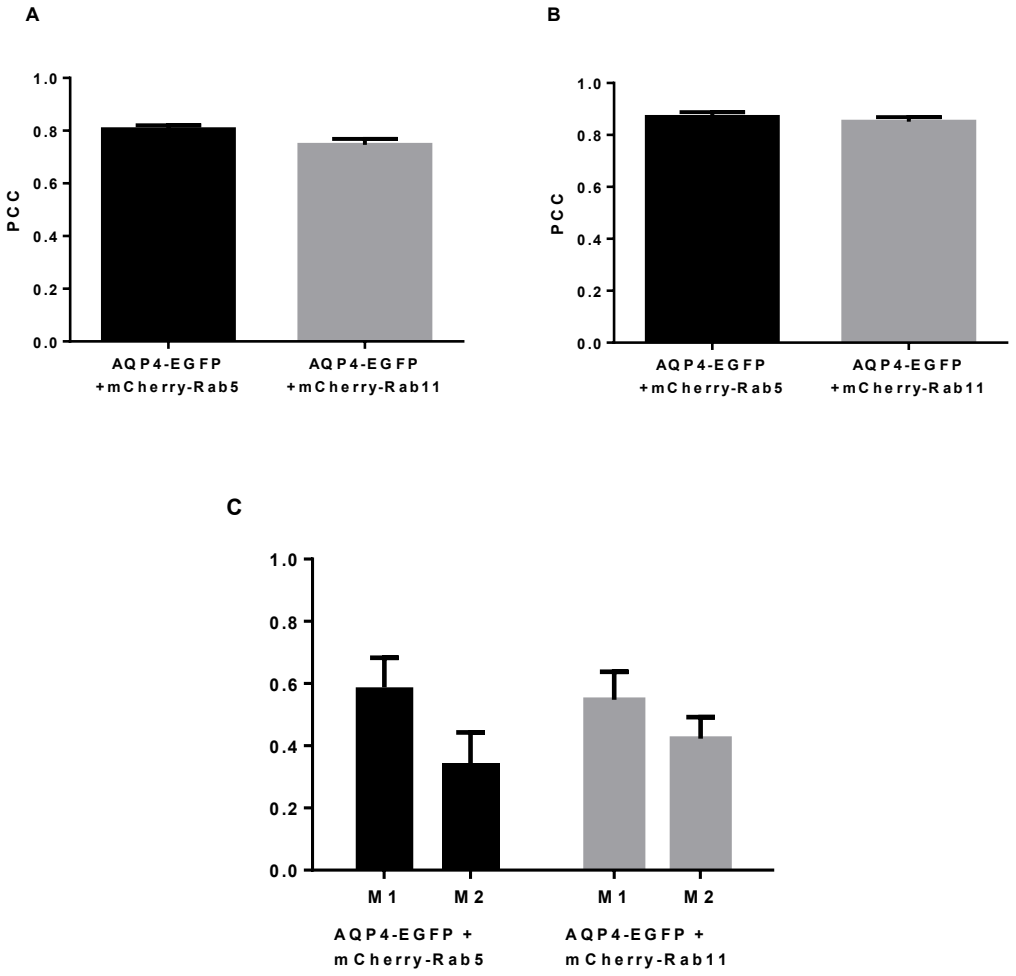

Figure 3-3: Quantification of AQP4 colocalisation with Rab5 and Rab11. Correlation in whole cells (A) and selected cells (B) and co-occurrence in selected cells (C) of AQP4-eGFP with mCherry-Rab5 and colocalisation of AQP4-eGFP with mCherry-Rab11 (C). The correlation of AQP4-eGFP with mCherry-Rab5 and mCherry-Rab11 was high (>0.7), showing that the green and red pixels were in the same space of the images. The M1 ratios of co-occurrence of AQP4-eGFP with mCherry-Rab5 and mCherry-Rab11 were high (>0.5), showing that red pixels were present in over half of the spaces where green pixels were. The M2 ratios of co-occurrence of AQP4-GFP with mCherry-Rab5 and mCherry-Rab11 were high (>0.5), showing that green pixels were present in over half of the spaces where red pixels were.

3.1.2 AQP2-GFP colocalizes with mCherry-Rab5 and mCherry-Rab11 in HEK293 cells

The localisation of AQP2-GFP in HEK293 cells has been shown previously, and there has been evidence presented to show that *in vivo* in rat inner medullary collecting duct cells, and *in vitro* in MDCK cells, AQP2 is present in Rab5-positive vesicles and Rab11-positive vesicles, suggesting a role of these in the trafficking of AQP2 (Yui *et al.*, 2013). A more recent description of AQP2 trafficking suggests that the water channel, once internalised is seen in the early endosome that is Rab5-positive, which then matures, and finally joins Rab11-positive recycling endosomes (Wang *et al.*, 2020). As this was the starting point for investigating the relationship between the two Rabs, confocal microscopy was used to confirm the colocalisation of transiently transfected AQP2-GFP with mCherry-Rab5 and mCherry-Rab11 in the HEK293 experimental model.

The images taken of AQP2-GFP (Figure 3-4A and D) show that, in isotonic conditions, it is localised in the cytoplasm. The same can be seen in the images of mCherry-Rab5 and mCherry-Rab11, which show a punctate distribution within the cytoplasm under isotonic conditions.

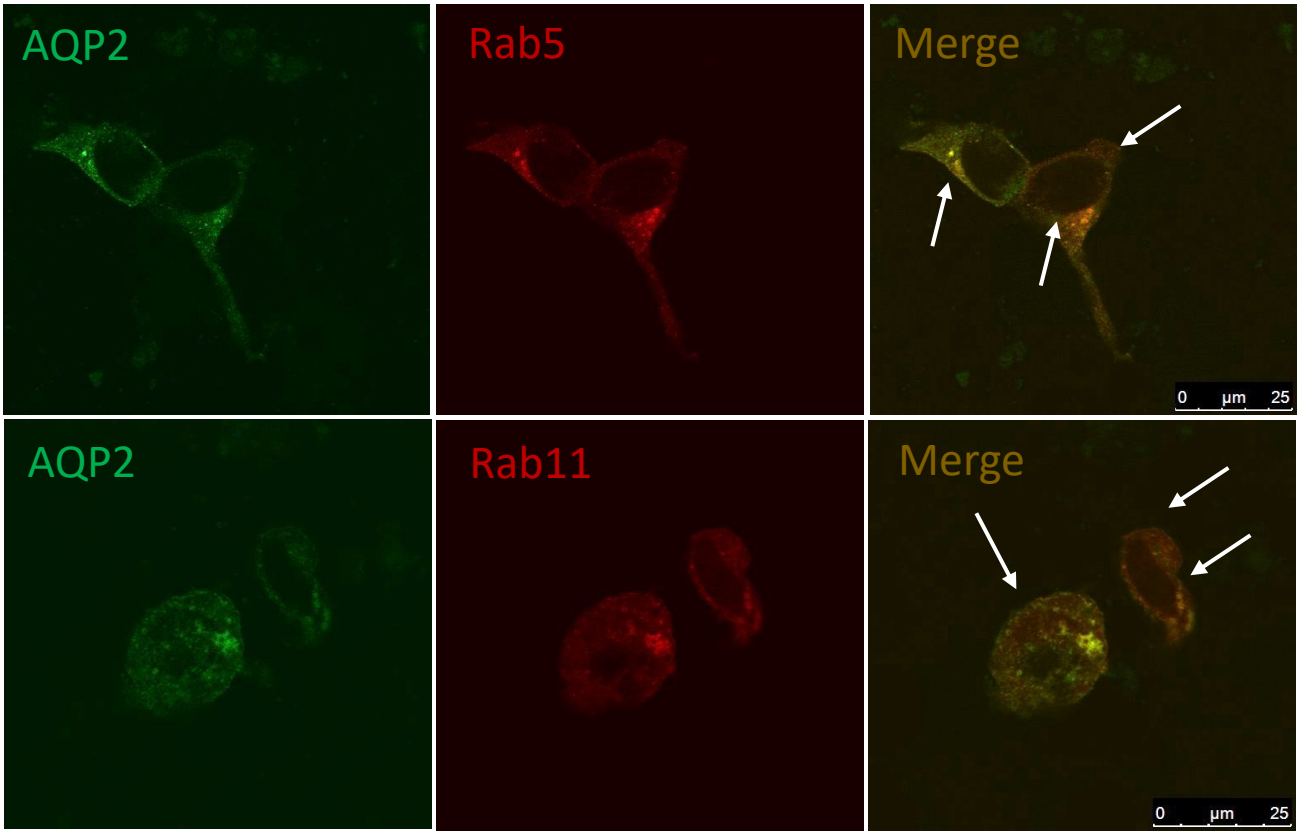

Figure 3-4: Colocalisation of AQP2 with Rab5 and Rab11 in HEK293 cells. Representative confocal images of HEK293 transfected with AQP2-GFP (green), mCherry-Rab5/mCherry-Rab11 (red) and the merged (yellow). Sequential images, 63x magnification. Localisation of red and green channel overlaps in many areas (white arrows). Scale bar is 25 µm.

As described above (see also Chapter 2, section 2.3.6), the PCC of AQP2-GFP and mCherry-Rab5 was found to be 0.72 (Figure 3-5A), which showed that the correlation between the location of the two proteins was high. This indicates that the AQP2-GFP and mCherry-Rab5 proteins strongly associate. However, the correlation of both proteins does not mean that colocalisation is occurring. The same can be said of the PCC of AQP2-GFP and mCherry-Rab11, which was 0.68 (figure 3-5A), again showing that the association of the two proteins was strong but without confirming colocalisation.

In order to determine whether the two fusion proteins were colocalizing, the Manders coefficients, M1 and M2, were calculated as described in Chapter 2, section 2.3.6. The M1 value for AQP2-GFP and mCherry-Rab5 was 0.51 and the M2 was 0.67, showing that where AQP2-GFP was present, mCherry-Rab5 overlapped in 51% of the pixels and where mCherry-Rab5 was present, AQP2-GFP overlapped in 67% of the pixels. The M1 value for AQP2-GFP and mCherry-Rab11 was 0.57 and the M2 was 0.69, showing that where AQP2-GFP was present, mCherry-Rab11 overlapped in 57% of the pixels and where mCherry-Rab11 was present, AQP2-GFP overlapped in 69% of the pixels.

These results show that AQP2-GFP colocalizes with both mCherry-Rab5 and mCherry-Rab11 positive endosomes and vesicles, respectively. These data were in agreement with previously published findings and suggest that AQP2 and AQP4 might use similar translocation mechanisms (Barile et al., 2005).

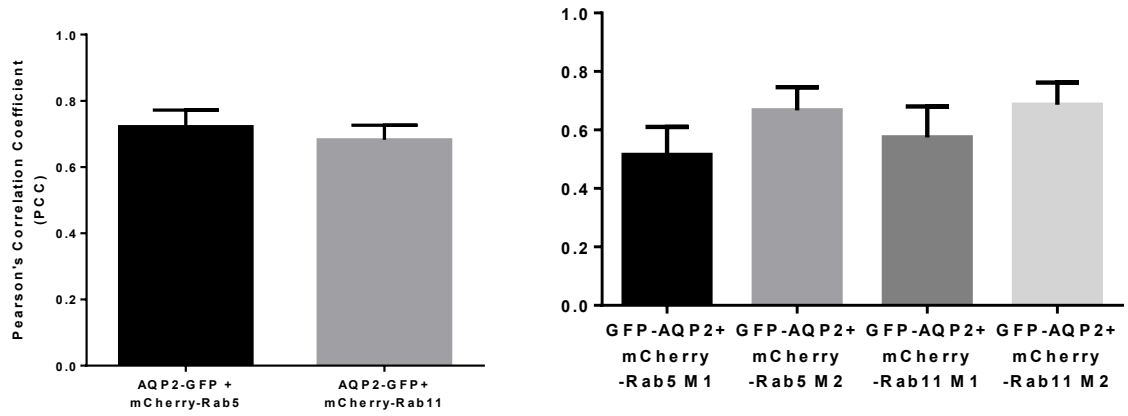

Figure 3-5: Quantification of AQP2 colocalisation with Rab5 and Rab11. Correlation (A) and co-occurrence (B) of AQP2-GFP with mCherry-Rab5 and colocalisation of AQP2-GFP with mCherry-Rab11 (B). The correlation of AQP2-GFP with mCherry-Rab5 and mCherry-Rab11 was high (>0.6), showing that the green and red pixels were in the same space of the images. The M1 ratios of co-occurrence of AQP2-GFP with mCherry-Rab5 and mCherry-Rab11 were high (>0.5), showing that red pixels were present in over half of the spaces where green pixels were. The M2 ratios of co-occurrence of AQP2-GFP with mCherry-Rab5 and mCherry-Rab11 were high (>0.6), showing that green pixels were present in over half of the spaces where red pixels were.

3.1.3 AQP4 translocation

The subcellular relocalisation of AQP4-eGFP following changes in tonicity in the extracellular environment has been shown before in HEK293 cells (Kitchen et al., 2015). Following exposure to a hypotonic environment for only a few seconds, AQP4 translocates from intracellular vesicles to the plasma membrane of HEK293 cells. The same is seen in response to hypoxia, which indicates that the use of hypotonicity as an *in vitro* model of cytotoxic oedema is appropriate (Kitchen et al., 2020). However, as mentioned previously, a clear picture of the complete molecular mechanism behind translocation, especially in response to changes in the surrounding environment, is largely missing.

Following the confirmation of AQP4-eGFP colocalizing with mCherry-Rab5 and mCherry-Rab11, the next step was to examine whether the two Rab GTPases were involved in the relocalisation of AQP4 in response to hypotonicity.

First, the optimal dilution of the medium was determined for these experiments. For each condition, the cells were placed in the medium diluted with water for 5 minutes, and relative membrane expression (RME) was measured (Figure 3-6). The 100% DMEM condition is the isotonic condition used as the control, and the 25% DMEM condition was the hypotonic condition used in subsequent experiments. The osmolarity of the control solution was measured to be 302 mOsm/kg, and the hypotonic was 77 mOsm/kg.

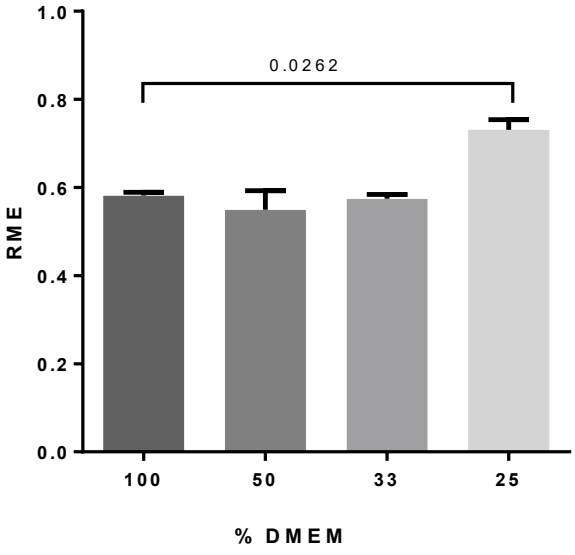

Figure 3-6: Localisation of AQP4 to the plasma membrane in isotonic and hypotonic conditions. HEK293 cells transfected with AQP4-eGFP were placed in an isotonic medium (100% DMEM) and moved to a range of dilutions of DMEM with water, ranging from 50% to 25%. The cells were imaged after 90 seconds and mean RME was calculated for AQP4-eGFP, averaged over 3 profiles/cell and 3 experimental repeats, $n = 3$. For each repeat, p values are

from a one-way analysis of variance followed by Tukey's correction. All data are presented as mean ± S.E.M.

The RME of AQP4 was measured, and this changed with changes in tonicity. In Figures 3-7A and B, at 30 seconds in an isotonic medium, the RME of AQP4 was approximately 0.4 which indicated, as expected, that less than half of the present AQP was found in the membrane. Following the addition of water, after 90 seconds, the RME of AQP4 rose to approximately 0.6, showing that AQP4 had translocated to the membrane following the change in tonicity. After 5 minutes, the RME of AQP4 was still approximately 0.6, which indicated that the relocalisation of the protein to the membrane occurred in a short period of time, most likely within the first 90 seconds.

The RME of Rab5 and Rab11 in Figures 3-7A and B, respectively, followed a similar pattern to that of AQP4. The RME of both Rabs at 30 seconds was approximately 0.4 and after a change in tonicity after 90 seconds, the RME of Rab5 and Rab11 rose to approximately 0.6, showing that a larger percentage of these was located in the plasma membrane following the change in tonicity. After 5 minutes, this stayed at approximately 0.6, which would again indicate that the movement of Rab5 and Rab11 occurred mostly within the first 90 seconds.

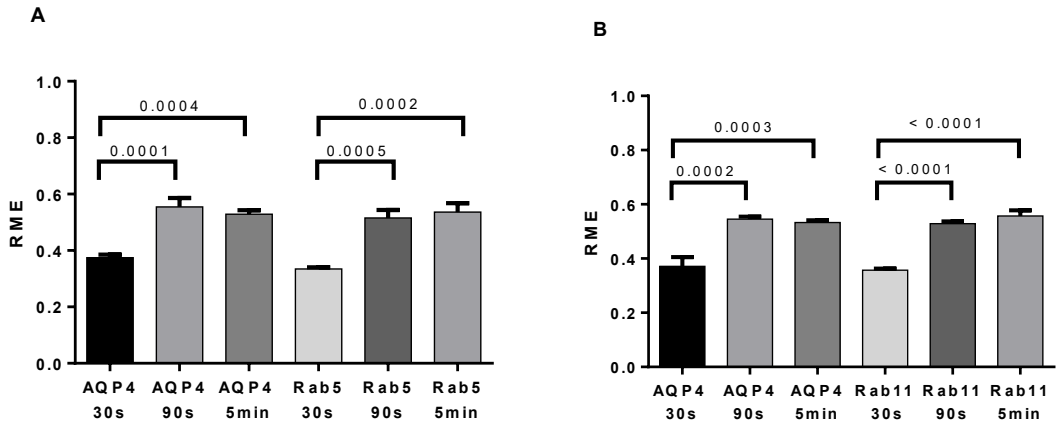

Figure 3-7: Quantification of AQP4, Rab5 and Rab11 RME in HEK293 cells. HEK293 cells were transfected with AQP4-eGFP and mCherry-Rab5 (A) or AQP4-eGFP and mCherry-Rab11 (B) and imaged by fluorescence microscopy in an isotonic solution after 30 seconds, then exposed to a hypotonic solution and imaged after 90 seconds and 5 minutes. Mean RME for AQP4-eGFP and mCherry tagged Rab5 and Rab11, averaged over 3 profiles/cell and 3 experimental repeats, n = 3. For each repeat, p values are from a one-way analysis of variance followed by Tukey's correction. All data are presented as mean ± S.E.M.

To further confirm the role of Rab5 and Rab11 in AQP4 translocation, dominant negative (DN) forms of the two proteins were used: mCherry-Rab5DN and DsRed-Rab11DN. Dominant negative mutants were selected to mimic a loss of function, with the Rabs unable to switch

from the inactive GDP to the active GTP. When comparing the RME of the co-transfected AQP4 and wild-type Rabs and the co-transfected AQP4 and dominant negative Rabs, there was a clear difference in distribution.

In Figure 3-8 at 30 seconds, the RME of AQP4-eGFP was approximately 0.4 in isotonic conditions, and 0.6 in hypotonic conditions. This indicated that when the extracellular environment changed, the AQP4 translocated to the membrane, as expected. In isotonic conditions, in the presence of Rab5 DN, the RME of AQP4 was approximately 0.6 which indicates that more than half of the present AQP was found in the membrane. Following the addition of water, the RME of AQP4 remained the same, suggesting that intracellular AQP4 did not further translocate to the membrane following the change in tonicity. Finally, the RME of AQP4 when co-transfected with Rab11 DN was approximately 0.4 in isotonic medium and remained the same in the hypotonic medium. These results suggest that tonicity-dependent AQP4 translocation is controlled by Rab5 and Rab11. The results also suggest that AQP4 is in a continuously cycling state between endosomes or vesicles and the plasma membrane, as the dominant negative Rab5 results showed the protein was "stuck" on the plasma membrane without the GTPase functioning properly, and the Rab11 dominant negative results showed the water channel "stuck" inside the vesicles.

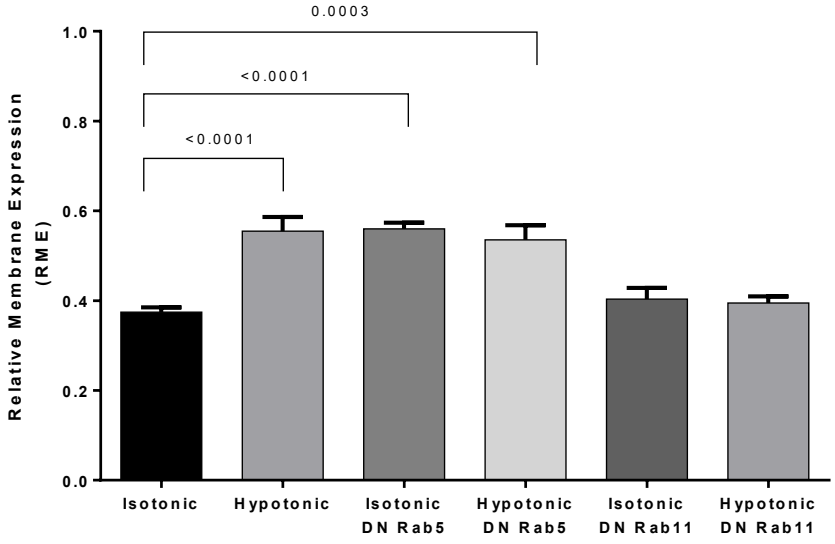

Figure 3-8: Quantification of AQP4 RME, in HEK293 cells co-transfected with Rab5DN and Rab11DN. HEK293 cells were transfected with AQP4-eGFP and mCherry-Rab5DN or AQP4-eGFP and DsRed-Rab11DN and imaged by fluorescence microscopy in an isotonic solution after 30 seconds, exposed to a hypotonic solution and imaged after 90 seconds and 5 minutes. Mean RME for AQP4, and AQP4 co-transfected with Rab5DN and Rab11DN, averaged over 3 profiles/cell and 3 experimental repeats, *n* = 3. Each column compared to

isotonic AQP4. For each repeat, *p* values are from one-way analysis of variance followed by Tukey's correction. All data are presented as mean ± S.E.M

3.2 Inhibition of membrane trafficking regulators

Following the confirmation of the role of Rab5 and Rab11 in the trafficking of AQP4, a further investigation was carried out to acquire a more detailed insight into the trafficking mechanism. This was achieved using pharmacological inhibitors of dynamin, clathrin-independent endocytosis, actin and microtubules using dynasore, filipin, cytochalasin D and Nocodazole, respectively.

The RME of AQP4 was measured as described in Chapter 2, section 2.3.7, both under isotonic and hypotonic conditions. When cells were pre-incubated with dynasore, the RME of AQP4 remained at 0.6, both in isotonic and hypotonic conditions, indicating that internalisation of AQP4 was impaired, with more AQP4 accumulating in the membrane compared to isotonic conditions in the absence of the inhibitor (Figure 3-9B). When cells were exposed to hypotonic conditions and then moved back to an isotonic environment, the RME of AQP4 did not change, showing this membrane accumulation was still present, regardless of tonicity.

When cells were pre-incubated with filipin, the RME of AQP4 was similar to that of the control (Figure 3-9C). When hypotonicity was introduced, the RME of AQP4 changed, and when returned back to isotonic conditions there was no significant difference. Following pre-incubation with nocodazole, the RME of AQP4 in isotonic medium was similar to that of the AQP4 control (Figure 3-9D), whereby there was a decreased expression of AQP4 in the plasma membrane, despite the change in tonicity. This indicates microtubules may play a role in the translocation mechanism of AQP4 since their inhibition led to a decreased movement of AQP4 to the plasma membrane. Finally, when cytochalasin D was added, the RME of AQP4 was approximately 0.6 (Figure 3-9E), which suggests a role of actin in the internalisation of AQP4, as more AQP4 was found at the plasma membrane than was brought back into the cell.

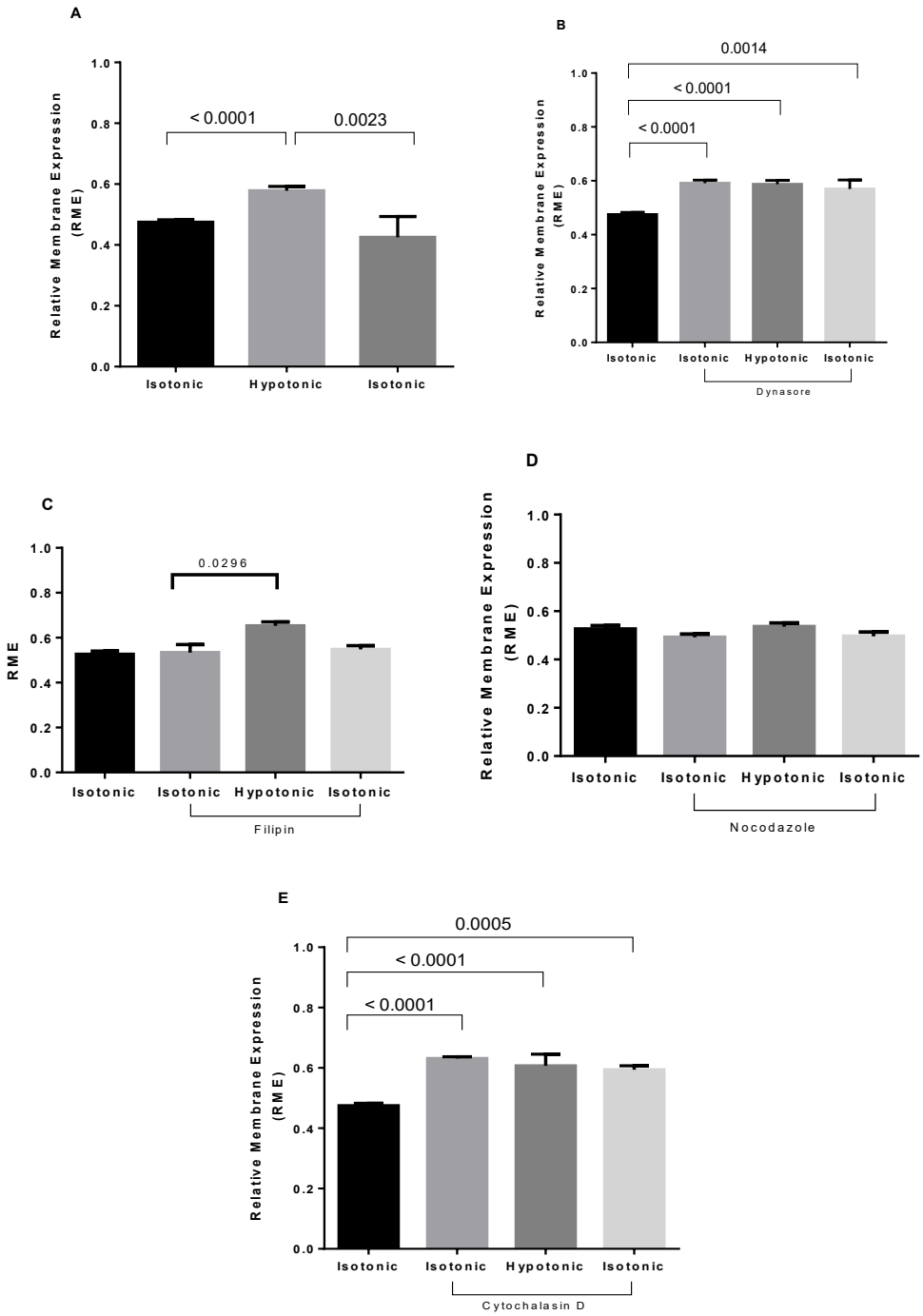

Figure 3-9: Inhibition of membrane trafficking regulators in HEK293 cells. HEK293 cells were transfected with AQP4-eGFP, inhibitors were added, and cells were imaged by fluorescence microscopy in an isotonic solution after 30 seconds, exposed to a hypotonic solution and imaged after 5 minutes, then returned to isotonic media and imaged after 5 minutes. From left to right clockwise, AQP4 no inhibitor (A), AQP4+dynasore (B), AQP4+filipin (C), AQP4+nocodazole (D), AQP4+ cytochalasin D (E). Mean RME for AQP4 averaged over 3 profiles/cell and 3 experimental repeats, $n = 3$. For each repeat, p values are from one-way analysis of variance followed by Tukey's correction. All data are presented as mean ± S.E.M.

3.3 Activation of the cytoskeleton

Following the inhibition experiments, the next step was to investigate the effect of activation of actin and microtubules by using jasplakinolide and paclitaxel. The RME of AQP4 was measured as described previously, both under isotonic and hypotonic conditions. When jasplakinolide was added, the RME of AQP4 remained similar to that of the control under isotonic conditions and increased under hypotonic conditions (Figure 3-10A). This indicates that translocation of AQP4 was not impaired. When cells were treated with paclitaxel, the RME did not change, staying at levels between 0.4 and 0.5 even when the cells were exposed to hypotonic conditions and then moved back to an isotonic environment (Figure 3-10B). This indicates an impairment of AQP4 movement to the membrane.

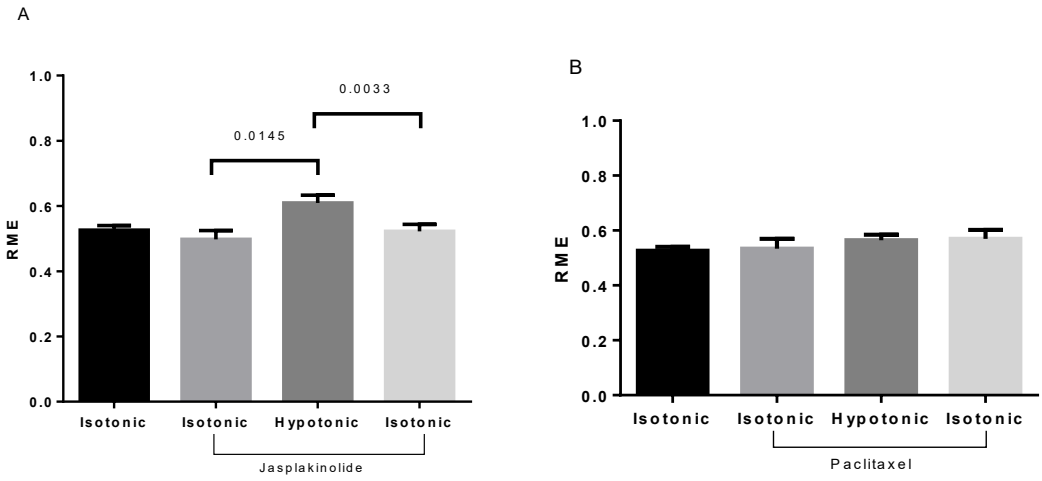

Figure 3-10: RME of HEK293 cells treated with cytoskeleton polymerisation activators. HEK293 cells were transfected with AQP4-eGFP, jasplakinolide and paclitaxel were added, and cells were imaged by fluorescence microscopy in an isotonic solution after 30 seconds, exposed to a hypotonic solution and imaged after 5 minutes, then returned to isotonic media and imaged after 5 minutes. (A) AQP4 + jasplakinolide, (B) AQP4+paclitaxel. Mean RME for AQP4 averaged over 3 profiles/cell and 3 experimental repeats, $n = 3$. For each repeat, p values are from one-way analysis of variance followed by Tukey's correction. All data are presented as mean ± S.E.M.

3.4 Discussion

The relocalisation of AQP4 is understood to occur when the hypoxic or hypotonic environment triggers an influx of calcium, through TRPV4, which binds to and activates CaM. Activated CaM activates adenylyl cyclase, which in turn leads to cAMP production that further activates PKA which phosphorylates AQP4 (Kitchen et al., 2015). However, following this phosphorylation there is little known about the membrane trafficking of the phosphorylated

AQP4. The results presented in this chapter begin to elucidate the mechanism by which AQP4 relocalises to the plasma membrane through vesicular trafficking.

3.4.1 AQP4-eGFP Colocalizes with mCherry-Rab5 and mCherry-Rab11

The two Rabs, Rab5 and Rab11, were chosen as likely to colocalize with AQP4 for these two reasons: the similarity of AQP trafficking mechanisms, and the fact that during internilsation, the most likely target is the Rab5-positive early endosome and subsequent recycling commonly occurs through Rab11-positive recycling endosome. The results showing the colocalisation of AQP4 with Rab5, and the colocalisation of AQP4 with Rab11, adds an additional level of knowledge step in the understanding of the movement of AQP4 to the plasma membrane. The involvement of Rab5 in membrane fusion between endocytic vesicles and early endosomes would indicate that where Rab5 and AQP4 colocalize, the latter has been internalized. Where Rab11 and AQP4 are colocalizing, the role of Rab11 in the recycling endosome would suggest that the water channel is in the process of being recycled to the surface. Thus, the colocalisation with both Rab5 and Rab11 suggests that these are involved in the translocation mechanism, and AQP4 indeed is internalized to the Rab5-positive early endosomes and is then recycled through the Rab11-positive recycling endosomes.

3.4.2 AQP2-GFP Colocalizes with mCherry-Rab5 and mCherry-Rab11

The results seen in Figure 3-5 show that AQP2 colocalizes with Rab5 and Rab11, confirming what was previously seen in the literature (Takata et al., 2008). This was also a confirmation that the fluorescent Rab constructs were functioning correctly. Whilst AQP2 translocation is triggered by vasopressin, the movement of AQPs has been shown to largely remain the same across cell types, something which was taken into account when predicting the role of Rab5 and Rab11 in the trafficking of AQP4.

3.4.3 mCherry-Rab5DN and dsRed-Rab11DN disrupts AQP4-eGFP trafficking

The results in Figure 3-8 show that when there is a Rab5(DN) mutant present, at least 55% of the AQP4 is localised to the plasma membrane, which is significantly higher when compared to the control. This would suggest that the recycling of AQP4 is impaired; many of the water channels are not being internalised, thus remaining on the cell surface and a decreased amount being internalised. When exposed to hypotonic conditions, no additional internalisation took place. In Figure 3-8, where Rab11(DN) is overexpressed, up to around 50% of AQP4 is present in the plasma membrane. Following the introduction of hypotonic conditions there is no change to the RME of AQP4, which would indicate there is no additional AQP4 reaching the plasma membrane, as it remains in vesicles. However, it is important to consider the fact that these results are indicative of only one timepoint, in either tonicity. The

recycling mechanism of AQP4, which has begun to be dissected here, is likely to be occurring constantly between the plasma membrane and vesicles. The use of the DN Rabs alters this cycle, either disrupting the movement from the plasma membrane to the early endosome (Rab5(DN)) or from the recycling endosome to the plasma membrane (Rab11(DN)). Again, these results also demonstrate a role of Rab5 and Rab11 in the translocation mechanism of AQP4. The DNRab5 outcompeted endogenous Rab5 and did not allow for AQP4 internalisation to the early endosome, and Rab11(DN) outcompeted endogenous Rab11 and stopped AQP4 recycling to the plasma membrane.

3.4.4 AQP4 trafficking is altered by dynasore, filipin, nocodazole and cytochalasin D

The use of inhibitors is a useful way of determining which elements of membrane trafficking machinery may be involved in the trafficking of AQP4. Dynasore, a dynamin inhibitor, was added to the cells following a 24-hour incubation with the transfection mix. The cells were imaged in isotonic conditions, the medium was then diluted, and cells were imaged before being returned to isotonic medium and imaged again. The results in Figure 3-9B showed that after being exposed to dynasore for 30 minutes, the majority of AQP4 was on the plasma membrane, with no change after the adjustments to tonicity. This would suggest that without functioning dynamin, endocytosis of AQP4 does not occur. This is in agreement with the function of dynamin in predominantly clathrin-mediated endocytosis, as it disrupts the formation of vesicles from the plasma membrane (Preta, Cronin & Sheldon, 2015). It should be noted that dynamin has also been shown to play a role in clathrin-independent endocytosis, so these results show that AQP4 internilsation potentially occurs in a dynamin-dependent manner.

The use of filipin complemented these results, as it helped confirm that it is unlikely that clathrin-independent endocytosis is mediating AQP4 internalisation. The results in Figure 3-9C showed that after being exposed to filipin there was no change in surface expression of AQP4 in isotonic conditions, and the movement of AQP4 to the membrane was not disrupted. This would suggest that whilst dynamin is involved in clathrin-mediated and clathrin-independent endocytosis, only clathrin-mediated endocytosis contributes to AQP4 internalisation.

The role of microtubules in trafficking has been assessed, with recent studies showing their involvement not only in positioning of organelles, but also their role in cargo transport to the plasma membrane in a quick and targeted manner (Fourriere et al., 2020). When nocodazole, a microtubule polymerization inhibitor, was added for 45 minutes, the RME of AQP4 remained at similar levels to the AQP4 control when moved to a hypotonic medium (Figure 3-9C). This would suggest that when microtubules are destabilized, there is no movement of AQP4 to the

plasma membrane. These data are in agreement with previous experiments showing the role of microtubules in the movement of AQP4 from the cytosol to the plasma membrane in MDCK cells (Mazzaferri, Costantino & Lefrancois, 2013), and with the additional element of hypotonicity-induced translocation, or lack thereof, provides one more dataset of interest. Much like the microtubules, actin plays a role in organelle positioning, as well as vesicular transport (DePina & Langford, 1999). So, with the addition of cytochalasin D, which disrupts actin polymerization, the RME of AQP4 remained high throughout the different tonicity (Figure 3-9D). This would suggest the mechanism of internalisation of AQP4 is potentially also dependent on actin, due to the lack of movement of AQP4 in response to the changes in tonicity.

3.4.5 AQP4 trafficking is not altered by jasplakinolide, but is altered by paclitaxel

This potential role of actin in AQP4 trafficking was further supported by the results in Figure 3-10A, where the addition of jasplakinolide that stabilised polymerisation of actin did not change the dynamics of AQP4 translocation in response to hypotonicity. The opposite was seen when paclitaxel was added, where the polymerisation of microtubules disrupted the movement of AQP4 to the plasma membrane. This could indicate the dynamic nature of microtubule polymerisation and depolymerisation is an element which contributes to the movement of AQP4, as opposed to just the formed microtubules being needed for the translocation to occur.

3.5 Future work

To further dissect the mechanism of AQP4 trafficking, a number of different steps could potentially be taken. First, the experiments have only been carried out at a single time-point and the potential changes to the cyclical movement of the AQP4 from plasma membrane to intracellular vesicles and back again would need to be investigated over time. This could be achieved through fluorescence recovery after photobleaching (Zheng et al., 2011), or suitable alternatives such as super-resolution and single-molecule localisation (Lelek et al., 2021). In addition to this, a useful experiment would be to expand the endosome types examined. The proportion of AQP4 sent to late endosomes for degradation could be determined using Rab7 as a marker for late endosomes, or the lysosomal marker LAMP-1.

A further examination of the role of clathrin could be done by carrying out similar studies to those with Rabs, to see whether clathrin colocalizes with AQP4 and whether changes to tonicity affect the localisation. Additionally, a knockout of clathrin and caveolin could be used to further examine which pathway is needed. However, it should be noted that pathways independent from clathrin and caveolin exist (Kumari, Mg & Mayor, 2010; Damm et al., 2005),

so a wider study into each of these and the potential role they could play in AQP4 internalisation would also be of interest.

Each compound which was selected as an inhibitor was used at a working concentration determined from the literature. Whilst this was not an ideal selection method because of the lack of experimental confirmation, the cell morphology remained the same when the compounds were added. A cell viability assay could also be carried out to confirm this.

The work in this chapter has been carried out in HEK293 cells, which do not express endogenous AQP4, so validating these results using astrocytes with endogenous AQP4 expression would be needed. This also means that the role of Rab5 and Rab11 may be different in the astrocytes, and it should be considered that the overexpression of Rab5 and Rab11 also could cause unexpected consequences, as well as the use of dominant negative Rabs. Finally, an investigation into the effects of each inhibitor would also be beneficial in determining the role of the cytoskeleton and dynamin in the translocation of endogenous AQP4.

The results presented in this chapter indicate that the mechanism of AQP4 subcellular relocalisation in HEK293 cells involves the Rab GTPases, Rab5 and Rab11. This, along with the inhibitor and activator studies provides an additional layer to understanding the membrane trafficking mechanism of AQP4 and could prove useful for identifying potential therapeutic targets for cytotoxic oedema.

4. Results - Investigating AQP4 trafficking mechanisms in human astrocytes

Following the confirmation of the role of Rab5, Rab11, dynamin and the cytoskeleton in the vesicular trafficking of AQP4 to and from the plasma membrane (Chapter 3), the aim of this chapter was to demonstrate the mechanism shown in HEK293 cells was seen in a physiologically relevant *in vitro* model. Primary human cortical astrocytes were used, with cell surface biotinylation chosen as suitable assay. Additionally, hypoxia was introduced as a more physiologically relevant trigger. This is because hypoxia occurs due to the reduction in blood flow at the injury site following TBI, as well as an overall decrease in oxidative metabolism in the brain (Vespa, 2016).

4.1 AQP4 cell surface expression in response to hypotonicity

Cell surface biotinylation is a useful tool to determine the cell surface expression of a protein (Tham, Joshi & Moukhles, 2016). In this case, AQP4 was the protein of interest, and following treatment with the compounds described in Table 1 of Chapter 2, and exposure to a hypotonic trigger, the surface expression was measured.

It is known that hypotonicity is a trigger of AQP4 relocalisation from the cytosol to the plasma membrane (Kitchen et al., 2015). In the case of the experiments in this chapter, the measured osmolarities were as follows: isotonic medium was 336 mOsm/kg; hypotonic medium was 85 mOsm/kg. This effect was seen in Figure 4-1A with the addition of a hypotonic medium, where there was a 50% increase in the surface expression of AQP4 compared to the isotonic (p = 0.0090). This control was subsequently used in Figures 4-1, 4-2, 4-3 and 4-4. When treated with the actin polymerisation inhibitor cytochalasin D, there was an overall increase in the surface expression of AQP4 in the isotonic condition when compared to the isotonic control (p = 0.0011). This remained almost unchanged with the hypotonic trigger (p = 0.0060) when compared to the isotonic control. Between the cells treated with cytochalasin D, the isotonic and hypotonic did not change surface localisation of AQP4 significantly.

When treated with the actin polymerisation stabiliser jasplakinolide, as seen in Figure 4-1B, the cell surface expression of AQP4 in isotonic conditions did not change significantly when compared to the isotonic control. The addition of the hypotonic medium caused an increase in AQP4 at the cell surface compared to the isotonic control (p = 0.0003) and the isotonic jasplakinolide-treated condition (p = 0.0016). The increase in cell surface expression of AQP4 in the control hypotonic medium when compared to the isotonic control was seen as expected (p = 0.0006).

A

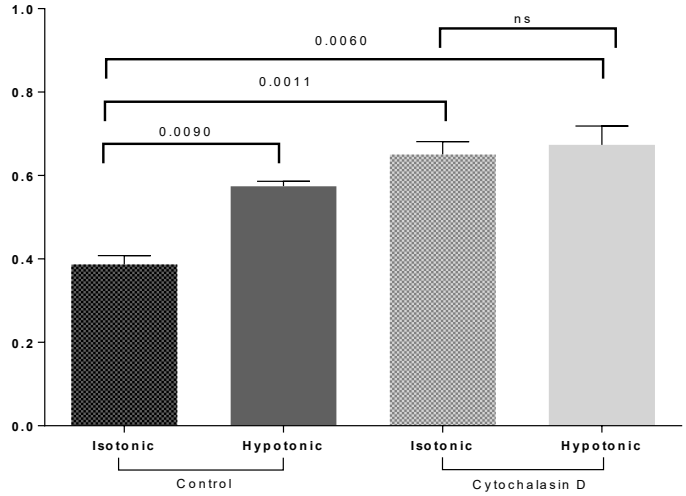

B

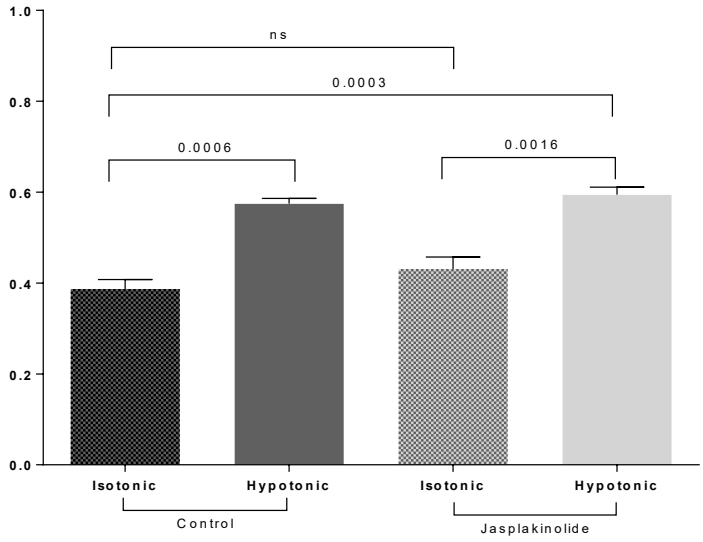

Figure 4-1: AQP4 surface localisation in response to actin-modifying compounds. Hypotonicity stimulates AQP4 relocalisation to the plasma membrane and treatment with 5μM cytochalasin D for 45 minutes disrupts subcellular relocalisation of AQP following a hypotonic trigger (A). Treatment with 0.15μM jasplakinolide for 30 minutes does not affect subcellular relocalisation of AQP following a hypotonic trigger (B). *n* = 3 for each repeat, *p*-values are from one-way analysis of variance followed by Tukey's correction. All data are presented as mean ± S.E.M

The next compound to be tested was the non-competitive dynamin inhibitor dynasore. The hypotonic control showed an increase of approximately 50% (p = 0.0048) compared to the isotonic control (Figure 4-2). When treated with dynasore, the isotonic cells showed an

increase in cell surface expression compared to the isotonic control cells (p = 0.0002), as did the hypotonic cells (p = 0.0003), with no significant change between the dynasore-treated isotonic and hypotonic conditions (Figure 4-2).

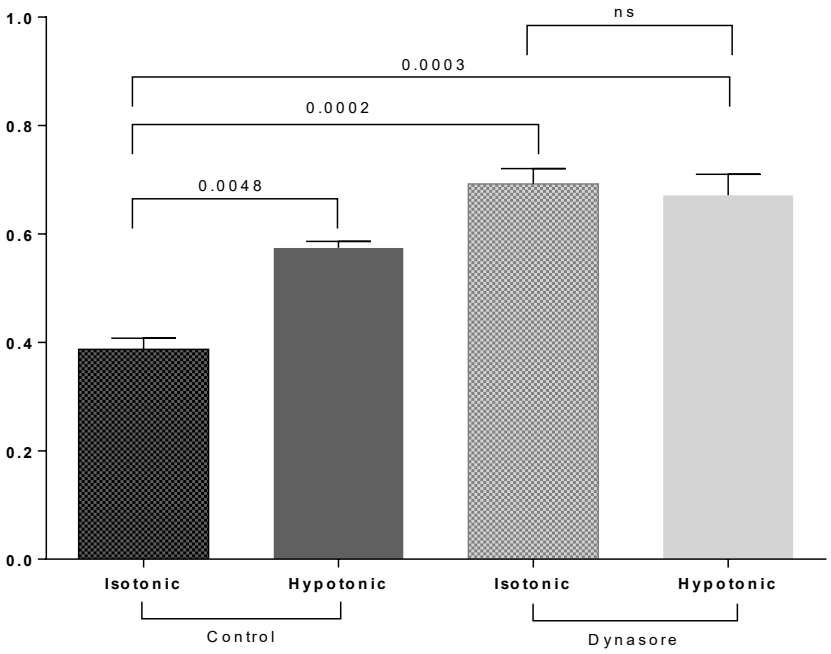

Figure 4-2: AQP4 surface localisation in response to dynamin inhibition. Hypotonicity stimulates AQP4 relocalisation to the plasma membrane and treatment with 80μM dynasore for 30 minutes disrupts subcellular relocalisation of AQP following a hypotonic trigger (A). n = 3 for each repeat, p-values are from one-way analysis of variance followed by Tukey's correction. All data are presented as mean ± S.E.M

The targeting of microtubule polymerisation was carried out using nocodazole as an inhibitor and paclitaxel as an activator. The hypotonic control showed an increase of approximately 50% (p = 0.0130) compared to the isotonic control (Figure 4-3A). In the group treated with nocodazole, the isotonic cells showed no significant change in cell surface expression compared to the isotonic control cells, whereas the hypotonic cells showed an increase when compared to the same group (p = 0.0013), with a significant increase also seen between the nocodazole-treated isotonic and hypotonic conditions (p = 0.0138) (Figure 4-3A).

In the paclitaxel-treated group, the isotonic cells showed no significant change compared to the isotonic controls, with the same being true of the hypotonic group (Figure 4-3B). The hypotonic control group did increase significantly (p = 0.0276) when compared to the isotonic control, as seen in the previous experiments (Figure 4-3B).

A

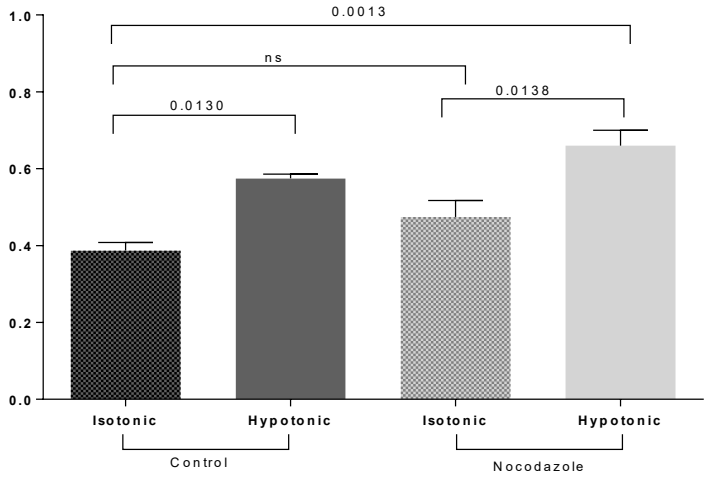

B

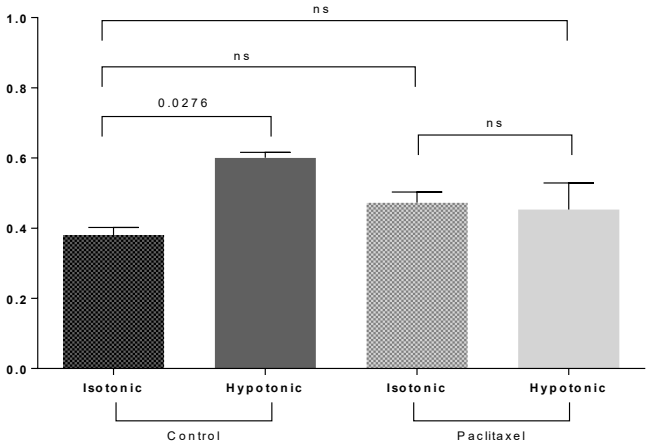

Figure 4-3: AQP4 surface localisation in response to microtubule-modifying compounds Hypotonicity stimulates AQP4 relocalisation to the plasma membrane and treatment with 30μM nocodazole for 45 minutes does not disrupt subcellular relocalisation of AQP following a hypotonic trigger (A). Treatment with 0.05μM paclitaxel for 20 minutes disrupts subcellular relocalisation of AQP following a hypotonic trigger (B). *n* = 3 for each repeat, *p*-values are from one-way analysis of variance followed by Tukey's correction. All data are presented as mean ± S.E.M

Finally, the last compound to be used as a treatment was filipin, an inhibitor of clathrin-independent endocytosis. The hypotonic control group again showed a significant increase ($p = 0.0026$) compared to the isotonic control (Figure 4-4). Following treatment with filipin, the isotonic group showed no significant change when compared to the isotonic control group,

whereas the hypotonic group showed an increase when compared to the same isotonic control (p = 0.0001) (Figure 4-4).

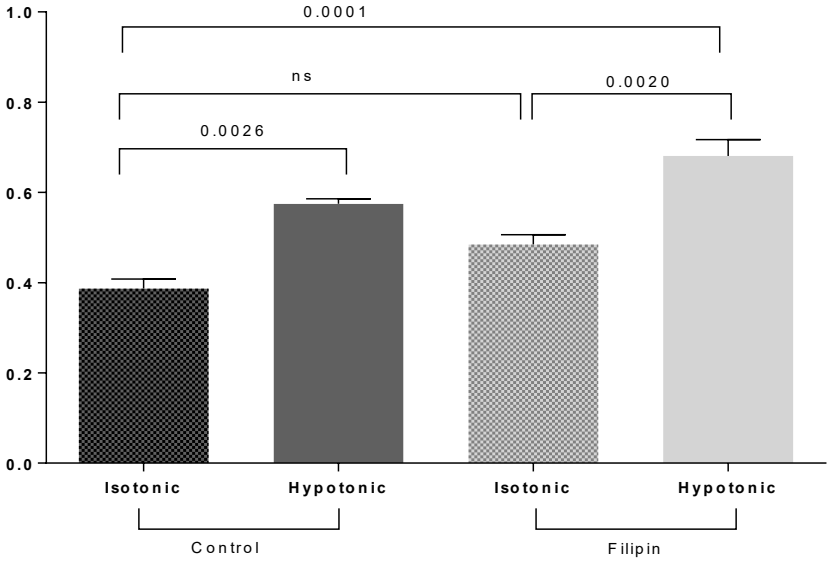

Figure 4-4: AQP4 surface localisation in response to clathrin-independent endocytosis inhibition. Hypotonicity stimulates AQP4 relocalisation to the plasma membrane and treatment with 30μM filipin for 20 minutes does not disrupt subcellular relocalisation of AQP4 following a hypotonic trigger (A). n = 3 for each repeat, p-values are from one-way analysis of variance followed by Tukey's correction. All data are presented as mean ± S.E.M

4.2 Reversibility of AQP4 cell surface localisation

The changes to AQP4 subcellular localisation after treatment with the compounds described in Table 1 of Chapter 2, and following a response to tonicity, resulted in a preliminary model of how AQP4 behaves when certain key elements of the proposed trafficking pathway are disrupted. However, it is known that the subcellular relocalisation of AQP4 in response to a change in tonicity is a reversible one (Kitchen et al., 2015). This return to isotonicity was therefore applied to the biotinylation assay, as an additional element to determine how the cytoskeleton and clathrin-dependent or -independent endocytosis might play a role not only in the movement of AQP4 to the cell surface, but also in its internalisation.

First, the isotonic control was placed in hypotonic conditions, and then returned to isotonic conditions (Figure 4-5). The trend was as expected with a significant increase of AQP4 at the

cell surface (p = < 0.0001), compared to the isotonic control and then a significant reduction in the cell surface expression of AQP4 when returned to isotonicity (p = < 0.0001) when compared to the hypotonic control. There was no significant difference between the isotonic control and the isotonic return control. The DMSO that was used to dissolve the compounds was also tested, to ensure the AQP4 localisation was not affected by it. At the highest concentration there was no change in the trend seen in the control. The AQP4 cell surface expression increased in the hypotonic compared to the isotonic condition (p = < 0.0001) and decreased when returned to the isotonic condition when compared to the hypotonic condition (p = < 0.0001).

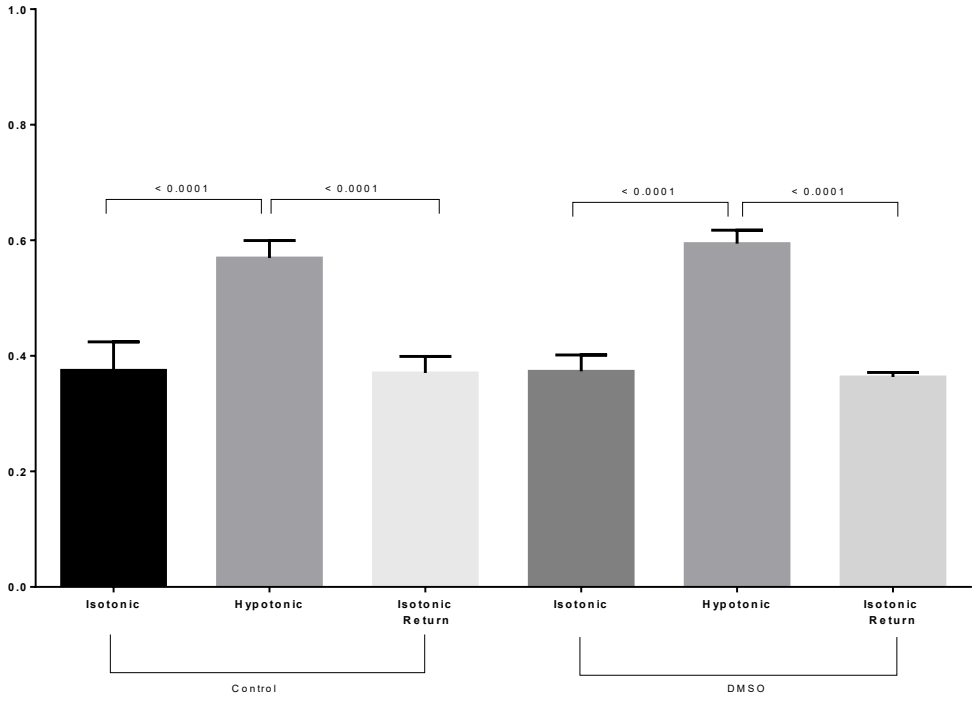

Figure 4-5: Hypotonicity stimulates AQP4 relocalisation to the plasma membrane in a reversible manner. Treatment with DMSO for 45 minutes does not disrupt subcellular relocalisation of AQP4 following a hypotonic trigger, and this can be reversed when isotonicity is restored. n = 3 for each repeat, p-values are from one-way analysis of variance followed by Tukey's correction. All data are presented as mean ± S.E.M

The treatment with dynasore shown in Figure 4-6 indicate that the addition of the compound to the isotonic cells increased the AQP4 cell surface expression when compared to the isotonic control (p = < 0.0001). Whilst there was no significant difference between the isotonic and hypotonic dynasore-treated cells, the levels remained the same when compared to the isotonic control. When the dynasore treatment was also applied with a return to isotonic conditions, there was again no change in the levels of AQP4 at the cell surface. The hypotonic dynasore treatment was significantly increased compared to the isotonic control (p = < 0.0001), as was

the isotonic return (p = < 0.0001). The control AQP4 cell surface expression increased in hypotonicity compared to the isotonic condition (p = 0.0011) and decreased when returned to isotonic conditions when compared to the control hypotonic condition (p = 0.0009).

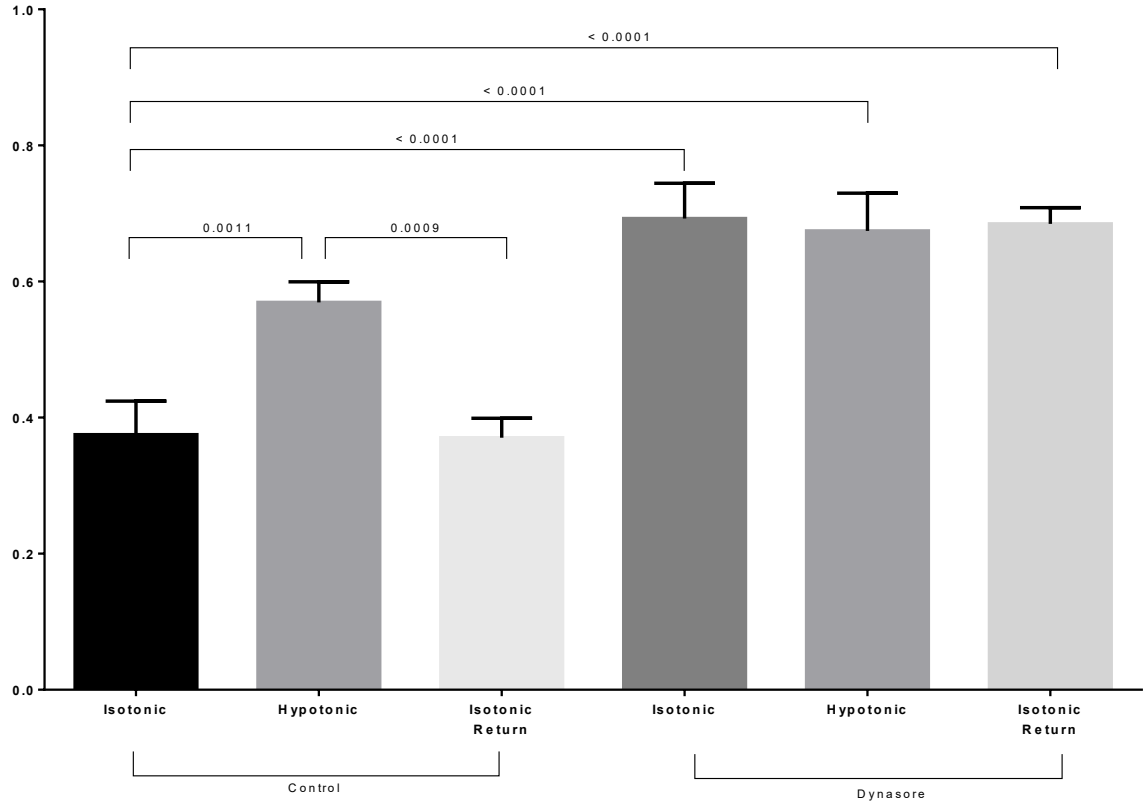

Figure 4-6: Hypotonicity stimulates AQP4 relocalisation to the plasma membrane in a reversible manner. Treatment with 80μM Dynasore for 30 minutes disrupts subcellular relocalisation of AQP following a hypotonic trigger, and this is not reversed when isotonicity is restored. n = 3 for each repeat, p-values are from one-way analysis of variance followed by Tukey's correction. All data are presented as mean ± S.E.M

The cytochalasin D treatment shown in Figure 4-7 also caused an increase to the AQP4 cell surface expression when compared to the isotonic control (p = <0.0002). Whilst there was no significant difference between the isotonic and hypotonic cytochalasin D - treated cells, the levels remained the same when compared to the isotonic control. When the cytochalasin D treatment was also applied with a return to isotonic conditions, there was again no change in the levels of AQP4 at the cell surface. Following hypotonic cytochalasin D treatment, AQP4 cell surface expression was significantly increased compared to the isotonic control (p = 0.0003) and the isotonic return (p = 0.0001). The control AQP4 cell surface expression increased in hypotonic conditions compared to the isotonic condition (p = 0.0048) and

decreased when returned to isotonic conditions when compared to the control hypotonic condition (p = 0.0040).

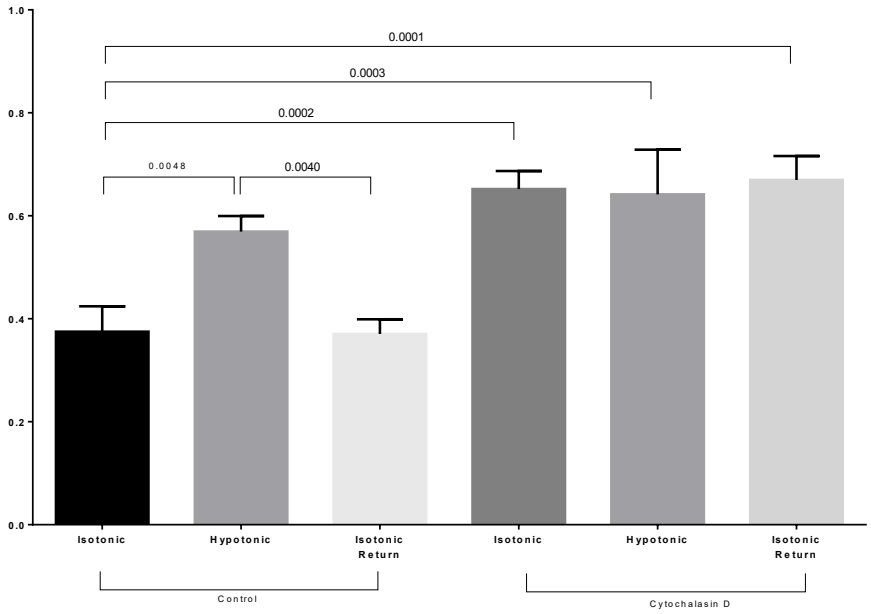

Figure 4-7: Hypotonicity stimulates AQP4 relocalisation to the plasma membrane in a reversible manner. Treatment with 5μM cytochalasin D for 45 minutes disrupts subcellular relocalisation of AQP following a hypotonic trigger, and this is not reversed when isotonicity is restored. n = 3 for each repeat, p-values are from one-way analysis of variance followed by Tukey's correction. All data are presented as mean ± S.E.M

Following on from the actin inhibitor study, the next compound to be used was the actin polymerisation stabiliser, jasplakinolide. Figure 4-8 shows that when treated with this, the basal level of cell surface AQP4 expression under isotonic conditions does not change significantly when compared to the control. The AQP4 cell surface expression did change under hypotonic conditions when compared to the isotonic control (p = 0.0044) and the isotonic jasplakinolide-treated group (p = 0.0011) and when isotonicity was restored, the cell surface expression was reduced again (p = 0.0009). The hypotonic control increased as expected when compared to the isotonic control (p = 0.0027) and the cell surface expression decreased when cells were returned to an isotonic condition (p = 0.0022).

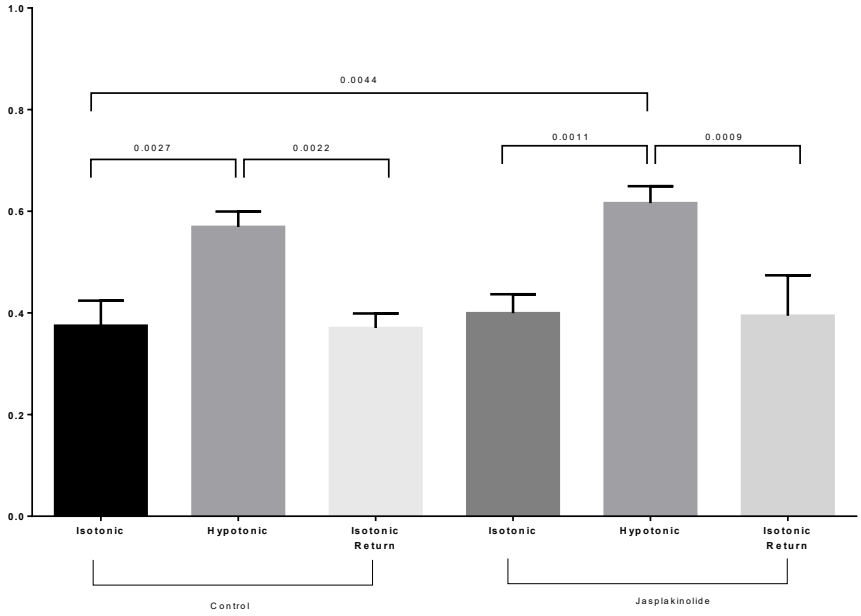

Figure 4-8: Hypotonicity stimulates AQP4 relocalisation to the plasma membrane in a reversible manner. Treatment with 0.15μM jasplakinolide for 30 minutes does not affect subcellular relocalisation of AQP4 following a hypotonic trigger, and this can be reversed when isotonicity is restored. *n* = 3 for each repeat, *p*-values are from one-way analysis of variance followed by Tukey's correction. All data are presented as mean ± S.E.M

The microtubule polymerisation inhibitor nocodazole did not seem to affect the basal level of AQP4 cell surface expression when compared to the isotonic control (Figure 4-9). However, under hypotonic conditions this expression increased compared to the isotonic control (p = 0.0141), and it increased even further when isotonicity was restored (p = 0.0365). The level of AQP4 cell surface expression in the hypotonic control increased as expected when compared to the isotonic control (p = 0.0075) and the cell surface expression decreased when cells were returned to an isotonic condition (p = 0.0012).

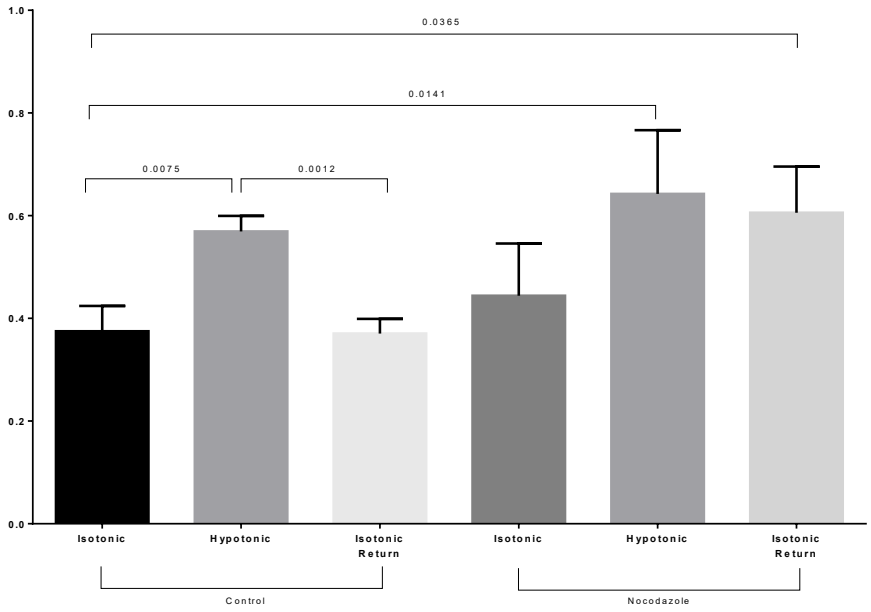

Figure 4-9: Hypotonicity stimulates AQP4 relocalisation to the plasma membrane in a reversible manner. Treatment with 30μM nocodazole for 45 minutes does not disrupt subcellular relocalisation of AQP following a hypotonic trigger. This is not reversed when isotonicity is restored. *n* = 3 for each repeat, *p*-values are from one-way analysis of variance followed by Tukey's correction. All data are presented as mean ± S.E.M

In Figure 4-10, the level of AQP4 cell surface expression in the hypotonic control increased when compared to the isotonic control ($p = 0.0246$) and the cell surface expression decreased back to basal levels when cells were returned to an isotonic condition ($p = 0.0211$). When microtubule polymerisation was stabilised using paclitaxel, there was no change in the cell surface expression of AQP4 when compared to the isotonic control (Figure 4-10) and this did not change under hypotonic conditions, or when there was a return to isotonicity.

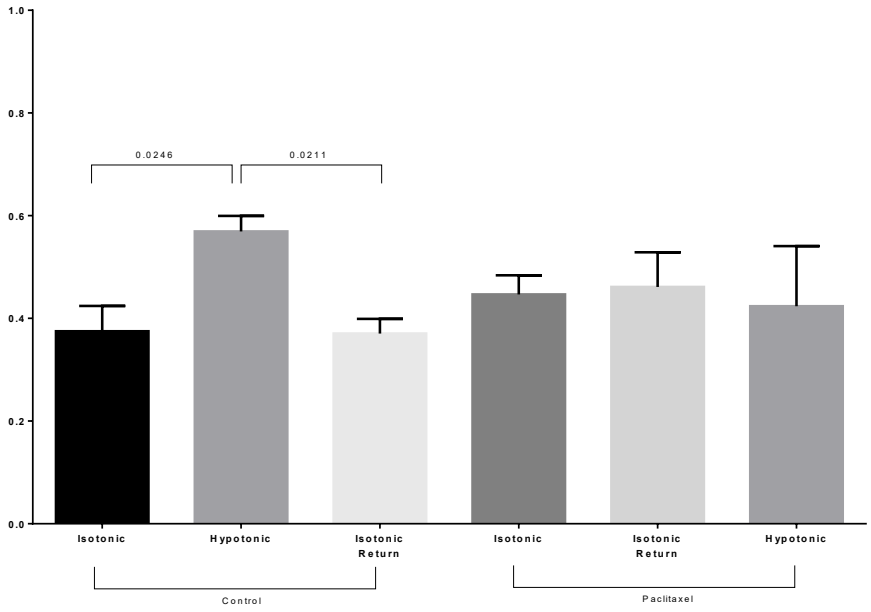

Figure 4-10: Hypotonicity stimulates AQP4 relocalisation to the plasma membrane in a reversible manner. Treatment with 0.05μM paclitaxel for 20 minutes disrupts subcellular relocalisation of AQP4 following a hypotonic trigger, and this does not change when isotonicity is restored. *n* = 3 for each repeat, *p*-values are from one-way analysis of variance followed by Tukey's correction. All data are presented as mean ± S.E.M

Lastly, the CIE inhibitor filipin was used to treat cells. The control conditions were the same as in previous figures, with the hypotonic control increasing when compared to the isotonic control ($p = 0.0021$) and the cell surface expression decreased back to previous levels when cells were returned to an isotonic condition ($p = 0.0017$) (figure 4-11). The Filipin-treated isotonic condition was not significantly different to the isotonic control, but the hypotonic Filipin treatment group showed an increase compared to the isotonic control ($p = <0.0001$) and the isotonic Filipin-treated group ($p = 0.0017$). When cells were returned to an isotonic medium and treated with Filipin, the surface expression of AQP4 reduced when compared to the hypotonic Filipin treatment group ($p = 0.0003$).

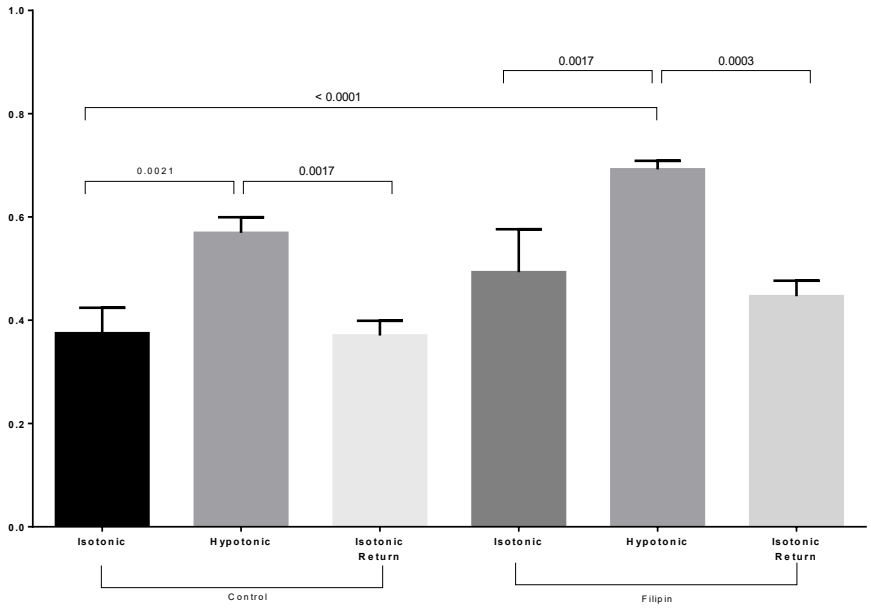

Figure 4-11: Hypotonicity stimulates AQP4 relocalisation to the plasma membrane in a reversible manner. Treatment with 30μM filipin for 20 minutes does not affect subcellular relocalisation of AQP4 following a hypotonic trigger, and this movement can be reversed when isotonicity is restored. *n* = 3 for each repeat, *p*-values are from one-way analysis of variance followed by Tukey's correction. All data are presented as mean ± S.E.M

4.3 Internalisation of AQP4 in response to hypotonicity

Apart from AQP4 cell surface expression, the percentage of AQP4 internalisation was measured using cell surface biotinylation, as described in Chapter 2, section 2.3.8, and either under untreated hypotonic to isotonic conditions (control) with time allowed for internalisation of AQP4, or with treatments and hypotonic to isotonic conditions with time allowed for internalisation, as well as the addition of glutathione to strip away any remaining biotinylated protein on the surface.

Treatment with cytochalasin D left around 86.99% of AQP4 at the cell surface, following a return to isotonicity (Figure 4-12A), suggesting the AQP4 was not internalised when actin polymerisation was disrupted. With actin polymerisation stabilised, there was 94.57% internalisation of AQP4 when the cells were returned to isotonic conditions (Figure 4-12B).

With dynasore treatment, there was almost no internalisation of AQP4, only 1.10% (Figure 4-12C), again indicating a disruption in the endocytic mechanism involving AQP4 translocation. In terms of microtubules, the nocodazole-treated group had only 56.42% of AQP4 internalised (Figure 4-12D), whereas the stabilisation of microtubules with paclitaxel led to an internalisation of 71.67% of the AQP4 from the surface (Figure 4-12E). The last treatment with

filipin again did not seem to disrupt internalisation of AQP4, with 85.72% being brought in from the cell surface (Figure 4-12F).

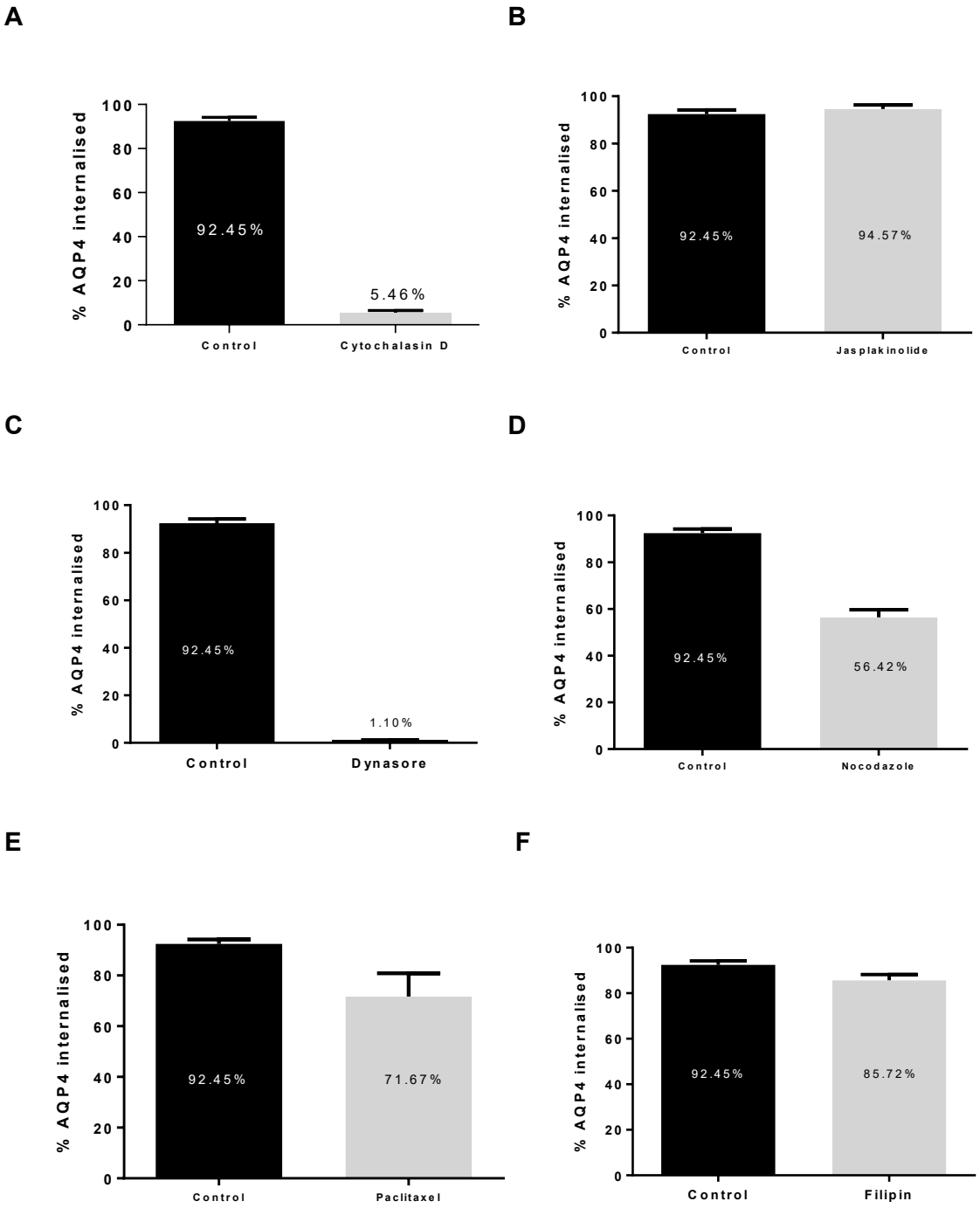

Figure 4-12: The percentage of AQP4 internalised following exposure to hypotonic then isotonic conditions when compared to a hypotonic untreated control and treatment with cytochalasin D (A), jasplakinolide (B), dynasore (C), nocodazole (D), paclitaxel (E) and filipin (F). Mean internalisation for AQP4 averaged over 3 technical repeats and 3 experimental repeats, *n* = 3. All data are presented as mean ± S.E.M.

4.4 Using hypoxia as a trigger for AQP4 subcellular relocalisation

Throughout this chapter, the trigger for AQP4 translocation has been hypotonicity. However, the physiological trigger leading to extracellular hypotonicity is hypoxia (Vespa, 2016). During normal conditions, there is a balance of solutes and hydroxyl radicals, whereas, in TBI this balance is disrupted (Hall et al., 2012). The damage to the astrocytes leads to a disruption of this homeostatic mechanism, through the increase of hydroxyl radicals and the formation of a hypoxic environment. In normal physiological conditions, these radicals are targeted by antioxidant systems, however, in injury this mechanism is dysfunctional (Bordone et al., 2019). The resulting hypoxic environment created by the free radicals leads to the formation of an osmotic gradient that drives the movement of water into the astrocytes, which swell to form cytotoxic oedema (Bordone et al., 2019).

This mechanism was confirmed, with a translocation of AQP4 occurring both under hypoxic conditions and hypotonic conditions (Figure 4-13).

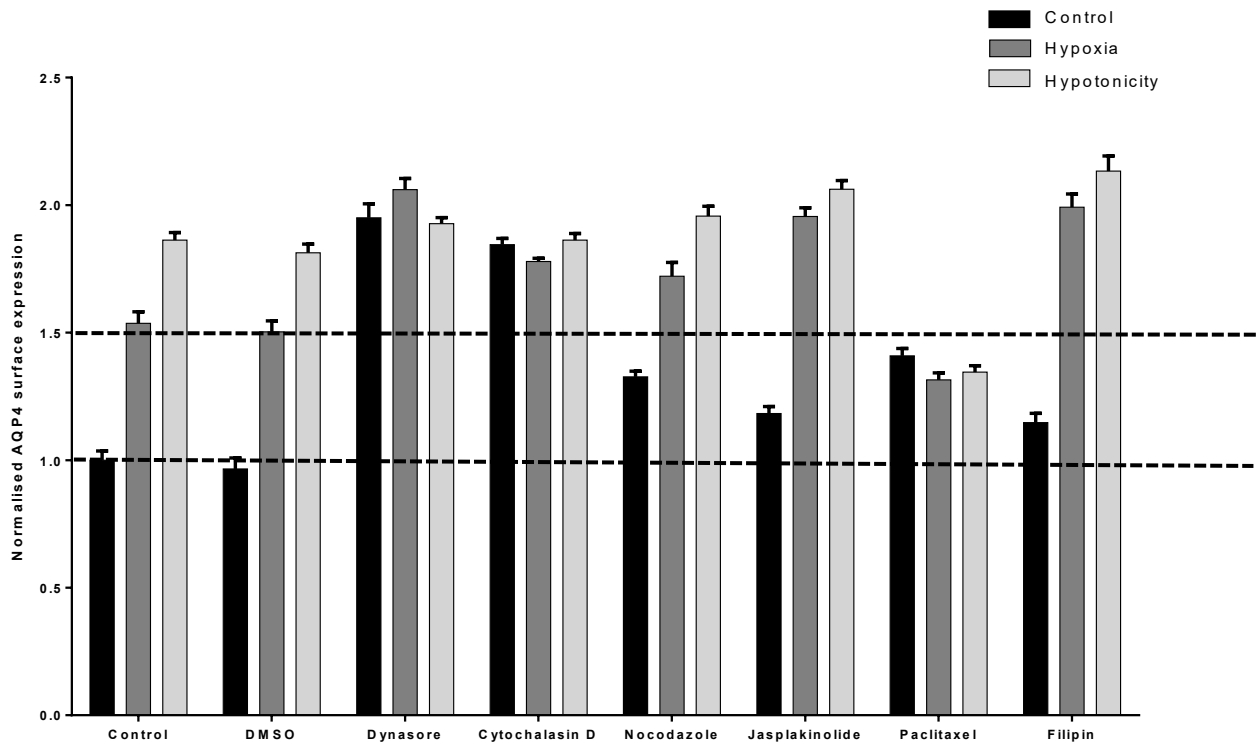

Figure 4-13: AQP4 surface expression in primary human astrocytes following exposure to hypoxia, hypotonicity and compounds targeting membrane trafficking components. Treatment with DMSO does not affect subcellular relocalisation of AQP4 following a hypotonic trigger or exposure to hypoxia. Treatment with dynasore disrupts subcellular relocalisation of AQP4 following a hypotonic trigger or exposure to hypoxia. Treatment with cytochalasin D disrupts subcellular relocalisation of AQP4 following a hypotonic trigger or exposure to hypoxia. Treatment with nocodazole does not affect subcellular relocalisation of AQP4 following a hypotonic trigger or exposure to hypoxia. Treatment with jasplakinolide does not affect subcellular relocalisation of AQP4 following a hypotonic trigger or exposure to hypoxia.

Treatment with paclitaxel disrupts affect subcellular relocalisation of AQP4 following a hypotonic trigger or exposure to hypoxia. Treatment with filipin does not affect subcellular relocalisation of AQP4 following a hypotonic trigger or exposure to hypoxia $n = 3$ for each repeat, p-values are from one-way analysis of variance followed by Tukey's correction. All data are presented as mean ± S.E.M.

4.5 Discussion

The work carried out in this chapter has shown that AQP4 trafficking in primary human astrocytes happens in a similar manner to that in HEK293 cells and therefore confirms that HEK cells are an appropriate model for use when investigating AQP4 trafficking. This is because endogenous AQP4 behaved in a similar way to the transiently transfected AQP4-EGFP in HEK293 cells. This is of use to note as an alternative to primary human astrocytes, due to the maintenance of the cells being more expensive and time-consuming. Additionally, transfection efficiency with primary human astrocytes was very low (approximately 3%), which meant any work to confirm Rab5 and Rab11 colocalisation with AQP4 was not possible. The use of hypotonicity has also been shown to be an appropriate trigger for AQP4 subcellular relocalisation, with no major differences when compared to hypoxia (Kitchen et al., 2020). This was also confirmed by the results seen in Figure 4-13.

4.5.1 Actin

The actin cytoskeleton and its remodelling are an integral part of the trafficking machinery of the cell (Lanzetti, 2007). More specifically, with regards to AQP2, actin has been shown to directly bind to the water channel (Noda et al., 2004). This complex has been suggested to be integral to the targeting of AQP2 to the apical membrane of the kidney's collecting duct cells (Noda et al., 2008). Additionally, the movement of AQP2 to the membrane is dependent on the dissociation of the protein from G-actin, and the disruption of F-actin, which, if it remained polymerised would impede this relocalisation (Noda et al., 2008). Cytochalasin-D disrupts both F-actin and G-actin, which is something to consider in future experiments. If AQP trafficking mechanisms are conserved, then it would be possible for the same mechanism to be seen for AQP4 as in AQP2.

It has been shown previously in rat and mouse astrocytes that actin plays a role in AQP4 localisation in astrocytes (Nicchia et al., 2008). Actin and AQP4 co-localize with each other, and the use of cytochalasin-D to alter actin polymerisation subsequently disrupts AQP4 cell surface localisation (Nicchia et al., 2008). It should also be noted that in rat astrocytes, cytochalasin-D increases water permeability, which could explain the increase in AQP4 cell surface expression in isotonic cells (Figures 4-1A and 4-7). However, the hypotonic and hypoxic trigger in these groups did not significantly change the expression of AQP4 at the

surface, indicating that the absence of newly polymerised actin leads to no AQP4 movement to the plasma membrane (Figure 4-1A, 4-7, 4-13). When returning the cells to isotonic conditions, there was no decrease in the cell surface expression of AQP4 (Figure 4-7). This also suggests that actin polymerisation is needed for the internalisation of AQP4, not just its movement to the cell membrane. This is also suggested by the percentage of internalised AQP4 in Figure 4-12A where cells were treated with cytochalasin-D, exposed to hypotonicity, and returned to isotonic conditions and there was minimal AQP4 internalised.

On the other hand, when actin polymerisation was stabilised with jasplakinolide, there was no disruption of the subcellular relocalisation in response to the hypotonic and hypoxic triggers (Figure 4-1B, 4-8 and 4-13). When isotonicity was restored, there was a decrease of AQP4 at the plasma membrane (Figure 4-8), and a percentage of internalisation that corresponded closely to the control (4-12B). These data also suggest that when actin polymerisation occurs, the ability of AQP4 to move from the cytosol to the plasma membrane is not disrupted.

However, actin polymerisation is a highly dynamic process, and the role of actin in both the movement and targeting of AQP4 would need to be investigated further.

4.5.2 Microtubules

The potential role of microtubules in the trafficking of AQP4 has briefly been described, with a suggestion that the disruption of the network impedes this movement (Mazzaferri, Costantino & Lefrancois, 2013). When moving from the cytosol to the plasma membrane, vesicles containing GFP-tagged AQP4 were shown to move along cytoskeletal structures. When nocodazole was used, this movement along this trajectory was disrupted.

When nocodazole was used as an inhibitor, the movement of AQP4 to the membrane in response to hypotonicity was not disrupted, with no significant increase in expression under isotonic conditions compared to the isotonic control (Figure 4-3A). However, under the same treatment with a return to isotonicity, the internalisation was impaired compared to the control return to isotonicity (Figure 4-9). This was also seen in the percentage of AQP4 internalised, which was only 56.42% (Figure 4-12D). The data suggest that the effect of nocodazole may not be as direct as expected, and the disruption of microtubule polymerisation could affect the speed of AQP4 internalisation, but perhaps not the movement of the protein to the membrane. When microtubules were stabilised, there was no change in basal AQP4 cell surface expression under isotonic conditions compared to the isotonic control, however there was also no movement of AQP4 to the plasma membrane under hypotonic conditions (Figures 4-3B and 4-10). When the cells were returned to an isotonic environment, again there was no change in the AQP4 cell surface expression (Figure 4-10). The percentage of AQP4 internalised was more than that of the cells treated with nocodazole, 71.67% (Figure 4-12E).

Much like actin, the microtubule network is a dynamic one, with the added complexity of movement in different directions along the fibres. This is something that should be considered when undertaking further work.

4.5.3 Dynamin

Dynamin, a major player in clathrin-mediated endocytosis, is responsible for assisting vesicle fission from the membrane during this process (Cheng et al., 2021). There have been some clathrin adaptor complexes identified as having a role in AQP4 trafficking, but once endocytosed, the water channel is targeted for degradation (Madrid et al., 2001). The main interest for this thesis is the recycling of AQP4 from the cytosol to the membrane, so these adaptor complexes were not considered as a target. Instead, dynamin, which has been shown to play a role in the internalisation of AQP4 through its interaction with dystroglycan, was selected (Tham, Joshi & Moukhles, 2016).

The data shown in Figures 4-2 and 4-6, suggest that dynamin inhibition interferes with the surface expression of AQP4, both by preventing an increase in the AQP4 at the membrane in response to hypotonicity, and by stopping any internalisation of AQP4 once returned to hypotonicity. This was also seen when the percentage of AQP4 internalised was compared to the control (Figure 4-12C). Overall, these results showed a very similar trend to the HEK293 results in Chapter 3.

4.5.4 Clathrin-independent endocytosis

More recently, clathrin-independent endocytosis has been described as playing a potential role in AQP4 surface trafficking. The role of caveolins especially has been suggested to interact with the water channel during internalisation (Filchenko et al., 2020). Here, filipin was used to disrupt CIE, with a view to determine whether or not this is needed for AQP4 to move from the plasma membrane to the cytosol.

As seen in Figures 4-4 and 4-11, there was no disruption of AQP4 movement when filipin was used. This was to be expected, because if the endocytic machinery was disrupted then the recycling of AQP4 should not change. However, in Figure 4-11 it was seen that there was also no disruption in the internalisation of AQP4. Additionally, the percentage of AQP4 that is internalised when filipin was used was 85.72% (Figure 4-12F). So, this suggests that CIE is overall not needed for AQP4 internalisation.

5 Results – Investigating AQP4 trafficking using *C. elegans* as an *in vivo* model

The overall aim of the project was to gain a better understanding of the molecular mechanism of AQP4 trafficking. Following on from the *in vitro* studies in HEK293 cells and primary human astrocytes, which shared a common mechanism (Chapters 3 and 4) the next step was to see how these results translated to an *in vivo* model. The model organism *C. elegans* was chosen with a view to develop it for high-throughput screening of AQP membrane trafficking regulators.

To achieve this, the initial stage was to establish whether *C. elegans* GFP-AQP-4 and GFP-AQP-1 change intracellular localization following changes in tonicity. This was done by optimising imaging and fluorescence quantification methods for GFP-tagged AQPs in *C.elegans* and screening an RNAi trafficking mini library to analyse key membrane trafficking regulators and their effect on localization of GFP-AQP-4.

8.1 *C. elegans* as a model organism

To understand biological processes, model organisms are widely used (Irion & Nüsslein-Volhard, 2022). They are useful in a laboratory setting because, among other things, many of them can be maintained easily and have a short life span. In this project, *C. elegans* was used as a model.

The use of *C. elegans* as a model organism is relatively recent, but already the developmental fate of each somatic cell is known (Krause, 1999), as is the complete genome sequence (C. elegans Sequencing Consortium, 1998). The life span of *C. elegans* is short, only approximately 14 days. While the worms go through specific life cycle stages, the reproductive cycle is complete in the first third of the life span, and the number of progenies is approximately 300.

5.2 AQPs in *C. elegans*

In *C. elegans*, there are 8 aquaporin-encoding genes: *aqp-1, aqp-2, aqp-3, aqp-4, aqp-5, aqp-6, aqp-7* and *aqp-8* in comparison to the thirteen human AQPs. Like the human AQPs, there are some that transport water and some that transport both water and glycerol (Huang *et al.,* 2007). This can be seen in the phylogenetic tree and sequence alignment shown in Huang *et al.* (2007), and in Figure 5-0.

The expression of AQP-4 is in the apical membrane of the intestine. AQP-4 in *C. elegans* is homologous to human AQP8. The expression of AQP-1 is predominantly in the basolateral membrane of the intestine. AQP-1 in *C. elegans* has been suggested to be homologous to either human AQP7 and/or AQP9 based on its function (Lee, Murphy and Kenyon, 2009). The

function of AQPs in the worm, though clearly useful in osmoregulatory tissues, is not essential to the process of osmotic homeostasis (Huang et al., 2007).

The intestinal location of both AQP-4 and AQP-1 was another reason for the selection of the two. Due to the polarized nature of the intestinal cell of *C. elegans*, and the size of it, it is easier to visualise (Chen et al., 2006). This has been shown previously, with the basolateral membrane and apical membrane responsible for exchange and uptake of molecules to and from the body and the environment, respectively (Gleason et al., 2016). Any abnormal basolateral exchange can be seen as an increase in endosomes containing fluid, again showing the ease with which trafficking defects can be identified in the *C. elegans* intestine (Chen et al., 2006).

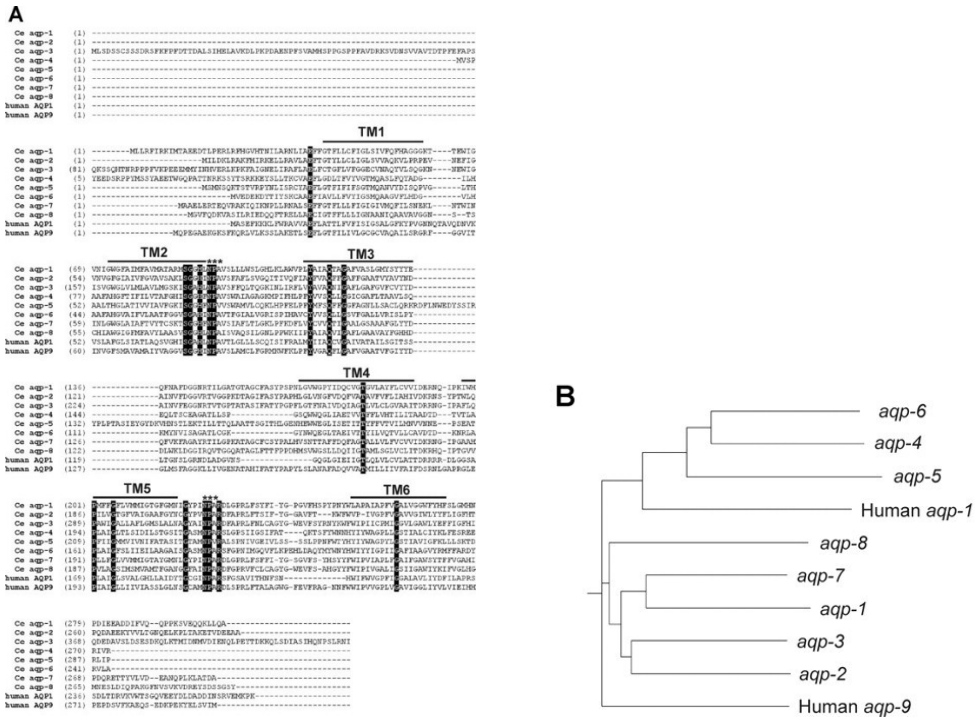

Figure 5-0: Alignment of *C. elegans* aquaporins with human AQP-1 and AQP-9 (A) and a phylogenetic tree (B) (adapted from Huang *et al*, 2007) **.**

5.3 Tonicity-induced translocation of GFP-AQP-4 in live *C. elegans*

5.3.1 Localisation of GFP-AQP-4 in *C. elegans*

The localisation of GFP-AQP-4 in *C. elegans* in response to different tonicities was investigated using fluorescence microscopy. Each tonicity condition had the following osmolarity measurements: Control was 168 mOsm/kg, hypotonic was 43 mOsm/kg, and hypertonic was 354 mOsm/kg. The *C. elegans* AQP-4 was selected because of the ease with

which it can be imaged in the intestine, and due to the availability of a transgenic strain. A search of the literature was done to determine which concentration could be used for each condition (isotonic, hypotonic and hypertonic). The worms were synchronised to L4 stage and were grown on plates of either isotonic, hypertonic or hypotonic conditions and images were taken at 24-hours (Figure 5-1) and 48-hours (Figure 5-2).

A Control (53 mM NaCl)

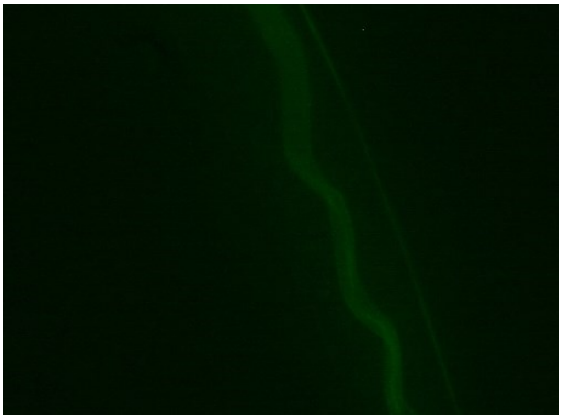

B Hypertonic (100 mM NaCl)

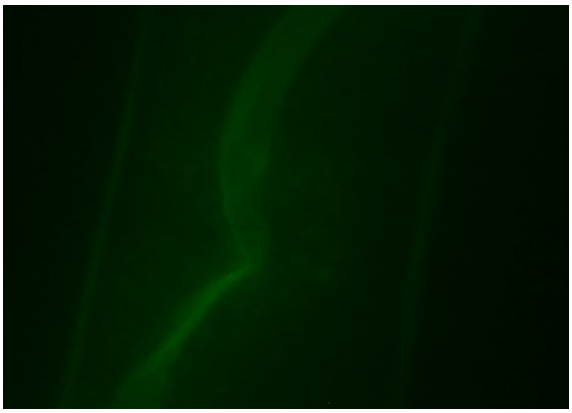

C Hypertonic (400 mM NaCl)

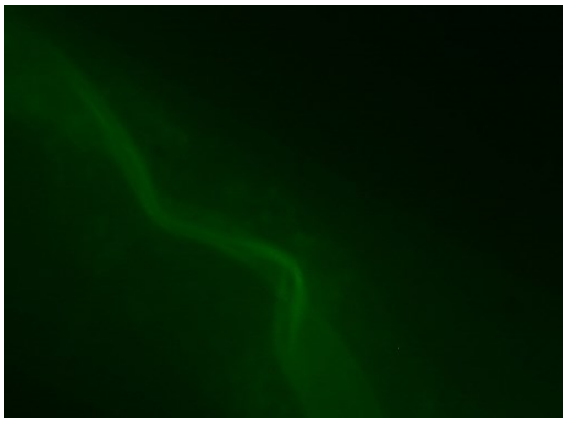

D Hypotonic (0 mM NaCl)

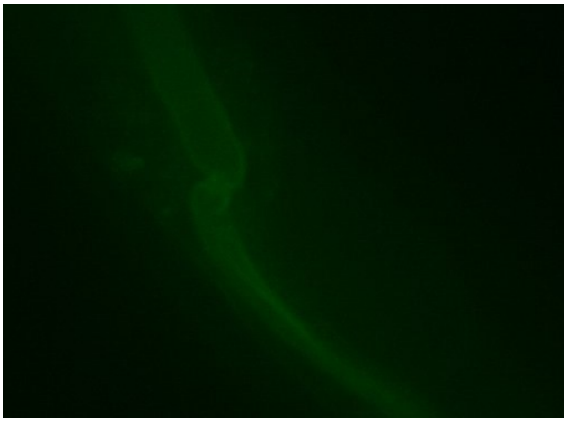

Figure 5-1: Localisation of GFP-AQP-4 in *C. elegans* intestine in apical membrane at different NaCl concentrations after 24-hours using fluorescence microscopy (x63 magnification) (n=3). Exposure to isotonic conditions (A) shows GFP-AQP-4 expression in the apical membrane of the intestine. Exposure to hypertonic conditions (B and C) shows a slight increase in GFP-AQP-4 intensity compared to isotonic. Exposure to hypotonic conditions (D) shows similar intensity to isotonic.

A Control (53 mM NaCl)

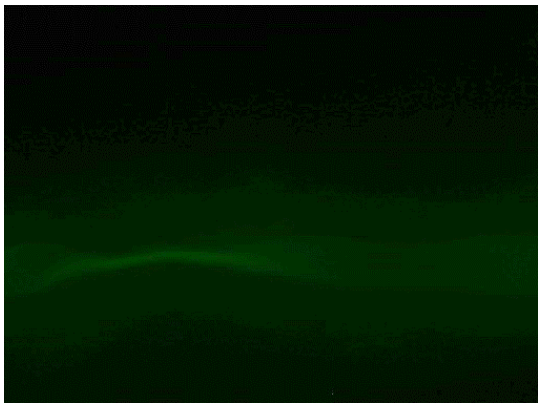

B Hypertonic (100 mM NaCl)

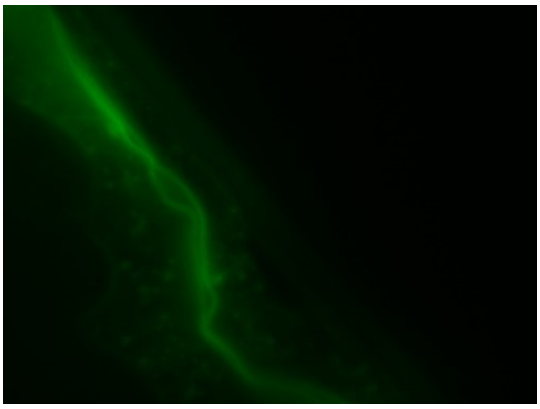

C Hypertonic (400 mM NaCl)

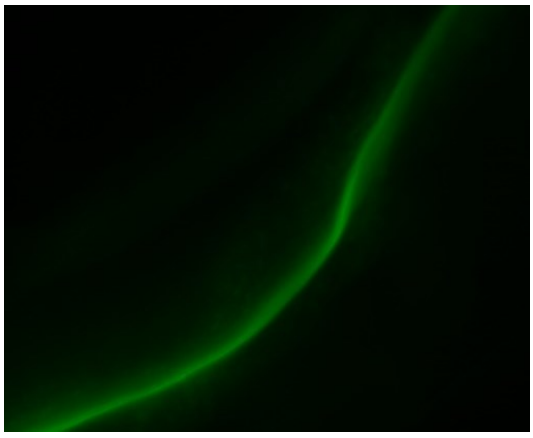

D Hypotonic (0 mM NaCl)

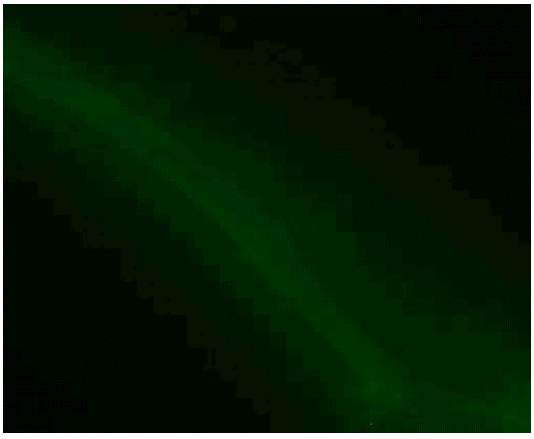

Figure 5-2: Localisation of GFP-AQP-4 in *C. elegans* intestine in apical membrane at different NaCl concentrations after 48-hours using fluorescence microscopy (x63 magnification) (n=3). Exposure to isotonic conditions (A) shows GFP-AQP-4 expression in the apical membrane of the intestine. Exposure to hypertonic conditions (B and C) shows a visible increase in GFP-AQP-4 intensity compared to isotonic. Exposure to hypotonic conditions (D) shows similar intensity to isotonic.

Both time points showed a similar pattern of GFP-AQP-4 intensity in response to different tonicities. At 24-hours, GFP-AQP-4 was clearly expressed in the apical membrane of the intestine (Figure 5-1A-D). Following exposure to hypertonic conditions there was a slight increase in the intensity of the fluorescence (Figure 5-1B, 6.1C) in comparison to the control (Figure 5-1A). Following exposure to hypotonic conditions (Figure 5-1D) there did not seem to be a change in the intensity of the fluorescence in comparison to the control (Figure 5-1A). At 48-hours, there was a visible increase in fluorescence intensity following exposure to the hypertonic conditions (Figure 5-2B, 6-2C) compared to the control and no visible difference was seen in the hypotonic conditions (Figure 5.2D) in comparison to the control (Figure 5-2A).

5.3.2 Quantification of GFP-AQP-4 expression in *C. elegans*.

The intensity of GFP-AQP-4 expression seen in Figures 5 and 6 was measured to determine the expression in response to changes in tonicity. The intensity at the two time points for the different concentrations of NaCl was compared to the total of the corresponding control (Figure 5-3). All data are shown as mean ± SEM.

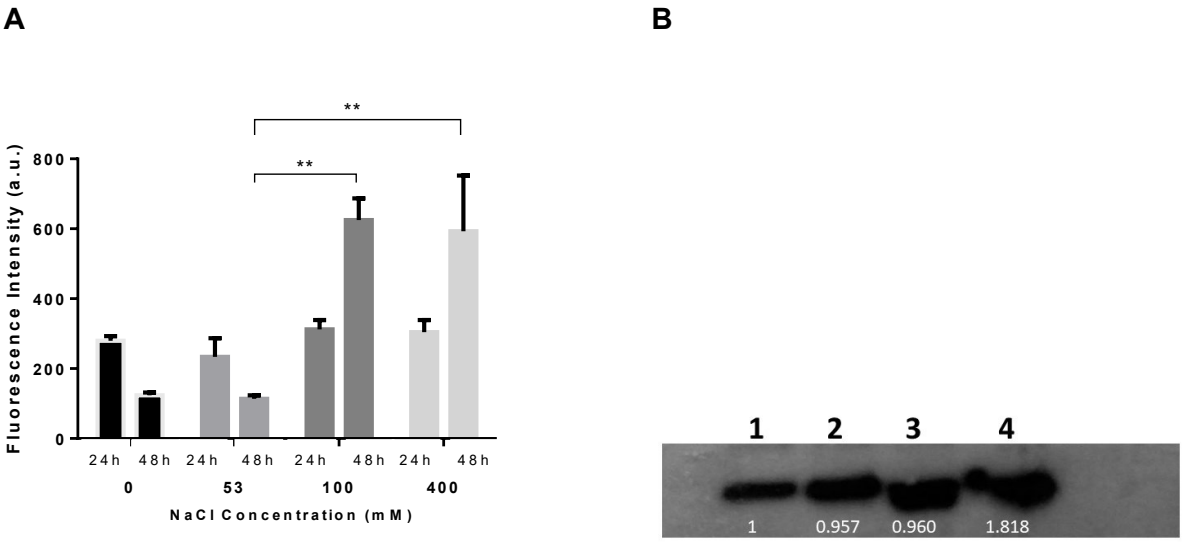

Figure 5-3: Expression and quantification of GFP-AQP-4. (A) Fluorescence intensity of GFP-AQP-4 following 24-hour and 48-hour exposure to hypotonic, isotonic and hypertonic conditions. Both hypertonic conditions showed an increase in fluorescence intensity and the isotonic and hypotonic conditions showed a decrease after 48-hours. Graphs are shown as mean ± SEM, n=10 for each time point and concentration which were repeated 3 times. (B) Western blot with samples from isotonic (1), hypotonic (2) and hypertonic (3 and 4) conditions after 48-hours. The values in white show the intensity of each band. Each lane was loaded with membranes extracted from 20 whole worms.

Figure 5-3A shows that there were changes in fluorescence intensity over 48-hours for every tonicity change. This indicates that there was an overall increase in expression of GFP-AQP-4. The one-way ANOVA carried out on the 24-hour timepoints showed that there was no significant change between the control (isotonic at 53 mM) and the hypertonic (100 mM NaCl and 400 mM NaCl) conditions. The one-way ANOVA carried out for 48-hours indicated that there was a significant change between the control (isotonic at 53 mM) and the hypertonic (100 mM NaCl and 400 mM NaCl) conditions and no significant change between the hypotonic (0 mM) condition and the control.

The expression of GFP-AQP-4 in *C. elegans* following 48-hour exposure to different tonicities was detected by Western Blot (Figure 5-3B). The intensity values of each band were expressed as values normalised to the isotonic condition. No loading control was shown in Figure 5-3B, due to technical issues with the Western Blot (no expression shown). This is an

experiment that needs further optimisation, due to the importance of the loading control. However, because of time constraints this was not possible. Whilst this additional loading control would be beneficial, it should be noted that an equal amount of worms were used to load each well.

5.4 RNAi knockdown of membrane trafficking regulators

Following the confirmation of GFP-AQP-4 localisation in the apical intestine and the change in fluorescence intensity in response to different tonicities, the next step was to begin examining the trafficking pathway of GFP-AQP-4.

The intensity of GFP-AQP-4 fluorescence was measured to determine the expression in response to RNAi knockdown of a number of key membrane trafficking regulatory genes (Figure 5-4). All data are shown as mean ± SEM. c

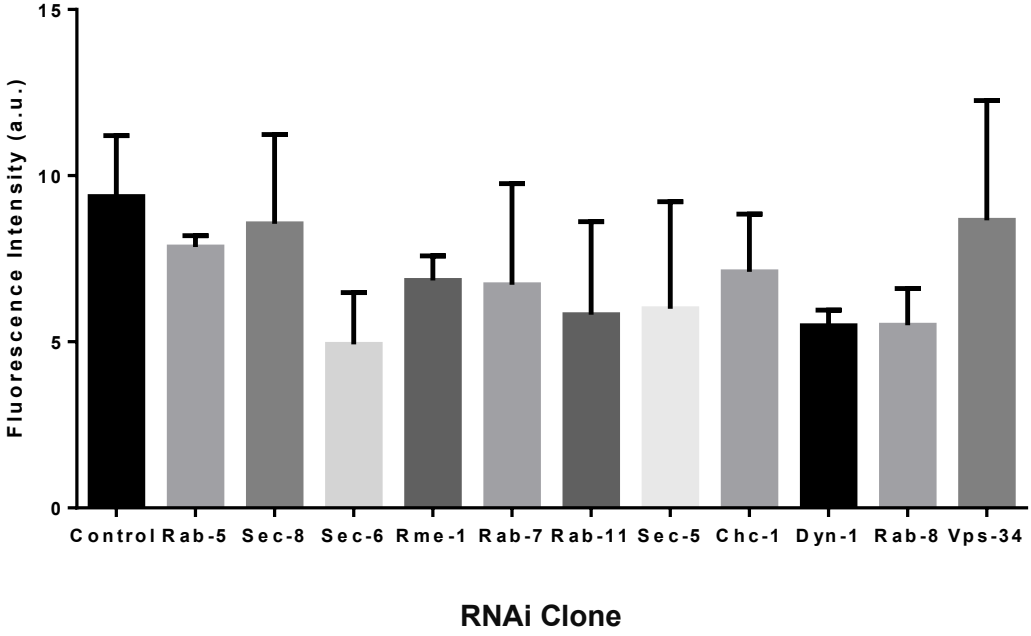

Figure 5-4: Fluorescence intensity of GFP-AQP-4 following 24-hours on RNAi plates to knock down membrane trafficking at different steps. Graphs are shown as mean ± SEM, n=10 for each time experiment which was repeated 3 times.

Figure 5-4 shows that there were small changes in fluorescence intensity between the control and each RNAi experiment over the 24-hours. The one-way ANOVA carried out demonstrated that there were no significant changes in AQP-4-GFP fluorescence intensity at the apical

membrane between the control worms and worms where each of the knocked down trafficking regulators was knocked down by RNAi.

5.5 Tonicity-induced translocation of GFP-AQP-4 in dissected *C. elegans* intestines

In the cell work described in Chapters 3 and 4, the changes in AQP4 translocation were very rapid. However, in *C. elegans*, this was only seen after 48-hours, suggesting the need for an experimental setup to match that of the mammalian cells. The previous experiments were carried out on live worms, however, in order to optimise the assay to screen for changes in localisation of GFP-AQP-4, dissected *C. elegans* intestines were used to determine if there was a rapid response to different tonicities. This was investigated using fluorescence microscopy using the GFP-tagged protein. The worms were grown on isotonic plates and then dissected in either isotonic, hypertonic or hypotonic dissection buffers for 10 minutes, fixed and images were taken. The osmolarity of each buffer was measured and found to be as follows: 0mM NaCl was 103 mOsm/kg, 100mM NaCl was 158 mOsm/kg, and 400mM NaCl was 428 mOsm/kg.

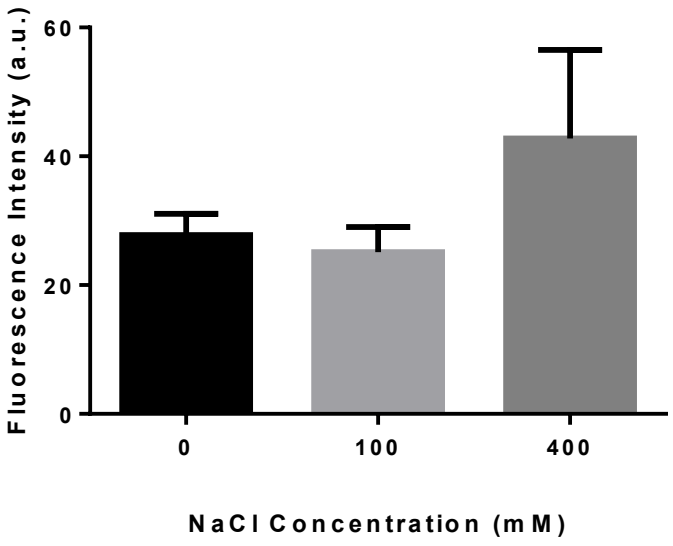

Figure 5-5: Fluorescence intensity of GFP-AQP-4 following 10-minute dissection in hypotonic, isotonic and hypertonic dissection buffers. Graphs are shown as mean ± SEM, n=10 for each concentration, which was repeated 3 times

Figure 5-5 shows that there were small changes in fluorescence intensity between hypotonic (0 mM) and isotonic (100 mM) conditions and between hypertonic (400 mM) and isotonic (100

mM) conditions. The one-way ANOVA carried out showed that there was no significant change between each of the dissection buffers.

5.6 RNAi knockdown of membrane trafficking regulators followed by tonicity-induced translocation of GFP-AQP-4 in dissected *C. elegans* intestines

Figure 5-4 showed there was a decrease in GFP-AQP-4 fluorescence intensity when *rab-5* and *rab-11* were knocked down with RNAi, as was seen in Chapters 3 and 4. These two clones were chosen as the starting point for examining the membrane trafficking of GFP-AQP-4. The proteins are found along two different parts of the membrane trafficking pathway. The function of RAB-5 involves membrane fusion during endocytosis, between endocytic vesicles and early endosomes. The function of RAB-11 is as an apical recycling regulator.

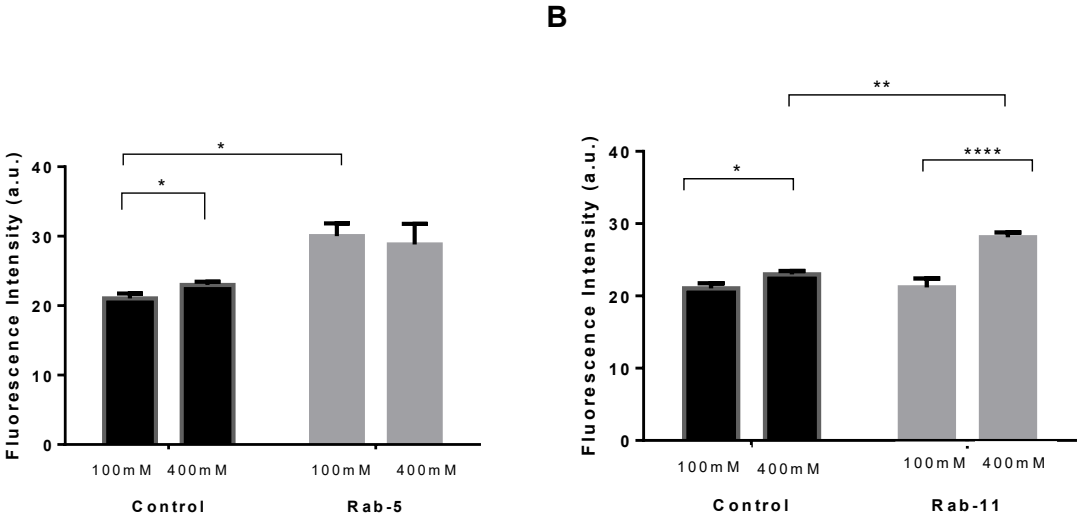

Figure 5-6: Fluorescence intensity of GFP-AQP-4 following gene knockdown for 24-hours followed by dissection in isotonic and hypertonic conditions. The hypertonic condition for Rab-5 (A) showed an increase in fluorescence intensity compared to the control and the hypertonic condition for Rab-11 (B) showed an increase in fluorescence intensity compared to the control. The isotonic condition for Rab-5 (A) showed an increase in fluorescence intensity and the isotonic condition for Rab-11 (B) showed similar values to the control. Graphs are shown as mean ± SEM, n=10 for each concentration and experiment which were repeated 3 times.

Figure 5-6 showed that there were changes in fluorescence intensity of GFP-AQP-4 following gene knockdown of both *rab-5* and *rab-11* for 24-hours followed by dissection in isotonic and hypertonic conditions. A one-way ANOVA showed that there was a significant increase between the isotonic condition for *rab-5* compared to the isotonic condition for the control and a significant change between the hypertonic condition for *rab-11* compared to the hypertonic

condition of the control. There were also significant changes between the control and between both the conditions of *rab-11*.

5.7 RNAi control experiments

The membrane trafficking regulators that were used in the RNAi experiments, were tested in the YP170 strain as a control experiment (Figure 5-7). In *C. elegans* yolk protein expression is induced at L4 stage and continues throughout adult life. Yolk protein is secreted from the intestine into the body cavity and endocytosed by oocytes that express yolk protein receptor. Yolk protein is further stored in vesicles that are in oocytes and later in the embryos. RFP-tagged YP170 is used to visualise any disruptions to endocytosis or secretion of the protein, which can be seen through the abnormal accumulation of yolk protein (Figure 5-7) either in the intestine (indicative of impaired secretion) or the body cavity (indicative of impaired endocytosis).

In *C. elegans* the RNAi is usually confirmed by the presence of a phenotype. RFP-YP170 essay is well established endocytosis essay and has previously confirmed that the clones used in this study demonstrated yolk trafficking phenotype (Balklava et al, 2007). This experiment was therefore done to confirm that the RNAi clones used were functioning as expected namely, the same clones as the ones that were used for the experiments seen in Figures 6-4 and 6-6.

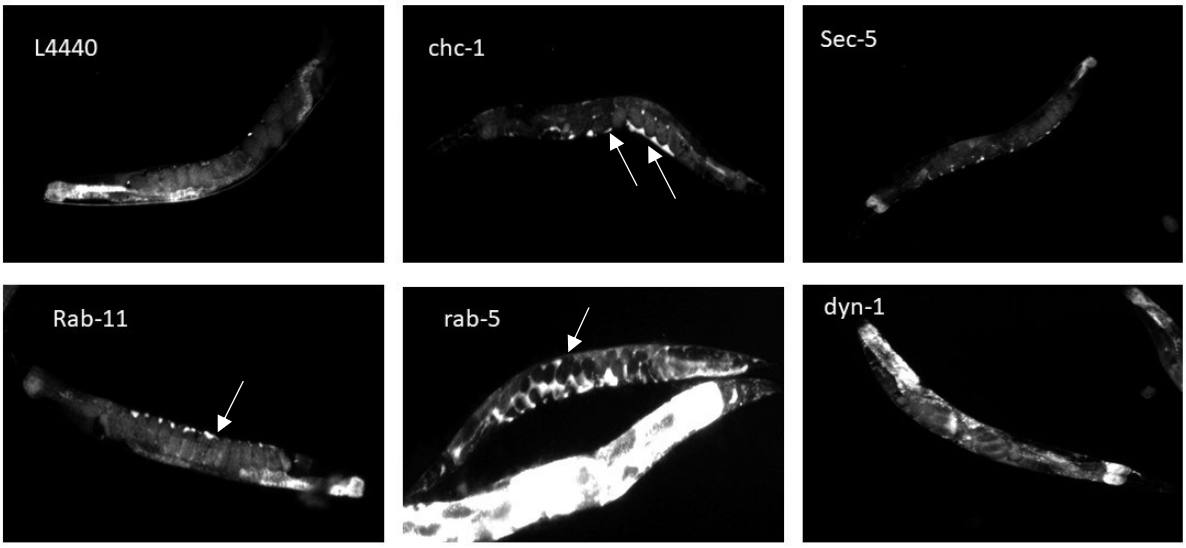

Figure 5-7: Localisation of YP170-RFP in the *C. elegans* body cavity. Images were taken following 24-hours on RNAi plates to knock down key membrane trafficking regulators. The white arrows indicate examples of abnormal accumulation of the yolk protein.

Figure 5-7 shows the control (L4440) phenotype expressing RFP in oocytes, with a change in RFP expression for each of the RNAi knock down experiments and excess yolk in the body

cavity. The knockdown of *rab-11* and *sec-5* was weakest, with only some excess yolk compared to the control.

5.8 Discussion

The trafficking of AQP-4 is of significance in terms of cytotoxic oedema due to its function as a water channel but also because it can be targeted for developing future oedema therapies or related water transport issues such as meningitis. Whilst hypotonicity is a key component of cytotoxic oedema, the chronic effects of hypo- and hypertonic states on astrocytes have severe consequences on brain function such as disability or even death. Therefore, an understanding of the role of AQP4 in both would be beneficial. However, on a molecular level, the use of a high throughput screen to identify trafficking modulators of AQPs could be an important development. The similarities seen in the translocation mechanisms of most AQPs would be enough to begin examining the possibility of *C. elegans* as a model to screen for this. The experiments in this chapter involved using *C. elegans* to investigate the localisation, quantify the expression and characterise the movement of GFP-AQP-4 in response to changes in tonicity, as well as the potential for using the worms as a high-throughput model. In order to understand this, *C. elegans* were grown on either isotonic, hypotonic or hypertonic plates or dissected in isotonic or hypertonic buffers. In addition to the response of GFP-AQP-4 fluorescence intensity in response to changes in tonicity, the gene knockdown of certain membrane trafficking regulators was investigated using RNAi. All of this was done with the aim of determining whether *C. elegans* is a viable model to investigate GFP-AQP-4 trafficking any further. The GFP-tagged AQP-4 was an ideal target to undergo this type of screening, due to the ease with which *C. elegans* can be imaged using fluorescence microscopy.

The fluorescence microscopy carried out showed the expression of GFP-AQP-4 in the apical membrane of the intestine (figures 5-1 and 5-2). There was a significant increase in the fluorescence intensity following 48-hour exposure to the hypertonic conditions, with a non-significant decrease in the intensity following exposure to hypotonic conditions (Figure 5-3A). These changes in fluorescence intensity indicate that a change in gene expression may be occurring due to the amount of time between initial plating on the different tonicities and when the images were taken. The western blot that was done showed changes in band density between each of the three conditions – isotonic, hypotonic and hypertonic (Figure 5-3B) – further indicating that there are changes to gene expression that are happening. However, there were technical issues with the western blot process, and even though 20 worms were loaded into each lane to achieve equal loading as seen in Figure 5-3B, this still needs to be repeated with a loading control in order to confirm the result seen. The previous attempts at using an actin antibody was unsuccessful and did not yield any detectable bands.

In mammalian cells, previous studies have shown that an increase in fluorescence intensity occurs when cells expressing human AQP4-GFP are exposed to a hypotonic condition (Kitchen *et al*, 2015), and this was seen in the work carried out in previous chapters. This change occurred over a very short time (30 seconds), clearly indicating a change in localisation. The changes seen in the worms in response to hypertonicity as opposed to a hypoosomolarity suggest that there may be another osmoregulatory mechanism present in the worms, and that GFP-AQP-4 may not be an essential part of whole animal water homeostasis in worms, a similar result to that seen by Huang *et al* (2015).

The work discussed above was all done on live worms, over 24-hours and 48-hours. As mentioned previously, potentially speeding up the process could show whether there are changes other than gene expression, namely changes to localisation of GFP-AQP-4 that have occurred in response to the changes in tonicity.

When comparing to previously published data, the results from both live worms and dissected intestines show a different effect. Kitchen *et al* (2015) described an increase in human AQP4 expression when cells were moved from an isotonic medium to a hypotonic medium.

The next method used to investigate the response of GFP-AQP-4 in response to changes in tonicity was done on dissected intestines. Most of the same concentrations were used as on the live worms. The results seen in the fluorescence intensity for 53 mM and 100 mM in the dissected intestines were similar, so 100 mM was used as the isotonic concentration, leaving 400 mM as hypertonic and 0 mM as hypotonic (Figure 5-5). *C. elegans* were dissected in buffers with different concentrations of NaCl, meaning the cells of the intestines were directly exposed to the buffers with different tonicities for only 10 minutes. The pattern of results was similar to that seen *in vivo*, with an increase between the hypertonic and the isotonic and no real difference between the hypotonic and isotonic (Figure 5-5). However, despite the changes being observed within 10 minutes, the actual units of fluorescence were much lower in the dissected samples compared to the units of the live samples. This was similar to what was seen in the cell work in terms of timings of the change in AQP4 surface expression changing, but in *C. elegans* this was seen in hypertonic as opposed to hypotonic buffer.

Next, in order to begin investigating the potential membrane trafficking mechanism of GFP-AQP-4, RNAi was applied to some of the membrane trafficking components that could be involved. The changes seen in the live *C. elegans* were not significant (Figure 5-4), however, they provided a starting point for which genes to target for the RNAi in dissected intestines.

Thus, *rab-5* and *rab-11* were knocked down and the changes seen in fluorescence intensity indicated that the RAB-5 protein is involved in the trafficking of GFP-AQP-4 (Figure 5-6), while RAB-11 is not involved in the mechanism.

Rab-5 plays a role in membrane fusion during early endocytosis, between endocytic vesicles and early endosomes (Sato, 2014). The increase of GFP-AQP-4 fluorescence intensity seen between *rab-5* and the control for isotonic conditions was significant, whereas the increase of GFP-AQP-4 fluorescence intensity seen between *rab-5* and the control for hypertonic conditions was not. The slight decrease seen between the isotonic condition and hypertonic condition for *rab-5* was not significant, indicating that there was no real effect of the change in tonicity to the expression, only the knock down of the gene. However, the overall increase of GFP-AQP-4 fluorescence intensity for *rab-5* (Figure 5-6A) suggests an accumulation of it at the apical membrane, indicating the potential role of Rab-5 as a transporter of GFP-AQP-4 to the early endosome. A similar mechanism to the one that could potentially be occurring with GFP-AQP-4 has been seen in AQP2 transport, where Rab5-positive vesicles contribute to the movement intracellularly from the membrane (Yui *et al.,* 2013).

The results of the RAB-11 experiment also showed a significant increase of GFP-AQP-4 fluorescence intensity when compared to the control for hypertonic conditions (Figure 5-6B), however there did not seem to be a significant difference of GFP-AQP-4 fluorescence intensity between the control and *rab-11* isotonic conditions. The increase of GFP-AQP-4 fluorescence intensity for *rab-11* (Figure 5-6B) again suggests an accumulation of it at the apical membrane. RAB-11 functions as an apical recycling regulator and so knocking this down was an opportunity to determine whether the recycling of GFP-AQP-4 was dependent on this protein. However, RAB-11 playing a role in the trafficking of GFP-AQP-4 is not likely, due to only a small difference between that and the control (Figure 5-6B). A Rab11 dependent recycling pathway is essential for the mechanism seen with mammalian AQP-2, with Rab11-positive vesicles (Vukićević *et al.*, 2016). One consideration when reviewing the results, was the control experiment carried out on the YP170 strain, which showed a very small qualitative difference between *rab-11* and the control (Figure 11). This could mean that the bacterial clone used was not functioning properly and perhaps there is a different conclusion that can be drawn if a new one is used, or that the RNAi would need to be carried out over 48-hours instead of just 24-hours.

The use of live *C. elegans* as a model has some advantages and disadvantages. The time taken to complete each of the experiments – 48-hours overall – is not conducive to a quick screen and would mean gene expression changes could not be excluded. Additionally, the RNAi experiments carried out in live worms had large error bars (Figure 5-4), which indicate the precision of the results was low. Instead, using the dissected intestines is a more appropriate way to examine changes in localisation. Firstly, because the two experiments (tonicity change and RNAi) can be combined, secondly by doing RNAi and then dissecting intestines, the intestinal cells are only exposed for ten minutes to changes in tonicity and offers

a quicker way of screening through the membrane trafficking regulators and their potential role in GFP-AQP-4 trafficking and finally because of the similarity between the results of the dissected intestines compared to the live worms. However, the dissection of worms was overall more time-consuming and would not be applicable as a high-throughput screening method.

There are several short-term experiments that would be a useful addition to this piece of work. Firstly, the results seen when using RNAi in dissected *C. elegans* intestines were only for *rab-11* and *rab-5* knockdown. The next steps would be to knock down *chc-1*, *dyn-1* and *sec-5*, which regulate different steps of the membrane trafficking pathway and determine if these play a role in GFP-AQP-4 trafficking. The completion of the western blot, following any more appropriate troubleshooting, to determine whether there is indeed a change in expression as opposed to localisation in GFP-AQP-4 following 48-hour exposure to different tonicities. Due to the fact that the role of GFP-AQP-4 in whole animal osmoregulation and the differences to those from mammalian cells *in vitro*, the role of GFP-AQP-1 in *C. elegans* should also be examined further to determine whether or not it plays a different role in the intestine compared to GFP-AQP-4.

6. General Discussion

The aim of this thesis was to examine the membrane trafficking of aquaporin-4 (AQP4) and determine the key molecular players in this process. This was done through the use of HEK293 cells as a model, primary human astrocytes as a physiologically relevant model, and *C. elegans* as an *in vivo* model. Throughout the thesis the importance of AQP4 in the CNS, both under homeostatic conditions and disease states, has been highlighted. Despite there being a more recent body of work describing the effects of disrupting AQP4 subcellular relocalisation, it is still not clear how this relocalisation occurs. The already well-described trafficking of aquaporin-2 (AQP2) was used as an example to begin selecting relevant targets, and the cell lines were utilised to investigate the main trafficking pathways that were thought to be contributing to the movement of the water channel from within the cytosol to the plasma membrane. Additionally, the *in vivo* model was investigated in the screening of potential membrane trafficking regulators, in order to achieve a faster determination of important components of the AQP4 vesicular trafficking mechanism.

6.1 *In vitro* studies

Membrane protein trafficking mechanisms are complex, requiring several key regulators and key steps in order for the process to be completed successfully. The AQP trafficking pathways differ between the water channel, with each depending on different triggers and different mechanisms to contribute to the movement from within the cell to the plasma membrane and *vice versa.* Whilst some of this is known information, a large part of the vesicular trafficking of AQPs is unknown. Despite there being a few AQPs with well-described trafficking mecahnisms, such as AQP1 and AQP2, the regulation of these is not the same as that of AQP4. Using the model of AQP2 trafficking, which has been elucidated to a much greater degree than AQP4, the following similarities can be inferred from the data presented in Chapters 3 and 4.

Figure 6-1 shows a comparison between the known elements of AQP2 internalisation and recycling and the investigated pathways of AQP4.

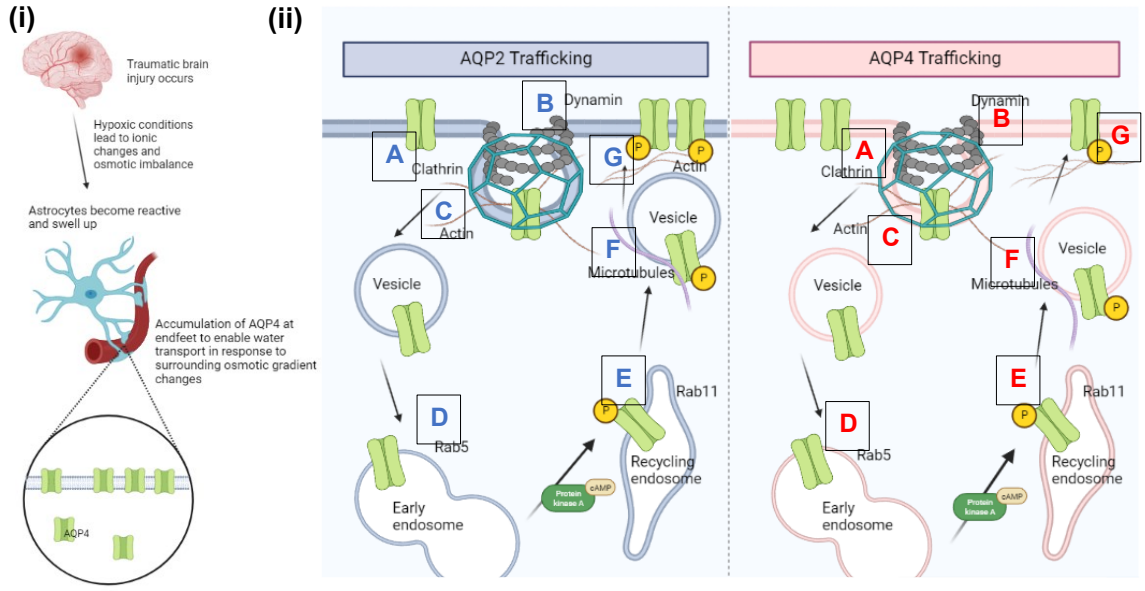

Figure 6-1: A simplified breakdown of how AQP4 may be triggered to move to the membrane following TBI (i), and a comparison of known elements of the trafficking mechanism of AQP2 and the trafficking mechanisms of AQP4 established through the work of Chapter 4 (ii). Blue letters represent the AQP2 pathway, and red letters represent the AQP4 pathway (Created with Biorender.com).

Beginning from the plasma membrane, AQP2 is internalised through clathrin-mediated endocytosis (Figure 6-1A). It has been shown to colocalise with clathrin in clathrin-coated pits (Noda & Sasaki, 2005; Sun et al., 2002). In Chapters 3 and 4, the internalisation of AQP4-eGFP in HEK293 cells, and endogenous AQP4 in primary human astrocytes was shown to not be disrupted when clathrin-independent endocytosis was blocked, indicating that perhaps the internalisation is CME-dependent like AQP2, which is why the involvement of clathrin in AQP4 internalisation is still to be further confirmed (Figure 6-1A). In 2001 it was suggested that there is evidence of clathrin playing a role in AQP4 internalisation through the AP2-adaptor complex interacting directly with the water channel (Madrid et al., 2001). Also, more recently, it was shown that the internalisation of AQP4 can be regulated by clathrin interacting with dynamin, due to the increase in AQP4 cell surface expression when chlorpromazine was used to inhibit the formation of clathrin-coated pits (Tham, Joshi & Moukhles, 2016). However, it has also been shown that AQP2 internilsation may occur through association with caveolin-1, as both were seen to be present in caveolar structures (Aoki et al., 2012). This caveolin-1 interaction has been seen with AQP4 as well *in vivo*. Mice with a knockout of caveolin-1 showed a decrease in AQP4 expression at the membrane after ischemia (Filchenko et al., 2020).

In CME, and CIE involving caveolae, dynamin is a key mediator of internalisation. It has been shown in a number of studies that AQP2 is dependent on dynamin for endocytosis (Figure 6-1B), both by inhibition of dynamin through the use of small molecules, or with dominant

negative forms of the GTPase (Dollerup et al., 2015; Sun et al., 2002). This could explain why, despite disruption of CIE, AQP4 is marginally internalised (although not to a significant level), as seen in Chapters 3 and 4. The dynamin function is not impaired when filipin is used, so the turnover may be slower, but the internalisation of AQP4 can still occur through the CME pathway. This also suggests that the AQP4 channel is going through a constant turnover, cycling between the cytosol and the plasma membrane. However, in Chapter 3, when dynasore was used to inhibit dynamin function, there was an increase of AQP4-eGFP at the surface under isotonic conditions, and no change to that surface expression under hypotonic conditions or when isotonicity was restored. This was seen again with endogenous AQP4 in Chapter 4, where the cell surface expression of AQP4 did not change under different tonicities, and the percentage internalisation of AQP4 from the cell surface was minimal. These results agree with what has been described before in terms of dynamin involvement in AQP4 internalisation (Tham, Joshi & Moukhles, 2016). It is highly likely that whilst AQP4 may not go through just CIE or CME, the internalisation process is dependent on dynamin function (figure 6-1B).

The actin cytoskeleton is involved in the endocytic process. As mentioned in Chapter 1, actin remodelling contributes to CME, through remodelling of the filaments, contributing to membrane invagination and aiding in vesicle fission. With regards to AQP2 internalisation, the actin cytoskeleton was proposed to play a role in this, but it was subsequently shown that inhibiting actin polymerisation both through cytochalasin D treatment and lantrunculin B treatment, did not affect AQP2 trafficking (Tajika et al., 2005). However, a more recent publication proposed that the conversion of F-actin to G-actin was what allowed AQP2-positive vesicles to be internalised (Wang et al., 2017), showing that in fact AQP2 endocytosis can be affected by the actin cytoskeleton structure (Figure 6-1C). When examining the role of actin in the internalisation of AQP4, cytochalasin D was selected as the actin polymerisation inhibitor, and jasplakinolide as the actin polymerisation stabiliser. The results seen in Chapter 3, show that even when treated with cytochalasin D, there is no change in the cell surface expression of AQP4-eGFP when hypotonicity is introduced, or when isotonicity is restored. This suggests that when actin is unable to polymerise, and F-actin cannot be formed, AQP4 is unable to move both to and from the surface of the cell. This was also seen in endogenous AQP4 in Chapter 4 where the internalisation percentage of AQP4 when isotonicity was restored to the hypotonic cells was very low. With the stabilisation of the actin filaments, the movement of AQP4-eGFP as seen in Chapter 3 and the endogenous AQP4 in Chapter 4 was not disrupted under hypotonic conditions – the increase expected under untreated conditions was seen – and the cell surface expression decreased to basal levels once the cells were placed back in

an isotonic environment. These results suggest that unlike for AQP2, the actin cytoskeleton, and perhaps more specifically F-actin, is necessary for AQP4 internalisation (Figure 6-1C).

Once the vesicle containing the AQP2 is internalised, it is localised to a Rab5-positive early endosome (Wong et al., 2020; Wang et al., 2020). Rab5 is required for endosome biogenesis, and is the Rab GTPase found on the early endosome. The images shown in Chapter 3, and subsequent analysis, agreed with this where HEK293 cells transiently transfected with AQP2-GFP were shown to colocalise with Rab5 (Figure 6-1D). Due to the similarities in the trafficking mechanisms of aquaporins, it was proposed that Rab5 would also colocalise with AQP4. In Chapter 3, HEK293 cells transiently transfected with AQP4-eGFP were shown to colocalise with Rab5 (Figure 6-1D).

Following the sorting that occurs in the early endosome, AQP2 is targeted to the recycling endosome, where Rab5 switches to Rab11 (Sönnichsen et al., 2000). This conversion has not been studied extensively, but has been shown to be required for a functioning recycling process to occur (Mani et al., 2016; Haas et al., 2005; Sun et al., 2012). It has been shown previously that AQP2 colocalises with Rab11 in vesicles (Chen et al., 2012; Barile et al., 2005; Nedvetsky et al., 2007). This is something that was also shown in Chapter 3, where HEK293 cells transiently transfected with AQP2-GFP were shown to colocalise with Rab11 (Figure 6-1E). Using this knowledge of AQP2 recycling, in Chapter 3 HEK293 cells transiently transfected with AQP4-eGFP were shown to colocalise with Rab11 (Figure 6-1E). This again suggests that the AQP4 is constantly cycling from the plasma membrane to the cytosol and *vice versa*.

Microtubules have been shown to be an important component of AQP2 trafficking (Figure 6-1F). They have been associated with both the internalisation of the water channel as well as targeting to the cell surface (Breton & Brown, 1998; Noda & Sasaki, 2005; Tajika et al., 2005). When AQP4 relative membrane expression was measured in Chapter 3 in cells treated with nocodazole, it prevented AQP4 membrane localisation in response to the hypotonicity trigger and then prevented AQP4 from returning to basal levels after isotonicity was restored. When microtubules were stabilised with paclitaxel, it prevented AQP4 from localising to the membrane in response to hypotonicity. This was different to what was seen in Chapter 4 with endogenous AQP4 expression at the cell surface. The nocodazole did not disrupt the movement to the plasma membrane from the cytoplasm, but instead only disrupted the internalisation. This could indicate that the dynamic movement of the microtubules is essential to AQP4 movement, but that the microtubules are not needed for movement to the plasma membrane but are needed for the internalisation of the AQP4 (Figure 6-1F). This would agree with data shown for AQP2, where nocodazole treatment at high concentrations gave rise to a

change in the distribution of AQP2 vesicles, with an increase of vesicles in the cytoplasm (Tajika et al., 2005).

Apart from the involvement of the actin cytoskeleton in internalisation of AQP2, the movement of AQP2-positive vesicles are also dependent on actin cytoskeleton dynamics (Figure 6-1G). It was first proposed that the actin cytoskeleton, and more specifically the F-actin state, was required to depolymerize to allow for the movement of AQP2 to the plasma membrane (Noda et al., 2008). However, it has been shown that AQP2 is in fact the trigger for this depolymerization, which is a consequence of the AQP2 movement (Yui et al., 2011). Something different was seen with the AQP4-eGFP in Chapter 3 and the endogenous AQP4 in Chapter 4. When actin was depolymerised with cytochalasin D, there was no movement to the membrane when hypotonicity was used as a trigger. However, when actin was polymerised, there was no disruption to the translocation mechanism in response to hypotonicity or a return to isotonicity. This suggests that actin would still need to be polymerised for there to be a movement of AQP4 to the surface (Figure 6-1G) – this still agrees with the fact that AQP2 also requires some element of the actin cytoskeleton for the translocation to the plasma membrane to occur. It should be noted that the experiments were carried out in different cell systems, which means that whilst there are common elements of trafficking, there may be differences too.

Finally, one thing to consider for all of the *in vitro* work completed, is that there was no measurement of water permeability. The assumption that there is an increase in the basal level of AQP4 at the plasma membrane due to the hypotonic changes was not fully investigated. The cell swelling aspect of an increase in AQP4 at the membrane is one that has been shown before to suggest that there is a functional water permeability change (Kitchen et al., 2015). However, this was not examined here. The results of both Chapter 3 and Chapter 4 suggest that there is a need for further determination of the water permeability of the cells, both without the compound treatments, and with the treatments. The solute permeability of the astrocytes was also not the focus of the experiments, but would be an important determinant of the polarization of the cells in a physiologically relevant context, and would most likely assist in the translocation of AQP4 (Lopes et al., 2018). The astrocytic osmotic permeability is most likely affected by the increase or decrease of AQP4 in the plasma membrane, as the water channels increase the permeability of the membranes (King, Yasui & Agre, 2000). However, with the addition of compounds that can interact with elements of the cell structure that can disrupt the permeability, there needs to be consideration of additional factors, and this is something that will be discussed in the future work.

6.2 *In vivo* studies

The work carried out in Chapter 5 gave an insight into the relocalisation of AQP-4 in response to changes in tonicity. Whilst the results were the reverse of those seen in the mammalian cells – hypotonicity versus hypertonicity as the subcellular relocalisation trigger – this could still provide an insight into developing a screening method for membrane trafficking regulators of AQP4. The necessity to use dissected intestines slowed down the process, and this would not be conducive to a high-throughput screening method. However, the understanding that whilst there are what seem to be expression changes over the 24- and 48-hour whole-worm experiment, these changes are also seen after just ten minutes' exposure to a hypertonic buffer.

The human AQP4 is not homologous to the *C. elegans* AQP-4, but its use as a model cannot be disregarded. In previous work, the model of anoxia was used in C. elegans to mimic oedema formation, with results that strongly suggest that an *aqp-4* deletion can increase survival and reduce water permeability (LaMacchia & Roth, 2015). This suggests that the results seen in animal studies, specifically knockout mice, can be mirrored in another model organism (Verkman et al., 2006). This decrease in the water intake of the worm is of interest, because of the relevance to the effects of oedema formation. Once swelling occurs, a treatment plan is not always feasible and this leads to severe consequences down the line – removing the aqp-4 in the worm increased survival, something that would not be as clear-cut in a mammalian system due to the need for a bidirectional movement of water and for it to be cleared out.

Finally, to address the results in association with the aims set out in the introduction of the thesis:

1. The trafficking mechanism of AQP4 was further dissected through the use of HEK293 cells. Through this it was determined that the key contributors to the vesicular movement of AQP4 in this system were dynamin, microtubules, and actin.
2. The HEK293 data were used to investigate the membrane trafficking regulators human primary cortical astrocytes, and the results showed that dynamin and actin still play a role in the vesicular movement, but microtubules are not necessary for this.
3. It was determined that *C. elegans* cannot be used as an appropriate *in vivo* model for screening potential trafficking partners of AQP4.

6.3 Future Work

Following on from the work carried out in Chapters 3 and 4, there are several subsequent studies that could be carried out to deepen our understanding of the AQP4 vesicular trafficking mechanism. First, it would be useful to gain an understanding of whether endogenous Rab5 and Rab11 function in a similar way with endogenous AQP4. This, along with an additional step of examining Rabs involved in the lysosomal pathway would give a more well-rounded view of the movement of AQP4 from internalisation to recycling, to degradation. The challenge of how to follow these up would be that there is a very minimal availability of Rab-specific inhibitors.

Additionally, an examination of the effect of different compounds on the same elements of the membrane trafficking pathways could aid in deciphering more specifically the key players in the movement of AQP4. This could be, for example an alternative actin polymerisation inhibitor such as colcemid, or cytochalasin B to determine which part of the actin disruption is in fact affecting the AQP4 translocation to and from the membrane. Additionally, transfecting HEK293 cells with fluorescently labelled tubulin and actin and monitoring the changes in structure over time, in response to different concentrations of the compounds over a longer time period, in the presence of AQP4-eGFP, would also demonstrate whether these changes affect AQP4 translocation.

Something else to consider would be to measure the water permeability of cells when treated with the compounds. The increase in AQP4 cell surface expression seen at the plasma membrane, even under isotonic conditions, could be caused by an increase in water permeability of the treated cells.

Following on from the work carried out in cell lines, the *in vivo* model of *C. elegans* could be expanded further. Whilst the results showed a change in AQP4 surface expression under a hypertonic condition, the membrane trafficking regulators that were involved were still similar to those seen to affect AQP4 in the HEK293 and primary astrocytes. Using this, optimisation experiments could be used to develop a high-throughput screen using *C. elegans*, as long as the right conditions were selected. Additionally, an exploration of the other 6 AQPs and their response to different tonicities combined with RNAi would be of use to determine the similarities across the water channels in *C. elegans.*

Moving forward from the work carried out in Chapter 5, it would be particularly beneficial to understand how the AQP1 in *C. elegans*, which is found in the basolateral membrane of the intestine, is expressed in response to changes in tonicity. Both AQP1 and AQP4 may not be needed for osmoregulation but uncovering whether they function together or irrespective of each other by knocking them down would also be of interest.

References

Akinc, A., Thomas, M., Klibanov, A.M. & Langer, R. (2005) Exploring polyethylenimine-mediated DNA transfection and the proton sponge hypothesis. *The Journal of Gene Medicine.* 7 (5), 657–663. doi:10.1002/jgm.696.

Alberts, B., Johnson, A., Walter, P., Lewis, J., et al. (2008) *Molecular Biology of the Cell*. 5Rev Ed edition. New York, Garland Publishing Inc,US.

Almeida-Souza, L., Frank, R.A.W., García-Nafría, J., Colussi, A., Gunawardana, N., Johnson, C.M., Yu, M., Howard, G., Andrews, B., Vallis, Y. & McMahon, H.T. (2018) A Flat BAR Protein Promotes Actin Polymerization at the Base of Clathrin-Coated Pits. *Cell*. 174 (2), 325-337.e14. doi:10.1016/j.cell.2018.05.020.

Amiry-Moghaddam, M. (2004). Alpha syntrophin deletion removes the perivascular but not the endothelial pool of aquaporin-4 at the blood-brain barrier and delays the development of brain oedema in an experimental model of acute hyponatremia. The FASEB Journal.

Aoki, T., Suzuki, T., Hagiwara, H., Kuwahara, M., Sasaki, S., Takata, K. & Matsuzaki, T. (2012) Close Association of Aquaporin-2 Internilsation with Caveolin-1. *Acta Histochemica et Cytochemica*. 45 (2), 139–146. doi:10.1267/ahc.12003.

Badaut, J., Lasbennes, F., Magistretti, P.J. & Regli, L. (2002) Aquaporins in Brain: Distribution, Physiology, and Pathophysiology. *Journal of Cerebral Blood Flow & Metabolism*. 22 (4), 367–378. doi:10.1097/00004647-200204000-00001.

Balklava, Z., Pant, S., Fares, H. & Grant, B.D. (2007) Genome-wide analysis identifies a general requirement for polarity proteins in endocytic traffic. *Nature Cell Biology*. 9 (9), 1066–1073.

Balklava, Z. and Sztul, E. (2013). Studying Membrane Trafficking in the Worm C. elegans by RNA Interference. *Methods for Analysis of Golgi Complex Function*, pp.51-68.

Barile, M., Pisitkun, T., Yu, M.-J., Chou, C.-L., Verbalis, M.J., Shen, R.-F. & Knepper, M.A. (2005) Large-Scale Protein Identification in Intracellular Aquaporin-2 Vesicles from Renal Inner Medullary Collecting Duct. *Molecular & cellular proteomics : MCP*. 4 (8), 1095–1106. doi:10.1074/mcp.M500049-MCP200.

Benfenati, V., Caprini, M., Dovizio, M., Mylonakou, M., Ferroni, S., Ottersen, O. and Amiry-Moghaddam, M. (2011). An aquaporin-4/transient receptor potential vanilloid 4 (AQP4/TRPV4) complex is essential for cell-volume control in astrocytes. Proceedings of the National Academy of Sciences, 108(6), pp.2563-2568.

Bitsikas, V., Corrêa, I.R., Jr & Nichols, B.J. (2014) Clathrin-independent pathways do not contribute significantly to endocytic flux S.R. Pfeffer (ed.). *eLife*. 3, e03970. doi:10.7554/eLife.03970.

Bonifacino, J. and Glick, B. (2004). The Mechanisms of Vesicle Budding and Fusion. *Cell*, 116(2), pp.153-166.

Boussif, O., Lezoualc'h, F., Zanta, M.A., Mergny, M.D., Scherman, D., Demeneix, B. & Behr, J.P. (1995) A versatile vector for gene and oligonucleotide transfer into cells in culture and in vivo: polyethylenimine. *Proceedings of the National Academy of Sciences of the United States of America*. 92 (16), 7297–7301.

Brandhorst, D., Zwilling, D., Rizzoli, S.O., Lippert, U., Lang, T. & Jahn, R. (2006) Homotypic fusion of early endosomes: SNAREs do not determine fusion specificity. *Proceedings of the National Academy of Sciences*. 103 (8), 2701–2706. doi:10.1073/pnas.0511138103.

Breton, S. & Brown, D. (1998) Cold-induced microtubule disruption and relocalization of membrane proteins in kidney epithelial cells. *Journal of the American Society of Nephrology: JASN*. 9 (2), 155–166. doi:10.1681/ASN.V92155.

C. elegans Sequencing Consortium (1998) Genome sequence of the nematode C. elegans: a platform for investigating biology. *Science (New York, N.Y.)*. 282 (5396), 2012–2018. doi:10.1126/science.282.5396.2012.

Carmosino, M., Procino, G., Tamma, G., Mannucci, R., Svelto, M. & Valenti, G. (2012) Trafficking and phosphorylation dynamics of AQP4 in histamine-treated human gastric cells. *Biology of the Cell*. 99 (1), 25–36. doi:10.1042/BC20060068.

Casella, J.F., Flanagan, M.D. & Lin, S. (1981) Cytochalasin D inhibits actin polymerization and induces depolymerization of actin filaments formed during platelet shape change. *Nature*. 293 (5830), 302–305. doi:10.1038/293302a0.

Cassimeris, L.U., Wadsworth, P. & Salmon, E.D. (1986) Dynamics of microtubule depolymerization in monocytes. *The Journal of Cell Biology*. 102 (6), 2023–2032. doi:10.1083/jcb.102.6.2023.

Chen, C.C.-H., Schweinsberg, P.J., Vashist, S., Mareiniss, D.P., Lambie, E.J. & Grant, B.D. (2006) RAB-10 Is Required for Endocytic Recycling in the Caenorhabditis elegans Intestine□D. *Molecular Biology of the Cell*. 17, 12.

Chen, Q., Peng, H., Lei, L., Zhang, Y., Kuang, H., Cao, Y., Shi, Q., Ma, T. and Duan, E. (2010). Aquaporin3 is a sperm water channel essential for postcopulatory sperm osmoadaptation and migration. *Cell Research*, 21(6), pp.922-933.

Chen, Y., Rice, W., Gu, Z., Li, J., Huang, J., Brenner, M.B., Hoek, A.V., Xiong, J., Gundersen, G.G., Norman, J.C., Hsu, V.W., Fenton, R.A., Brown, D. & Lu, H.A.J. (2012) Aquaporin 2 Promotes Cell Migration and Epithelial Morphogenesis. *Journal of the American Society of Nephrology*. 23 (9), 1506–1517. doi:10.1681/ASN.2012010079.

Cheng, X., Chen, K., Dong, B., Yang, M., Filbrun, S.L., Myoung, Y., Huang, T.-X., Gu, Y., Wang, G. & Fang, N. (2021) Dynamin-dependent vesicle twist at the final stage of clathrin-mediated endocytosis. *Nature Cell Biology*. 23 (8), 859–869. doi:10.1038/s41556-021-00713-x.

Chu, H., Huang, C., Ding, H., Dong, J., Gao, Z., Yang, X., Tang, Y. & Dong, Q. (2016) Aquaporin-4 and Cerebrovascular Diseases. *International Journal of Molecular Sciences*. 17 (8), 1249. doi:10.3390/ijms17081249.

Conner, A.C., Bill, R.M. & Conner, M.T. (2013) An emerging consensus on aquaporin translocation as a regulatory mechanism. *Molecular Membrane Biology*. 30 (1), 101–112. doi:10.3109/09687688.2012.743194.

Conner, M.T., Conner, A.C., Brown, J.E.P. & Bill, R.M. (2010) Membrane Trafficking of Aquaporin 1 Is Mediated by Protein Kinase C via Microtubules and Regulated by Tonicity. *Biochemistry*. [Online] 49 (5), 821–823. Available from: doi:10.1021/bi902068b.

Cooper, G.M. (2000) Structure and Organization of Actin Filaments. *The Cell: A Molecular Approach. 2nd edition*. https://www.ncbi.nlm.nih.gov/books/NBK9908/.

Damm, E.-M., Pelkmans, L., Kartenbeck, J., Mezzacasa, A., Kurzchalia, T. & Helenius, A. (2005) Clathrin- and caveolin-1–independent endocytosis : entry of simian virus 40 into cells devoid of caveolae. *Journal of Cell Biology*. 168 (3), 477–488. doi:10.1083/jcb.200407113.

Danziger, J. and Zeidel, M. (2014). Osmotic Homeostasis. Clinical Journal of the American Society of Nephrology, 10(5), pp.852-862.

Dávalos, A., Shuaib, A. and Wahlgren, N. (2000). Neurotransmitters and pathophysiology of stroke: Evidence for the release of glutamate and other transmitters/mediators in animals and humans. Journal of Stroke and Cerebrovascular Diseases, 9(6), pp.2-8.

Day, R., Kitchen, P., Owen, D., Bland, C., Marshall, L., Conner, A., Bill, R. and Conner, M. (2014). Human aquaporins: Regulators of transcellular water flow. *Biochimica et Biophysica Acta (BBA) - General Subjects*, 1840(5), pp.1492-1506.

Denker, B., Smith, B., Kuhajda, F. and Agre, P. (1988). Identification, purification, and partial characterization of a novel Mr 28,000 integral membrane protein from erythrocytes and renal tubules. J. Biol. Chem, 263, pp.15634-15642.

DePina, A.S. & Langford, G.M. (1999) Vesicle transport: the role of actin filaments and myosin motors. *Microscopy Research and Technique*. 47 (2), 93–106. doi:10.1002/(SICI)1097-0029(19991015)47:2<93::AID-JEMT2>3.0.CO;2-P.

Dollerup, P., Thomsen, T.M., Nejsum, L.N., Færch, M., Österbrand, M., Gregersen, N., Rittig, S., Christensen, J.H. & Corydon, T.J. (2015) Partial nephrogenic diabetes insipidus caused by a novel AQP2 variation impairing trafficking of the aquaporin-2 water channel. *BMC Nephrology*. 16 (1), 217. doi:10.1186/s12882-015-0213-3.

Ferguson, S.M., Raimondi, A., Paradise, S., Shen, H., Mesaki, K., Ferguson, A., Destaing, O., Ko, G., Takasaki, J., Cremona, O., O' Toole, E. & De Camilli, P. (2009) Coordinated actions of actin and BAR proteins upstream of dynamin at endocytic clathrin-coated pits. *Developmental cell*. 17 (6), 811–822. doi:10.1016/j.devcel.2009.11.005.

Fiebig, K.M., Rice, L.M., Pollock, E. & Brunger, A.T. (1999) Folding intermediates of SNARE complex assembly. *Nature Structural Biology*. 6 (2), 117–123. doi:10.1038/5803.

Filchenko, I., Blochet, C., Buscemi, L., Price, M., Badaut, J. & Hirt, L. (2020) Caveolin-1 Regulates Perivascular Aquaporin-4 Expression After Cerebral Ischemia. *Frontiers in Cell and Developmental Biology*. 8. doi:10.3389/fcell.2020.00371.

Fourriere, L., Jimenez, A.J., Perez, F. & Boncompain, G. (2020) The role of microtubules in secretory protein transport. *Journal of Cell Science*. 133 (2). doi:10.1242/jcs.237016.

Francesca, B. and Rezzani, R. (2010). Aquaporin and Blood Brain Barrier. Current Neuropharmacology, 8(2), pp.92-96.

Fukuda, A.M. & Badaut, J. (2012) Aquaporin 4: a player in cerebral oedema and neuroinflammation. *Journal of Neuroinflammation*. 9 (1), 279. doi:10.1186/1742-2094-9-279.

Galizia, L., Pizzoni, A., Fernandez, J., Rivarola, V., Capurro, C. and Ford, P. (2012). Functional interaction between AQP2 and TRPV4 in renal cells. Journal of Cellular Biochemistry, 113(2), pp.580-589.

Galperin, E. & Sorkin, A. (2003) Visualization of Rab5 activity in living cells by FRET microscopy and influence of plasma-membrane-targeted Rab5 on clathrin-dependent endocytosis. *Journal of Cell Science*. 116 (23), 4799–4810. doi:10.1242/jcs.00801.

Gleason, A.M., Nguyen, K.C.Q., Hall, D.H. & Grant, B.D. (2016) Syndapin/SDPN-1 is required for endocytic recycling and endosomal actin association in the Caenorhabditis elegans intestine. *Molecular Biology of the Cell*. 27 (23), 3746–3756. doi:10.1091/mbc.E16-02-0116.

Gopal Krishnan, P.D., Golden, E., Woodward, E.A., Pavlos, N.J. & Blancafort, P. (2020) Rab GTPases: Emerging Oncogenes and Tumor Suppressive Regulators for the Editing of Survival Pathways in Cancer. *Cancers*. 12 (2), 259. doi:10.3390/cancers12020259.

Grant, B.D. & Donaldson, J.G. (2009) Pathways and mechanisms of endocytic recycling. *Nature Reviews Molecular Cell Biology*. 10 (9), 597–608. doi:10.1038/nrm2755.

Haas, A.K., Fuchs, E., Kopajtich, R. & Barr, F.A. (2005) A GTPase-activating protein controls Rab5 function in endocytic trafficking. *Nature Cell Biology*. 7 (9), 887–893. doi:10.1038/ncb1290.

Hedfalk, K., Törnroth-Horsefield, S., Nyblom, M., Johanson, U., Kjellbom, P. & Neutze, R. (2006) Aquaporin gating. *Current Opinion in Structural Biology*. 16 (4), 447–456. doi:10.1016/j.sbi.2006.06.009.

Hoffmann, E., Lambert, I. and Pedersen, S. (2009). Physiology of Cell Volume Regulation in Vertebrates. Physiological Reviews, 89(1), pp.193-277.

Holzinger, A. (2009) Jasplakinolide: an actin-specific reagent that promotes actin polymerization. *Methods in Molecular Biology (Clifton, N.J.)*. 586, 71–87. doi:10.1007/978-1-60761-376-3_4.

Horwitz, S.B. (1994) Taxol (paclitaxel): mechanisms of action. *Annals of Oncology: Official Journal of the European Society for Medical Oncology*. 5 Suppl 6, S3-6.

Huang, C.G., Lamitina, T., Agre, P. & Strange, K. (2007) Functional analysis of the aquaporin gene family in Caenorhabditis elegans. *American Journal of Physiology. Cell Physiology*. 292 (5), C1867-1873. doi:10.1152/ajpcell.00514.2006.

Hurley, J.H., Boura, E., Carlson, L.-A. & Różycki, B. (2010) Membrane Budding. *Cell*. [Online] 143 (6), 875–887. Available from: doi:10.1016/j.cell.2010.11.030.

Hutagalung, A.H. & Novick, P.J. (2011) Role of Rab GTPases in Membrane Traffic and Cell Physiology. *Physiological Reviews*. [Online] 91 (1), 119–149. Available from: doi:10.1152/physrev.00059.2009.

Iacovetta, C., Rudloff, E. and Kirby, R. (2012). The role of aquaporin 4 in the brain. *Veterinary Clinical Pathology*.

Irion, U. & Nüsslein-Volhard, C. (2022) Developmental genetics with model organisms. *Proceedings of the National Academy of Sciences*. 119 (30), e2122148119. doi:10.1073/pnas.2122148119.

Ishibashi, K. (2006) Aquaporin subfamily with unusual NPA boxes. *Biochimica et Biophysica Acta (BBA) - Biomembranes*. 1758 (8), 989–993. doi:10.1016/j.bbamem.2006.02.024.

Ishibashi, K., Tanaka, Y. & Morishita, Y. (2021) The role of mammalian superaquaporins inside the cell: An update. *Biochimica et Biophysica Acta (BBA) - Biomembranes*. 1863 (7), 183617. doi:10.1016/j.bbamem.2021.183617.

Jin, B., Rossi, A. and Verkman, A. (2011). Model of Aquaporin-4 Supramolecular Assembly in Orthogonal Arrays Based on Heterotetrameric Association of M1-M23 Isoforms. Biophysical Journal, 100(12), pp.2936-2945.

Jovic, M., Sharma, M., Rahajeng, J. & Caplan, S. (2010) The early endosome: a busy sorting station for proteins at the crossroads. *Histology and histopathology*. 25 (1), 99–112.

Jung, J.S., Bhat, R.V., Preston, G.M., Guggino, W.B., Baraban, J.M. & Agre, P. (1994a) Molecular characterization of an aquaporin cDNA from brain: candidate osmoreceptor and regulator of water balance. *Proceedings of the National Academy of Sciences of the United States of America*. 91 (26), 13052–13056.

Jung, J.S., Preston, G.M., Smith, B.L., Guggino, W.B. & Agre, P. (1994b) Molecular structure of the water channel through aquaporin CHIP. The hourglass model. *Journal of Biological Chemistry*. 269 (20), 14648–14654. doi:10.1016/S0021-9258(17)36674-7.

Kimelberg, H. (2004). Water homeostasis in the brain: Basic concepts. *Neuroscience*, 129(4), pp.851-860.

Kimelberg, H. (2005). Astrocytic swelling in cerebral ischemia as a possible cause of injury and target for therapy. *Glia*, 50(4), pp.389-397.

Kitchen, P., Conner, M., Bill, R. and Conner, A. (2016). Structural Determinants of Oligomerization of the Aquaporin-4 Channel. Journal of Biological Chemistry, 291(13), pp.6858-6871.

Kitchen, P., Day, R., Salman, M., Conner, M., Bill, R. and Conner, A. (2015). Beyond water homeostasis: Diverse functional roles of mammalian aquaporins. Biochimica et Biophysica Acta (BBA) - General Subjects, 1850(12), pp.2410-2421.

Kitchen, P., Day, R.E., Taylor, L.H.J., Salman, M.M., et al. (2015) Identification and Molecular Mechanisms of the Rapid Tonicity-induced Relocalisation of the Aquaporin 4 Channel. *The Journal of Biological Chemistry*. [Online] 290 (27), 16873–16881. Available from: doi:10.1074/jbc.M115.646034.

Kitchen, P., Salman, M.M., Halsey, A.M., Clarke-Bland, C., MacDonald, J.A., Ishida, H., Vogel, H.J., Almutiri, S., Logan, A., Kreida, S., Al-Jubair, T., Winkel Missel, J., Gourdon, P., Törnroth-Horsefield, S., Conner, M.T., Ahmed, Z., Conner, A.C. & Bill, R.M. (2020) Targeting Aquaporin-4 Subcellular Localisation to Treat Central Nervous System Oedema. *Cell*. 181 (4), 784-799.e19. doi:10.1016/j.cell.2020.03.037.

Klatzo, I. (1967). Presidential Address*. Journal of Neuropathology & Experimental Neurology, 26(1), pp.1-14.

Kovtun, O., Dickson, V.K., Kelly, B.T., Owen, D.J. & Briggs, J.A.G. (2020) Architecture of the AP2/clathrin coat on the membranes of clathrin-coated vesicles. *Science Advances*. 6 (30), eaba8381. doi:10.1126/sciadv.aba8381.

Kozono, D., Yasui, M., King, L. and Agre, P. (2002). Aquaporin water channels: atomic structure molecular dynamics meet clinical medicine. Journal of Clinical Investigation, 109(11), pp.1395-1399.

Krause, M. (1999) *Cell Fate Determination in Caenorhabditis elegans | SpringerLink*. 1999. https://link.springer.com/chapter/10.1007/978-3-642-59828-9_16 [Accessed: 22 September 2022].

Kreida, S. & Törnroth-Horsefield, S. (2015) Structural insights into aquaporin selectivity and regulation. *Current Opinion in Structural Biology*. 33, 126–134. doi:10.1016/j.sbi.2015.08.004.

Kumari, S., Mg, S. & Mayor, S. (2010) Endocytosis unplugged: multiple ways to enter the cell. *Cell Research*. 20 (3), 256–275. doi:10.1038/cr.2010.19.

Kwon, T.-H., Frøkiær, J. & Nielsen, S. (2013) Regulation of aquaporin-2 in the kidney: A molecular mechanism of body-water homeostasis. *Kidney Research and Clinical Practice*. [Online] 32 (3), 96–102. Available from: doi:10.1016/j.krcp.2013.07.005.

LaMacchia, J.C. & Roth, M.B. (2015) Aquaporins-2 and -4 regulate glycogen metabolism and survival during hypotonic-anoxic stress in Caenorhabditis elegans. *American Journal of Physiology - Cell Physiology*. 309 (2), C92–C96. doi:10.1152/ajpcell.00131.2015.

Lanzetti, L. (2007) Actin in membrane trafficking. *Current Opinion in Cell Biology*. 19 (4), 453–458. doi:10.1016/j.ceb.2007.04.017.

Lau, A.W. & Chou, M.M. (2008) The adaptor complex AP-2 regulates post-endocytic trafficking through the non-clathrin Arf6-dependent endocytic pathway. *Journal of Cell Science*. 121 (Pt 24), 4008–4017. doi:10.1242/jcs.033522.

Lee, S., Murphy, C. and Kenyon, C. (2009). Glucose Shortens the Life Span of C. elegans by Downregulating DAF-16/FOXO Activity and Aquaporin Gene Expression. Cell Metabolism, 10(5), pp.379-391.

Lelek, M., Gyparaki, M.T., Beliu, G., Schueder, F., Griffié, J., Manley, S., Jungmann, R., Sauer, M., Lakadamyali, M. & Zimmer, C. (2021) Single-molecule localization microscopy. *Nature Reviews Methods Primers*. 1 (1), 1–27. doi:10.1038/s43586-021-00038-x.

Liang, D., Bhatta, S., Gerzanich, V. and Simard, J. (2007). Cytotoxic oedema: mechanisms of pathological cell swelling. Neurosurgical Focus, 22(5), pp.1-9.

Lim, A., Tiu, S., Li, Q. and Qi, R. (2003). Direct Regulation of Microtubule Dynamics by Protein Kinase CK2. Journal of Biological Chemistry, 279(6), pp.4433-4439.

Liu, X., Bandyopadhyay, B., Nakamoto, T., Singh, B., Liedtke, W., Melvin, J. and Ambudkar, I. (2006). A Role for AQP5 in Activation of TRPV4 by Hypotonicity: Concerted Involvement Of Aqp5 And Trpv4 In Regulation Of Cell Volume Recovery. Journal of Biological Chemistry, 281(22), pp.15485-15495.

Longo, P.A., Kavran, J.M., Kim, M.-S. & Leahy, D.J. (2013) Transient Mammalian Cell Transfection with Polyethylenimine (PEI). *Methods in enzymology*. 529, 227–240. doi:10.1016/B978-0-12-418687-3.00018-5.

Macia, E., Ehrlich, M., Massol, R., Boucrot, E., Brunner, C. & Kirchhausen, T. (2006) Dynasore, a cell-permeable inhibitor of dynamin. *Developmental Cell*. 10 (6), 839–850. doi:10.1016/j.devcel.2006.04.002.

Madrid, R., LeMaout, S., Barrault, M.-B., Janvier, K., Benichou, S. & Mérot, J. (2001) Polarized trafficking and surface expression of the AQP4 water channel are coordinated by serial and regulated interactions with different clathrin–adaptor complexes. *The EMBO Journal*. 20 (24), 7008–7021. doi:10.1093/emboj/20.24.7008.

Mani, M., Lee, U.H., Yoon, N.A., Kim, H.J., Ko, M.S., Seol, W., Joe, Y., Chung, H.T., Lee, B.J., Moon, C.H., Cho, W.J. & Park, J.W. (2016) Developmentally regulated GTP-binding protein 2

coordinates Rab5 activity and transferrin recycling. *Molecular Biology of the Cell*. 27 (2), 334–348. doi:10.1091/mbc.e15-08-0558.

Manley, G., Fujimura, M., Ma, T., Noshita, N., Filiz, F., Bollen, A., Chan, P. and Verkman, A. (2000). Aquaporin-4 deletion in mice reduces brain oedema after acute water intoxication and ischemic stroke. Nature Medicine, 6(2), pp.159-163.

Markou, A., Unger, L., Abir-Awan, M., Saadallah, A., Halsey, A., Balklava, Z., Conner, M., Törnroth-Horsefield, S., Greenhill, S.D., Conner, A., Bill, R.M., Salman, M.M. & Kitchen, P. (2022) Molecular mechanisms governing aquaporin relocalisation. *Biochimica et Biophysica Acta (BBA) - Biomembranes*. 1864 (4), 183853. doi:10.1016/j.bbamem.2021.183853.

Mathai, J.C. & Agre, P. (1999) Hourglass Pore-Forming Domains Restrict Aquaporin-1 Tetramer Assembly. *Biochemistry*. 38 (3), 923–928. doi:10.1021/bi9823683.

Maxfield, F.R. & McGraw, T.E. (2004) Endocytic recycling. *Nature Reviews Molecular Cell Biology*. 5 (2), 121–132. doi:10.1038/nrm1315.

Mayor, S. & Pagano, R.E. (2007) Pathways of clathrin-independent endocytosis. *Nature Reviews Molecular Cell Biology*. 8 (8), 603–612. doi:10.1038/nrm2216.

Mazzaferri, J., Costantino, S. & Lefrancois, S. (2013) Analysis of AQP4 Trafficking Vesicle Dynamics Using a High-Content Approach. *Biophysical Journal*. [Online] 105 (2), 328–337. Available from: doi:10.1016/j.bpj.2013.06.010.

McMahon, H.T. & Boucrot, E. (2011) Molecular mechanism and physiological functions of clathrin-mediated endocytosis. *Nature Reviews Molecular Cell Biology*. [Online] 12 (8), 517–533. Available from: doi:10.1038/nrm3151.

Müller, M.P. & Goody, R.S. (2017) Molecular control of Rab activity by GEFs, GAPs and GDI. *Small GTPases*. 9 (1–2), 5–21. doi:10.1080/21541248.2016.1276999.

Nagelhus, E. and Ottersen, O. (2013). Physiological Roles of Aquaporin-4 in Brain. Physiological Reviews, 93(4), pp.1543-1562.

Nedvetsky, P.I., Stefan, E., Frische, S., Santamaria, K., Wiesner, B., Valenti, G., Hammer III, J.A., Nielsen, S., Goldenring, J.R., Rosenthal, W. & Klussmann, E. (2007) A Role of Myosin Vb and Rab11-FIP2 in the Aquaporin-2 Shuttle. *Traffic*. 8 (2), 110–123. doi:10.1111/j.1600-0854.2006.00508.x.

Nicchia, G.P., Rossi, A., Mola, M.G., Procino, G., Frigeri, A. & Svelto, M. (2008) Actin cytoskeleton remodeling governs aquaporin-4 localisation in astrocytes. *Glia*. 56 (16), 1755–1766. doi:10.1002/glia.20724.

NICE (2019) *Overview | Head injury: assessment and early management | Guidance | NICE*. [Online]. 2019. Available from: https://www.nice.org.uk/guidance/CG176 [Accessed: 15 June 2020].

Noda, Y. & Sasaki, S. (2005) Trafficking mechanism of water channel aquaporin-2. *Biology of the Cell*. 97 (12), 885–892. doi:10.1042/BC20040120.

Noda, Y., Horikawa, S., Kanda, E., Yamashita, M., Meng, H., Eto, K., Li, Y., Kuwahara, M., Hirai, K., Pack, C., Kinjo, M., Okabe, S. & Sasaki, S. (2008) Reciprocal interaction with G-actin and tropomyosin is essential for aquaporin-2 trafficking. *Journal of Cell Biology*. 182 (3), 587–601. doi:10.1083/jcb.200709177.

Noda, Y., Horikawa, S., Katayama, Y. & Sasaki, S. (2004) Water channel aquaporin-2 directly binds to actin. *Biochemical and Biophysical Research Communications*. 322 (3), 740–745. doi:10.1016/j.bbrc.2004.07.195.

Oh, P., McIntosh, D.P. & Schnitzer, J.E. (1998) Dynamin at the neck of caveolae mediates their budding to form transport vesicles by GTP-driven fission from the plasma membrane of endothelium. *The Journal of Cell Biology*. 141 (1), 101–114. doi:10.1083/jcb.141.1.101.

Papadopoulos, M. and Verkman, A. (2013). Aquaporin water channels in the nervous system. Nature Reviews Neuroscience, 14(4), pp.265-277.

Phongphanphanee, S., Yoshida, N. and Hirata, F. (2008). On the Proton Exclusion of Aquaporins: A Statistical Mechanics Study. Journal of the American Chemical Society, 130(5), pp.1540-1541.

Potokar, M., Stenovec, M., Jorgačevski, J., Holen, T., Kreft, M., Ottersen, O. and Zorec, R. (2013). Regulation of AQP4 surface expression via vesicle mobility in astrocytes. Glia, 61(6), pp.917-928.

Preta, G., Cronin, J.G. & Sheldon, I.M. (2015) Dynasore - not just a dynamin inhibitor. *Cell communication and signaling: CCS*. 13, 24. doi:10.1186/s12964-015-0102-1.

Rash, J., Pereda, A., Kamasawa, N., Furman, C., Yasumura, T., Davidson, K., Dudek, F., Olson, C., Li, X. and Nagy, J. (2004). High-resolution proteomic mapping in the vertebrate central nervous system: Close proximity of connexin35 to NMDA glutamate receptor clusters and colocalisation of connexin36 with immunoreactivity for zonula occludens protein-1 (ZO-1). Journal of Neurocytology, 33(1), pp.131-151.

Reuss, L. (2012). Water Transport Across Cell Membranes. *eLS*.

Roche, J. and Törnroth-Horsefield, S. (2017). Aquaporin Protein-Protein Interactions. *International Journal of Molecular Sciences*, 18(11), p.2255.

Rodnick-Smith, M., Luan, Q., Liu, S.-L. & Nolen, B.J. (2016) Role and structural mechanism of WASP-triggered conformational changes in branched actin filament nucleation by Arp2/3 complex. *Proceedings of the National Academy of Sciences*. 113 (27), E3834–E3843. doi:10.1073/pnas.1517798113.

Rossi, A., Crane, J. and Verkman, A. (2011). Aquaporin-4 Mz isoform: Brain expression, supramolecular assembly and neuromyelitis optica antibody binding. Glia, 59(7), pp.1056-1063.

Saadoun, S., Papadopoulos, M.C., Watanabe, H., Yan, D., Manley, G.T. & Verkman, A.S. (2005) Involvement of aquaporin-4 in astroglial cell migration and glial scar formation. *Journal of Cell Science*. 118 (Pt 24), 5691–5698. doi:10.1242/jcs.02680.

Sato, K. (2014). *C. elegans* as a model for membrane traffic. WormBook, pp.1-47.

Savage, D.F. & Stroud, R.M. (2007) Structural basis of aquaporin inhibition by mercury. *Journal of molecular biology*. [Online] 368 (3), 607–617. Available from: doi:10.1016/j.jmb.2007.02.070.

Schnitzer, J.E., Oh, P., Pinney, E. & Allard, J. (1994) Filipin-sensitive caveolae-mediated transport in endothelium: reduced transcytosis, scavenger endocytosis, and capillary permeability of select macromolecules. *Journal of Cell Biology*. 127 (5), 1217–1232. doi:10.1083/jcb.127.5.1217.

Semerdjieva, S., Shortt, B., Maxwell, E., Singh, S., Fonarev, P., Hansen, J., Schiavo, G., Grant, B.D. & Smythe, E. (2008) Coordinated regulation of AP2 uncoating from clathrin-coated vesicles by rab5 and hRME-6. *The Journal of Cell Biology*. 183 (3), 499–511. doi:10.1083/jcb.200806016.

Söllner, T., Whiteheart, S.W., Brunner, M., Erdjument-Bromage, H., Geromanos, S., Tempst, P. & Rothman, J.E. (1993) SNAP receptors implicated in vesicle targeting and fusion. *Nature*. 362 (6418), 318–324. doi:10.1038/362318a0.

Sönnichsen, B., De Renzis, S., Nielsen, E., Rietdorf, J. & Zerial, M. (2000) Distinct Membrane Domains on Endosomes in the Recycling Pathway Visualized by Multicolor Imaging of Rab4, Rab5, and Rab11. *The Journal of Cell Biology*. 149 (4), 901–914.

Sorbo, J., Moe, S., Ottersen, O. and Holen, T. (2008). The Molecular Composition of Square Arrays. Biochemistry, 47(8), pp.2631-2637.

Stokum, J.A., Gerzanich, V. & Simard, J.M. (2016) Molecular pathophysiology of cerebral oedema. *Journal of Cerebral Blood Flow & Metabolism*. [Online] 36 (3), 513–538. Available from: doi:10.1177/0271678X15617172.

Sun, L., Liu, O., Desai, J., Karbassi, F., Sylvain, M.-A., Shi, A., Zhou, Z., Rocheleau, C.E. & Grant, B.D. (2012) CED-10/Rac1 Regulates Endocytic Recycling through the RAB-5 GAP TBC-2. *PLOS Genetics*. 8 (7), e1002785. doi:10.1371/journal.pgen.1002785.

Sun, M., Honey, C., Berk, C., Wong, N. and Tsui, J. (2003). Regulation of aquaporin-4 in a traumatic brain injury model in rats. *Journal of Neurosurgery*, 98(3), pp.565-569.

Sun, T.-X., Van Hoek, A., Huang, Y., Bouley, R., McLaughlin, M. & Brown, D. (2002) Aquaporin-2 localization in clathrin-coated pits: inhibition of endocytosis by dominant-negative dynamin. *American Journal of Physiology. Renal Physiology*. 282 (6), F998-1011. doi:10.1152/ajprenal.00257.2001.

Tajika, Y., Matsuzaki, T., Suzuki, T., Ablimit, A., Aoki, T., Hagiwara, H., Kuwahara, M., Sasaki, S. & Takata, K. (2005) Differential regulation of AQP2 trafficking in endosomes by microtubules and actin filaments. *Histochemistry and Cell Biology*. 124 (1), 1–12. doi:10.1007/s00418-005-0010-3.

Takata, K., Matsuzaki, T., Tajika, Y., Ablimit, A., et al. (2008) Localisation and trafficking of aquaporin 2 in the kidney. *Histochemistry and Cell Biology*. [Online] 130 (2), 197–209. Available from: doi:10.1007/s00418-008-0457-0.

Tham, D.K.L., Joshi, B. & Moukhles, H. (2016) Aquaporin-4 Cell surface Expression and Turnover Are Regulated by Dystroglycan, Dynamin, and the Extracellular Matrix in Astrocytes. *PLoS ONE*. 11 (10). doi:10.1371/journal.pone.0165439.

Thomas, C.M. & Smart, E.J. (2008) Caveolae structure and function. *Journal of Cellular and Molecular Medicine*. 12 (3), 796–809. doi:10.1111/j.1582-4934.2008.00295.x.

Törnroth-Horsefield, S., Hedfalk, K., Fischer, G., Lindkvist-Petersson, K. and Neutze, R. (2015). Structural insights into eukaryotic aquaporin regulation. FEBS Letters, 584(12), pp.2580-2588.

Vandebroek, A. & Yasui, M. (2020) Regulation of AQP4 in the Central Nervous System. *International Journal of Molecular Sciences*. [Online] 21 (5). Available from: doi:10.3390/ijms21051603 [Accessed: 15 June 2020].

Vella, J. (2015). The central role of aquaporins in the pathophysiology of ischemic stroke. Frontiers in Cellular Neuroscience, 9.

Verbalis, J. (2007). How Does the Brain Sense Osmolality?. Journal of the American Society of Nephrology, 18(12), pp.3056-3059.

Verkman, A.S., Binder, D.K., Bloch, O., Auguste, K. & Papadopoulos, M.C. (2006) Three distinct roles of aquaporin-4 in brain function revealed by knockout mice. *Biochimica et Biophysica Acta (BBA) - Biomembranes*. 1758 (8), 1085–1093.

Vespa, P.M. (2016) Brain Hypoxia and Ischemia After Traumatic Brain Injury: Is Oxygen the Right Metabolic Target? *JAMA Neurology*. 73 (5), 504–505. doi:10.1001/jamaneurol.2016.0251.

Vukićević, T., Schulz, M., Faust, D. and Klussmann, E. (2016). The Trafficking of the Water Channel Aquaporin-2 in Renal Principal Cells—a Potential Target for Pharmacological Intervention in Cardiovascular Diseases. Frontiers in Pharmacology, 7.

Walz, W. and Mukerji, S. (1988). KCl movements during potassium-induced cytotoxic swelling of cultured astrocytes. Experimental Neurology, 99(1), pp.17-29.

Wang, P.-J., Lin, S.-T., Liu, S.-H., Kuo, K.-T., Hsu, C.-H., Knepper, M.A. & Yu, M.-J. (2017) Vasopressin-induced serine 269 phosphorylation reduces Sipa1l1 (signal-induced proliferation-associated 1 like 1)-mediated aquaporin-2 endocytosis. *Journal of Biological Chemistry*. 292 (19), 7984–7993. doi:10.1074/jbc.M117.779611.

Wang, T., Li, L. and Hong, W. (2017). SNARE proteins in membrane trafficking. *Traffic*, 18(12), pp.767-775.

Wang, W.-L., Su, S.-H., Wong, K.Y., Yang, C.-W., Liu, C.-F. & Yu, M.-J. (2020) Rab7 involves Vps35 to mediate AQP2 sorting and apical trafficking in collecting duct cells. *American Journal of Physiology-Renal Physiology*. 318 (4), F956–F970. doi:10.1152/ajprenal.00297.2019.

Wolburg, H., Wolburg-Buchholz, K., Fallier-Becker, P., Noell, S. and Mack, A. (2011). Structure and Functions of Aquaporin-4-Based Orthogonal Arrays of Particles. *International Review of Cell and Molecular Biology*, pp.1-41.

Wong, K.Y., Wang, W.-L., Su, S.-H., Liu, C.-F. & Yu, M.-J. (2020) Intracellular location of aquaporin-2 serine 269 phosphorylation and dephosphorylation in kidney collecting duct cells. *American Journal of Physiology-Renal Physiology*. 319 (4), F592–F602. doi:10.1152/ajprenal.00205.2020.

Yang, B., Zador, Z. and Verkman, A. (2008). Glial Cell Aquaporin-4 Overexpression in Transgenic Mice Accelerates Cytotoxic Brain Swelling. Journal of Biological Chemistry, 283(22), pp.15280-15286.

Yang, P., Liu, Z. and Mahmood, T. (2014). Western blot: Technique, theory and trouble shooting. North American Journal of Medical Sciences, 6(3), p.160.

Yui, N., Lu, H.A.J., Chen, Y., Nomura, N., et al. (2013) Basolateral targeting and microtubule-dependent transcytosis of the aquaporin-2 water channel. *American Journal of Physiology - Cell Physiology*. [Online] 304 (1), C38–C48. Available from: doi:10.1152/ajpcell.00109.2012.

Yui, N., Lu, H.J., Bouley, R. & Brown, D. (2011) AQP2 is necessary for vasopressin- and forskolin-mediated filamentous actin depolymerization in renal epithelial cells. *Biology Open*. 1 (2), 101–108. doi:10.1242/bio.2011042.

Zador, Z., Stiver, S., Wang, V. & Manley, G.T. (2009) Role of Aquaporin-4 in Cerebral Oedema and Stroke. *Handbook of experimental pharmacology*. [Online] (190), 159–170. Available from: doi:10.1007/978-3-540-79885-9_7.

Zakeri, A., Kouhbanani, M.A.J., Beheshtkhoo, N., Beigi, V., Mousavi, S.M., Hashemi, S.A.R., Karimi Zade, A., Amani, A.M., Savardashtaki, A., Mirzaei, E., Jahandideh, S. & Movahedpour, A. (2018) Polyethylenimine-based nanocarriers in co-delivery of drug and gene: a developing horizon. *Nano Reviews & Experiments*. 9 (1), 1488497. doi:10.1080/20022727.2018.1488497.

Zeuthen, T. (2001). How water molecules pass through aquaporins. Trends in Biochemical Sciences, 26(2), pp.77-79.

Zheng, C.-Y., Petralia, R.S., Wang, Y.-X. & Kachar, B. (2011) Fluorescence Recovery After Photobleaching (FRAP) of Fluorescence Tagged Proteins in Dendritic Spines of Cultured Hippocampal Neurons. *Journal of Visualized Experiments : JoVE*. (50), 2568. doi:10.3791/2568.

Zulkefli, K.L., Houghton, F.J., Gosavi, P. & Gleeson, P.A. (2019) A role for Rab11 in the homeostasis of the endosome-lysosomal pathway. *Experimental Cell Research*. 380 (1), 55–68. doi:10.1016/j.yexcr.2019.04.010.